1-2019

Local Lagged Adapted Generalized Method of Moments: An Innovative Estimation and Forecasting Approach and its Applications.

Olusegun Michael Otunuga
Marshall University, otunuga@marshall.edu

Gandaram S. Ladde

Nathan G. Ladde

Recommended Citation
Otunuga, O. M., Ladde, G. S., & Ladde, N. G. (2019). Local Lagged Adapted Generalized Method of Moments: An Innovative Estimation and Forecasting Approach and its Applications. Journal of Time Series Econometrics. 11(1): pp. https://doi.org/10.1515/jtse-2016-0024

Local Lagged Adapted Generalized Method of Moments: An Innovative Estimation and Forecasting Approach and its Applications[1,+]

OLUSEGUN M. OTUNUGA*
Department of Mathematics and Statistics, Marshall University, One John Marshall Dr,
Huntington, West Virginia, 25755, USA.
GANGARAM S. LADDE
Department of Mathematics and Statistics,University of South Florida, 4202 E. Fowler Avenue,
Tampa, Florida, 33620, USA.
NATHAN G. LADDE
CSM, 5775 Glenridge Dr NE,
Atlanta, Georgia, 30328, USA.

Abstract

In this work, an attempt is made to apply the Local Lagged Adapted Generalized Method of Moments (LLGMM) to estimate state and parameters in stochastic differential dynamic models. The development of LLGMM is motivated by parameter and state estimation problems in continuous-time nonlinear and non-stationary stochastic dynamic model validation problems in biological, chemical, engineering, energy commodity markets, financial, medical, physical and social sciences. The byproducts of this innovative approach (LLGMM) are the balance between model specification and model prescription of continuous-time dynamic process and the development of discrete-time interconnected dynamic model of local sample mean and variance statistic process (DTIDMLSMVSP). Moreover, LLGMM is a dynamic non-parametric method. The DTIDMLSMVSP is an alternative approach to the GARCH (1,1) model, and it provides an iterative scheme for updating statistic coefficients in a system of generalized method of moment/observation equation. Furthermore, applications of LLGMM to energy commodities price, U.S. Treasury Bill interest rate and the U.S.-U.K. foreign exchange rate data strongly exhibit its unique role, scope and performance, in particular, in forecasting and confidence-interval problems in applied statistics.

Keywords: Conceptual computational/theoretical parameter estimation scheme; Method of Moments; Nonparametric; Simulation; Forecasting; Mean Square Optimal Procedure; Reaction/response time delay.

Mathematics Classification Code : 37M05; 37M10; 62M10; 62G05; 62P05

*Corresponding Author. Email: otunuga@marshall.edu Phone: +1 (304) 696 3049.

[1]U.S. Patent Pending

+ This is a preprint of a paper whose final and definite form is with *Journal of Time Series Econometrics*, available at https://doi.org/10.1515/jtse-2016-0024. Submitted 08/30/2016; Revised 01/02/2018; Accepted 12/07/2018

1. Introduction

For the past 40 years, researchers [3, 9, 11, 15, 17, 18, 19, 42, 31, 32, 35, 36, 38, 39, 40, 41] have given a lot of attention to estimating continuous-time dynamic models from discrete time data sets. The Generalized Method of Moments (GMM) developed by Hansen [17] and its extensions [11, 18, 19] have played a significant role in literature related to the parameter and state estimation problems in linear and nonlinear stochastic dynamic processes.

Most of the existing parameter and state estimation techniques are centered around the usage of either overall data sets [11, 18, 19], batched data sets [7], or local data sets [39] drawn on an interval of finite length T. This leads to an overall parameter estimate on the interval.

In this paper, recently developed method referred to as an innovative method, called the "Local Lagged Adapted Generalized Method of Moments" (LLGMM) [30] is used to estimate state and parameters in stochastic differential dynamic models. The LLGMM approach [30] is composed of seven interconnected components: (1) development of stochastic mathematical model of continuous time dynamic process [23, 24], (2) development of the discrete-time interconnected dynamic model for statistic process, (3) utilizing the Euler-type discretized scheme [21] for nonlinear and non-stationary system of stochastic differential equations (1), (4) employing lagged adaptive expectation process [33] for developing generalized method of moment/observation equations, (5) introduction of the conceptual and computational parameter estimation problem, (6) formulation of the conceptual and computational state simulation scheme and (7) defining the mean square ϵ-sub-optimal procedure.

In fact, the LLGMM approach [30] is also applicable to apparently different dynamic processes that are in actuality conceptually similar dynamic processes in biological, chemical, engineering, financial, medical, physical and social sciences. Moreover, one of the goals of the parameter and state estimation problems is for model validation rather than model misspecification [11]. For the continuous-time dynamic model validation, we utilize existing real world data. The real world time varying data is drawn/recorded at discrete-time on a time interval of finite length. Because of this, instead of using existing econometric specification/Euler-type numerical scheme, we construct the stochastic numerical approximation scheme [21] using continuous time stochastic differential equations. In real world dynamic modeling problems [23, 24, 25, 33, 34], future states of continuous time dynamic processes are influenced by the past state history. This is due to the influence of response/reaction time delay processes [25, 29, 30, 33]. The influence of state history, the concept of lagged adaptive expectation process [33], and the idea of a moving average [20] are incorporated in the development of the DTIDMLSMVSP (we refer readers to Lemma 2.1 of [30]). The presented approach is more suitable and robust for forecasting problems than existing methods. It also provides upper and lower bounds for the forecasted state of the system. Moreover, its computational aspect is a nested "two scale hierarchic" quadratic mean-square optimization process whereas the existing GMM and its extensions are "single-shot".

The organization of this paper is as follows.

In Section 2, we utilize the theoretical components (1)-(7) of the LLGMM method. For easy reference, we construct a local observation system from nonlinear stochastic functional differential equations. This is based on the Itô-Doob stochastic differential formula, Euler-type numerical scheme in the context of the original stochastic systems of differential equations and the given data. In addition, we briefly outline a procedure to estimate the state and parameters, locally. Using the LLGMM components (2), (3) and (4), conceptual computational iterative scheme, state and parameter estimation scheme, the simulation processes are coordinated with a real world data process in Section 3. This has led to generate the following concepts: (a) local admissible set of lagged sample/data/ observation size, (b) local class of admissible lagged-adapted finite sequence of conditional sample/data, (c) local admissible sequence of parameter estimates and corresponding admissible sequence of simulated values, (d) ϵ-best sub-optimal admissible subset of set of m_k-size local conditional samples at time t_k in (a), (e) ϵ-sub-optimal lagged-adapted finite sequence of conditional sample/data, and (f) finally, the ϵ-best sub-optimal parameter estimates and simulated value at time t_k for $k = 1, 2, ..., N$. These are summarized in Section 3 in a systematic way. Moreover, the local lagged adaptive process and DTIDMLSMVSP generate a finite chain of discrete-time admissible sets/sub-data and a corresponding chain described by the simulation algorithm. Furthermore, in Section 4, the usefulness of the conceptual computational LLGMM algorithm is illustrated by applying the algorithm to energy commodity's price, U.S. Treasury Bill interest rate and the U.S.-U.K. foreign exchange rate data for the state and parameter estimation problems. The graphical, simulation and statistical results as well as the goodness-of-fit measures are also outlined. In Section 5, the LLGMM is applied to investigate the forecasting and confidence-interval problems in applied statistics. The presented results show the long-run prediction exhibiting a degree of confidence. Moreover, it exhibits a wider role and scope to play in the 21st century. Because of the knowledge of nanotechnology coupled with the usage of advancements in electronic communication systems/tools which exhibit that almost everything is dynamic, highly nonlinear, non-stationary and operating under endogenous and exogenous processes, a multitude of applications of the proposed model exists. A few by-products of LLGMM namely: (a) the development of the second component, DTIDMLSMVSP and its component with the GARCH as well as Ex Post Volatility work in Section 6, (b) the Aggregated Generalized Method of Moments(AGMM) (described in Section 7 and Appendix *Appendix B*) and (c) Orthogonal Condition Based Generalized Method of Moments (OCBGMM-Analytic) are compared in Section 7. Using the average of locally estimated parameters in LLGMM, an aggregated generalized method of moment (AGMM) is also developed and applied to six data sets in *Appendix B*. In fact, in Section 7, we summarize a comparative study between LLGMM and the existing parametric OCBGMM techniques. The details are outlined in *Appendix C*. The LLGMM method exhibits superior performance to the existing and newly developed OCBGMM methods. The LLGMM method is independent and dynamic. On the other hand, the OCBGMM method is highly dependent and static.

2. Theoretical Parametric Estimation Procedure

In this section, for the sake of completeness and easy reference, we outline the theoretical components (1), (3) and (4) of the LLGMM [30]. The outline is based on a mathematically rigorous theoretical state and parameter estimation procedure for any general continuous-time nonlinear and non-stationary stochastic dynamic model described by a system of stochastic differential equations [24]. As stated before, this work is not only motivated by the continuous-time dynamic model validation problem [29, 30] in the context of real data energy commodities, but also motivated by any continuous-time nonlinear and non-stationary stochastic dynamic model validation problems in biological, chemical, engineering, financial, medical, physical and social sciences. For the sake of comparison of the presented results, we also sketch the existing OCBGMM procedure [9, 10, 18, 19] that uses the entire time series data set for single-shot parameter and state estimates. It lacks the usage of Itô-Doob calculus, properties of stochastic differential equations and its connectivity with the usage of econometric specification based discretization scheme, orthogonality conditional vector and the quadratic form.

We consider a general system of stochastic differential equations under the influence of hereditary effects in both the drift and diffusion coefficients described by

$$d\mathbf{y} = \mathbf{f}(t, \mathbf{y}_t)dt + \boldsymbol{\sigma}(t, \mathbf{y}_t)d\mathbf{W}(t), \quad \mathbf{y}_{t_0} = \boldsymbol{\varphi}_0, \tag{2.1}$$

where $\mathbf{y}_t(\theta) = \mathbf{y}(t+\theta)$, $\theta \in [-\tau, 0]$, $\mathbf{f}$, $\boldsymbol{\sigma} : [0, T] \times C \to \mathfrak{R}^q$ are Lipschitz continuous bounded functionals; C is a Banach space of continuous functions defined on $[-\tau, 0]$ into $\mathfrak{R}^q$ equipped with the supremum norm; $W(t)$ is standard Wiener process defined on a complete filtered probability space $(\Omega, \mathcal{F}, (\mathcal{F}_t)_{t\geq 0}, \mathbb{P})$; $\boldsymbol{\varphi}_0 \in C$, and $\mathbf{y}_0(t_0 + \theta)$ is $(\mathcal{F})_{t_0}$ measurables; the filtration function $(\mathcal{F}_t)_{t\geq 0}$ is right-continuous, and each $\mathcal{F}_t$ with $t \geq t_0$ contains all $\mathbb{P}$-null events in $\mathcal{F}$; the solution process $\mathbf{y}(t_0, \boldsymbol{\varphi}_0)(t)$ of (2.1) is adapted and non-anticipating with respect to $(\mathcal{F})_{t\geq 0}$.

2.1. Transformation of System of Stochastic Differential Equations (2.1) [30]

Let $V \in C[[-\tau, \infty] \times \mathfrak{R}^q, \mathfrak{R}^m]$, and its partial derivatives V_t, $\frac{\partial V}{\partial \mathbf{y}}$, $\frac{\partial^2 V}{\partial \mathbf{y}^2}$ exist and continuous. We apply Itô-Doob stochastic differential formula [24] to V and obtain

$$dV(t, \mathbf{y}) = LV(t, \mathbf{y}, \mathbf{y}_t)dt + V_{\mathbf{y}}(t, \mathbf{y})\boldsymbol{\sigma}(t, \mathbf{y}_t)d\mathbf{W}(t), \tag{2.2}$$

where the L operator is defined by

$$\begin{cases} LV(t,\mathbf{y},\mathbf{y}_t) & = & V_t(t,\mathbf{y}) + V_{\mathbf{y}}(t,\mathbf{y})\mathbf{f}(t,\mathbf{y}_t) + \frac{1}{2}tr(V_{\mathbf{yy}}(t,y)b(t,\mathbf{y}_t)), \\ b(t,\mathbf{y}_t) & = & \boldsymbol{\sigma}(t,\mathbf{y}_t)\boldsymbol{\sigma}^T(t,\mathbf{y}_t). \end{cases} \tag{2.3}$$

2.2. Euler-type Discretization Scheme for (2.1) and (2.2) [30]

For (2.1) and (2.2), we present the Euler-type discretization scheme [21]:

$$\begin{cases} \Delta\mathbf{y}_i & = & \mathbf{f}(t_{i-1},\mathbf{y}_{t_{i-1}})\Delta t_i + \boldsymbol{\sigma}(t_{i-1},\mathbf{y}_{t_{i-1}})\Delta\mathbf{W}(t_i), \\ \Delta V(t_i,\mathbf{y}(t_i)) & = & LV(t_{i-1},\mathbf{y}(t_i),\mathbf{y}_{t_{i-1}})\Delta t_i + V_{\mathbf{y}}(t_{i-1},\mathbf{y}(t_{i-1}))\boldsymbol{\sigma}(t_{i-1},\mathbf{y}_{t_{i-1}})\Delta W(t_i), \quad i = 1,2,...,n. \end{cases} \tag{2.4}$$

Define $\mathcal{F}_{t_{i-1}} \equiv \mathcal{F}_{i-1}$ as the filtration process up to time t_{i-1}.

2.3. Formation of Generalized Moment Equations From (2.4)

With regard to the continuous time dynamic system (2.1) and its transformed system (2.2), the more general moments of $\Delta\mathbf{y}(t_i)$ are as follows:

$$\begin{cases} \mathbb{E}\left[\Delta\mathbf{y}(t_i)|\mathcal{F}_{i-1}\right] & = & \mathbf{f}(t_{i-1},\mathbf{y}_{t_{i-1}})\Delta t_i, \\ \mathbb{E}\left[\left(\Delta\mathbf{y}(t_i) - E\left[\Delta\mathbf{y}(t_i)|\mathcal{F}_{i-1}\right]\right)\left(\Delta\mathbf{y}(t_i) - E\left[\Delta\mathbf{y}(t_i)|\mathcal{F}_{i-1}\right]\right)^T|\mathcal{F}_{i-1}\right] & = & \boldsymbol{\sigma}(t_{i-1},\mathbf{y}_{t_{i-1}})\boldsymbol{\sigma}^T(t_{i-1},\mathbf{y}_{t_{i-1}})\Delta t_i, \\ \mathbb{E}\left[\Delta V(t_i,\mathbf{y}(t_i))|\mathcal{F}_{i-1}\right] & = & LV(t_{i-1},\mathbf{y}(t_i),\mathbf{y}_{t_{i-1}})\Delta t_i, \\ \mathbb{E}\left[\left(\Delta V(t_i,\mathbf{y}(t_i)) - E\left[\Delta V(t_i,\mathbf{y}(t_i))|\mathcal{F}_{i-1}\right]\right)\left(\Delta V(t_i,y(t_i)) - E\left[\Delta V(t_i,y(t_i))|\mathcal{F}_{i-1}\right]\right)^T|\mathcal{F}_{i-1}\right] & = & B(t_{i-1},\mathbf{y}(t_{i-1}),\mathbf{y}_{t_{i-1}}), \end{cases} \tag{2.5}$$

where $B(t_{i-1},\mathbf{y}(t_{i-1}),\mathbf{y}_{t_{i-1}}) = V_{\mathbf{y}}(t_{i-1},\mathbf{y}(t_{i-1}))b(t_{i-1},\mathbf{y}_{t_{i-1}})V_{\mathbf{y}}(t_{i-1},\mathbf{y}(t_{i-1}))^T\Delta t_i$, and T is the transpose of the matrix.

2.4. Basis for Local Lagged Adaptive Discrete-time Expectation Process

For $i = 1,2,...,n$, it follows from (2.4) and (2.5) that

$$\begin{cases} \Delta\mathbf{y}_i & = & E\left[\Delta\mathbf{y}(t_i)|\mathcal{F}_{i-1}\right] + \boldsymbol{\sigma}(t_{i-1},\mathbf{y}_{t_{i-1}})\Delta\mathbf{W}(t_i), \\ \Delta V(t_i,\mathbf{y}(t_i)) & = & E\left[\Delta V(t_i,\mathbf{y}(t_i))|\mathcal{F}_{i-1}\right] + V_{\mathbf{y}}(t_{i-1},\mathbf{y}(t_{i-1}))\boldsymbol{\sigma}(t_{i-1},\mathbf{y}_{t_{i-1}})\Delta\mathbf{W}(t_i), \; i = 1,2,...,n. \end{cases} \tag{2.6}$$

This provides the basis for the development of the concept of lagged adaptive expectation process [33] with respect to continuous time stochastic dynamic systems (2.1) and (2.2). This indeed leads to a formulation of m_k-local generalized method of moments at time t_k.

2.5. Block Orthogonality Condition Vector for (2.1) and (2.2) [30]

From (2.6), we note that one can define a block vector of orthogonality condition [10] as

$$H(t_{i-1},\mathbf{y}(t_i),\mathbf{y}(t_{i-1})) = \begin{pmatrix} \Delta\mathbf{y}(t_i) - \mathbf{f}(t_{i-1},\mathbf{y}(t_{i-1}))\Delta t_i \\ \Delta V(t_{i-1},\mathbf{y}(t_i)) - LV(t_{i-1},\mathbf{y}(t_{i-1},\mathbf{y}_{t_{i-1}}))\Delta t_i \end{pmatrix}. \tag{2.7}$$

Remark 2.1. Using the LLGMM method described in [30], we attempt to estimate the state and parameters of the stochastic differential dynamic model of the type (2.1). This involves the construction of Euler-type discretization scheme for (2.1) and (2.2) in Sub-section 2.2, the formation of generalized moment equations from (2.4) in Sub-section 2.3 and the basis for local lagged adaptive discrete-time expectation process in Sub-section 2.4. All of these are in the framework of correct mathematical reasoning. Further, it is logical and interconnected/interactive within the context of the continuous-time dynamic system (2.1). The theoretical parameter estimation procedure in this section adapts to and incorporates the continuous-time changes in the state and parameters of the system and moves into a discrete-time theoretical numerical schemes in (2.4) as a model validation of (2.1). It further successively moves in the local moment equations within the context of local lagged adaptive, local discrete-time statistic and computational processes in a natural, systematic and coherent manner.

We illustrate this by applying the LLGMM method [30] to estimate state and parameters in stochastic differential dynamic models for energy commodity price, U.S. Treasury Bill interest rate, and the U.S.-U.K. foreign exchange rate data.

2.6. Illustration 1: Dynamic Model for Energy Commodity Price [29, 30]

We consider the stochastic dynamic model for energy commodities [29, 30] described by the following nonlinear stochastic differential equation

$$dy = a(t)(\mu(t)-y)ydt + \sigma(t,y_t)ydW(t), \quad y_{t_0} = \boldsymbol{\varphi}_0, \tag{2.8}$$

where $y_t(\theta) = y(t+\theta)$; $\theta \in [-\tau, 0]$, $\mu, a : [t_0, T] \to \mathfrak{R}$ are continuous functions; the initial process $\boldsymbol{\varphi}_0 = \{y(t_0+\theta)\}_{\theta\in[-\tau,0]}$ is $\mathcal{F}_{t_0}$-measurable and independent of $\{W(t), t \in [t_0, T]\}$; $W(t)$ is a standard Wiener process defined in (2.1); $\sigma : [t_0, T] \times C \to \mathfrak{R}^+$ is a Lipschitz continuous and bounded functional; C is the Banach space of continuous functions defined on $[-\tau, 0]$ into $\mathfrak{R}$ equipped with the supremum norm.

The solution $y(t)$ of (2.8) satisfies

$$y(t) - y(t_0) = \int_{t_0}^{t} a(s)y(s)(\mu(s) - y(s))ds + \int_{t_0}^{t} \sigma(s, y_s)y(s)dW(s),$$

and

$$\mathbb{E}\left[y(t) - y(t_0)|\mathcal{F}_{s<t}\right] = \int_{t_0}^{t} a(s)y(s)(\mu(s) - y(s))ds.$$

Transformation of Stochastic Differential Equation (2.8): We pick a Lyapunov function $V(t, y) = \ln(y)$ in (2.2) for (2.8). Using Itô-differential formula [24], we have

$$d\left(\ln(y)\right) = \left[a(t)(\mu(t) - y) - \frac{1}{2}\sigma^2(t, y_t)\right]dt + \sigma(t, y_t)dW(t). \tag{2.9}$$

The Euler-type Discretization Schemes for (2.8) **and** (2.9) **[21, 30]**: By setting $\Delta t_i = t_i - t_{i-1}$, $a_i = a(t_i)$, $\mu_i = \mu(t_i)$, $\sigma_i = \sigma(t_i)$, $\Delta y_i = y(t_i) - y(t_{i-1})$, the combined Euler discretized scheme for (2.8) and (2.9) is

$$\begin{cases} \Delta y_i & = & a_{i-1}y_{i-1}(\mu_{i-1} - y_{i-1})\Delta t_i + \sigma(t_{i-1}, y_{t_{i-1}})y_{i-1}\Delta W(t_i), \quad y_{t_0} = \boldsymbol{\varphi}_0, \\ \Delta\left(\ln(y_i)\right) & = & \left[a_{i-1}(\mu_{i-1} - y_{i-1}) - \frac{1}{2}\sigma^2(t_{i-1}, y_{t_{i-1}})\right]\Delta t_i + \sigma(t_{i-1}, y_{t_{i-1}})\Delta W(t_i), \quad y_{t_0} = \boldsymbol{\varphi}_0. \end{cases} \tag{2.10}$$

where $\boldsymbol{\varphi}_0 = \{y_i\}_{i=-r}^{0}$ is a given finite sequence of $\mathcal{F}_0-$ measurable random variables, and it is independent of $\{\Delta W(t_i)\}_{i=0}^{N}$.

Generalized Moment Equations [30]: Applying conditional expectation to (2.10) with respect to $\mathcal{F}_{t_{i-1}} \equiv \mathcal{F}_{i-1}$, we obtain

$$\begin{array}{lcl} \mathbb{E}\left[\Delta y_i|\mathcal{F}_{i-1}\right] & = & a_{i-1}y_{i-1}(\mu_{i-1} - y_{i-1})\Delta t, \\ \mathbb{E}\left[\Delta\left(\ln(y_i)\right)|\mathcal{F}_{i-1}\right] & = & \left[a_{i-1}(\mu_{i-1} - y_{i-1}) - \frac{1}{2}\sigma^2(t_{i-1}, y_{t_{i-1}})\right]\Delta t, \\ \mathbb{E}\left[\left(\Delta\left(\ln(y_i)\right) - \mathbb{E}\left[\Delta\left(\ln(y_i)\right)|\mathcal{F}_{i-1}\right]\right)^2|\mathcal{F}_{i-1}\right] & = & \sigma^2(t_{i-1}, y_{t_{i-1}})\Delta t. \end{array} \tag{2.11}$$

Basis for Lagged Adaptive Discrete-time Expectation Process: From (2.11), (2.10) reduces to

$$\begin{cases} \Delta y_i & = & \mathbb{E}\left[\Delta y_i|\mathcal{F}_{i-1}\right] + \sigma(t_{i-1}, y_{t_{i-1}})y_{i-1}\Delta W(t_i), \\ \Delta\left(\ln(y_i)\right) & = & \mathbb{E}\left[\Delta\left(\ln(y_i)\right)|\mathcal{F}_{i-1}\right] + \sigma(t_{i-1}, y_{t_{i-1}})\Delta W(t_i). \end{cases} \tag{2.12}$$

(2.12) provides the basis for the development of the concept of lagged adaptive expectation process [33] with respect to continuous time stochastic dynamic systems (2.8) and (2.9).

Remark 2.2. Orthogonality Condition Vector for (2.8) **and** (2.9)

Using (2.10), (2.11) and (2.12), we further remark that the orthogonality condition vector [10] with respect to continuous-time stochastic dynamic model (2.8) is represented by

$$H(t_{i-1}, y(t_i), y(t_{i-1})) = \begin{pmatrix} \Delta y(t_i) - a(t_{i-1})y(t_{i-1})(\mu(t_{i-1}) - y(t_{i-1}))\Delta t_i \\ \Delta \ln(y(t_i)) - L\ln(y(t_{i-1}), y_{t_{i-1}})\Delta t_i \\ (\Delta \ln(y(t_i)) - L\ln(y(t_{i-1}), y_{t_{i-1}})\Delta t_i)^2 - \sigma^2(t_{i-1}, y_{t_{i-1}})\Delta t_i \end{pmatrix}. \tag{2.13}$$

where $L\ln(y(t_{i-1}), y_{t_{i-1}})\Delta t_i = \left(a(t_{i-1})(\mu(t_{i-1}) - y(t_{i-1})) - \frac{1}{2}\sigma^2(t_{i-1}, y_{t_{i-1}})\right)\Delta t_i$. Moreover, unlike the orthogonality condition vector defined in the literature [8, 10, 38], this orthogonality condition vector is based on the discretization scheme (2.10) associated with nonlinear continuous-time stochastic differential equations (2.8) and (2.9) and the Itô-Doob stochastic differential calculus [21, 24]

Local Observation System of Algebraic Equations [30]: Following definition for $k \in I_0(N)$, applying the LLGMM method [30] and using Definitions 2.3-2.7 of [30] together with the discretized form (2.12), we formulate a local observation/measurement process at time t_k as algebraic functions of m_k-local functions of restriction of the overall finite sample sequence $\{y_i\}_{i=-r}^{N}$ to a subpartition P_k in Definition 2.2 of [30]. Let $a_{t_{k*}}$ and $\mu_{t_{k*}}$ be estimates of a_t and μ_t, respectively, at each time t. We have

$$\begin{cases} \frac{1}{m_k}\sum\limits_{i=k-m_k}^{k-1} \mathbb{E}\left[\Delta y_i|\mathcal{F}_{i-1}\right] & = & a_{t_{k*}}\left[\frac{\mu_{t_{k*}}}{m_k}\sum\limits_{i=k-m_k}^{k-1} y_{i-1} - \frac{1}{m_k}\sum\limits_{i=k-m_k}^{k-1} y_{i-1}^2\right]\Delta t, \\ \frac{1}{m_k}\sum\limits_{i=k-m_k}^{k-1} \mathbb{E}\left[\Delta\left(\ln(y_i)\right)|\mathcal{F}_{i-1}\right] & = & a_{t_{k*}}\left[\mu_{t_{k*}} - \frac{1}{m_k}\sum\limits_{i=k-m_k}^{k-1} y_{i-1}\right]\Delta t - \frac{1}{2m_k}\sum\limits_{i=k-m_k}^{k-1} \mathbb{E}\left[\left(\Delta\left(\ln(y_i)\right) - \mathbb{E}\left[\Delta\left(\ln(y_i)\right)|\mathcal{F}_{i-1}\right]\right)^2|\mathcal{F}_{i-1}\right], \\ \hat{\sigma}_{m_k,k}^2 & = & \begin{cases} \frac{1}{m_k\Delta t}\sum\limits_{i=k-m_k}^{k-1} \mathbb{E}\left[\left(\Delta\left(\ln(y_i)\right) - \mathbb{E}\left[\Delta\left(\ln(y_i)\right)|\mathcal{F}_{i-1}\right]\right)^2|\mathcal{F}_{i-1}\right] & \text{if } m_k \text{ is small} \\ \frac{1}{(m_k-1)\Delta t}\sum\limits_{i=k-m_k}^{k-1} \mathbb{E}\left[\left(\Delta\left(\ln(y_i)\right) - \mathbb{E}\left[\Delta\left(\ln(y_i)\right)|\mathcal{F}_{i-1}\right]\right)^2|\mathcal{F}_{i-1}\right] & \text{if } m_k \text{ is large,} \end{cases} \end{cases} \tag{2.14}$$

where $m_k \in I_2(r+k-1) = \{2, 3, ..., r+k-1\}$ is defined as the local admissible sample/data observation size at time t_k (Definition 3.3 [30]). Following Definitions (2.5-2.7) in [30], we define $\bar{S}_{m_k,k}$ and $s_{m_k,k}^2$ as the m_k-local average/mean and m_k-local variance, respectively, corresponding to a local sequence $S_{m_k,k} = \{x_j\}_{k-m_k}^{k-1}$. From the third equation in (2.14), it follows that the average volatility square $\hat{\sigma}_{m_k,k}^2$ is given by

$$\hat{\sigma}_{m_k,k}^2 = \frac{s_{m_k,k}^2}{\Delta t}, \tag{2.15}$$

where $s_{m_k,k}^2$ is the local sample variance statistics for volatility at time t_k in the context of $x(t_i) = \Delta(\ln(y_i))$ satisfying the following discrete-time interconnected dynamic model of local sample mean $\bar{S}_{m_k,k}$ and variance $s_{m_k,k}^2$ processes (DTIDMLSMVSP)

$$
\begin{cases}
\bar{S}_{m_{k-p+1},k-p+1} = \frac{m_{k-p}}{m_{k-p+1}} \bar{S}_{m_{k-p},k-p} + \eta_{m_{k-p},k-p}, \quad \bar{S}_{m_0,0} = \bar{S}_0 \\
s^2_{m_k,k} = \begin{cases}
\frac{m_k-1}{m_k}\left[\sum_{i=1}^{p}\left[\frac{m_{k-i}}{\prod_{j=0}^{i-1} m_{k-j}}\right] s^2_{m_{k-i},k-i} + \frac{m_{k-p}}{\prod_{j=0}^{p-1} m_{k-j}} \bar{S}^2_{m_{k-p},k-p}\right] + \varepsilon_{m_{k-1},k-1}, & \text{for small } m_k, m_{k-1} \le m_k \\
\sum_{i=1}^{p}\left[\frac{m_{k-i}-1}{\prod_{j=0}^{i-1} m_{k-j}}\right] s^2_{m_{k-i},k-i} + \frac{m_{k-p}}{\prod_{j=0}^{p-1} m_{k-j}} \bar{S}^2_{m_{k-p},k-p} + \epsilon_{m_{k-1},k-1}, & \text{for large } m_k,\ m_{k-1} \le m_k \\
s^2_{m_i,i} = s^2_i,\ i \in I_{-p}(0), & \text{initial conditions}
\end{cases}
\end{cases}
\tag{2.16}
$$

where p is the order of the system (2.16) and

$$
\begin{cases}
\eta_{m_{k-p},k-p} = \frac{1}{m_{k-p+1}}\left[\sum_{i=-m_{k-p+1}+1}^{-m_{k-p}+1} F^i x_{k-p} - F^{-m_{k-p}+1} x_{k-p} - F^{-m_{k-p}} x_{k-p} + F^0 x_{k-p}\right], \\
\varepsilon_{m_{k-1},k-1} = \frac{m_k-1}{m_k}\left[\sum_{i=1}^{p} \frac{\left(F^{-i+1} x_{k-1}\right)^2}{\prod_{j=0}^{i-1} m_{k-j}} - \sum_{i=1}^{p} \frac{\left(F^{-i+1-m_{k-i}} x_{k-1}\right)^2}{\prod_{j=0}^{i-1} m_{k-j}} - \sum_{i=1}^{p} \frac{\left(F^{-i+2-m_{k-i}} x_{k-1}\right)^2}{\prod_{j=0}^{i-1} m_{k-j}}\right] \\
\qquad + \frac{m_k-1}{m_k}\left[\sum_{i=1}^{p}\left[\frac{\sum_{l=-i+2-m_{k-i+1}}^{-i+2-m_{k-i}} (F^l x_{k-1})^2}{\prod_{j=0}^{i-1} m_{k-j}}\right] + \sum_{i=1}^{p}\left[\frac{\sum_{\substack{l,s=-i+2-m_{k-i+1} \\ l\neq s}}^{-i+1} F^l x_{k-1} F^s x_{k-1}}{\prod_{j=0}^{i-1} m_{k-j}}\right]\right] \\
\qquad - \frac{1}{m_k} \sum_{\substack{l,s=-m_k+1 \\ l\neq s}}^{0} F^l x_{k-1} F^s x_{k-1}, \\
\epsilon_{m_{k-1},k-1} = \sum_{i=1}^{p} \frac{\left(F^{-i+1} x_{k-1}\right)^2}{\prod_{j=0}^{i-1} m_{k-j}} - \sum_{i=1}^{p} \frac{\left(F^{-i+1-m_{k-i}} x_{k-1}\right)^2}{\prod_{j=0}^{i-1} m_{k-j}} - \sum_{i=1}^{p} \frac{\left(F^{-i+2-m_{k-i}} x_{k-1}\right)^2}{\prod_{j=0}^{i-1} m_{k-j}} + \sum_{i=1}^{p}\left[\frac{\sum_{l=-i+2-m_{k-i+1}}^{-i+2-m_{k-i}} (F^l x_{k-1})^2}{\prod_{j=0}^{i-1} m_{k-j}}\right] \\
\qquad + \sum_{i=1}^{p}\left[\frac{\sum_{\substack{l,s=-i+2-m_{k-i+1} \\ l\neq s}}^{-i+1} F^l x_{k-1} F^s x_{k-1}}{\prod_{j=0}^{i-1} m_{k-j}}\right] - \frac{1}{m_k-1} \sum_{\substack{l,s=-m_k+1 \\ l\neq s}}^{0} F^l x_{k-1} F^s x_{k-1}
\end{cases}
\tag{2.17}
$$

For details, see [30] (Lemma 2.1) and [29].

Thus, by the application of the Implicit Function Theorem [2], we conclude that for every non-constant m_k-local sequence $\{x(t_i)\}_{i=k-m_k}^{k-1}$, there exists a unique solution $\hat{a}_{m_k,k} \equiv a_{t_k}$ and $\hat{\mu}_{m_k,k} \equiv \mu_{t_k}$ of system of algebraic equations (2.14) as a point estimates of $a(t)$ and $\mu(t)$, respectively, at time $t = t_k$, given by

$$
\begin{cases}
\hat{a}_{m_k,k} = \dfrac{\left(\frac{1}{m_k}\sum_{i=k-m_k}^{k-1} \Delta(\ln y_i) + \frac{s^2_{m_k,k}}{2}\right)\left(\frac{1}{m_k}\sum_{i=k-m_k}^{k-1} y_{i-1}\right) - \frac{1}{m_k}\sum_{i=k-m_k}^{k-1} \Delta y_i}{\frac{1}{m_k}\left[\sum_{i=k-m_k}^{k-1} y^2_{i-1} - \frac{1}{m_k}\left(\sum_{i=k-m_k}^{k-1} y_{i-1}\right)^2\right]\Delta t} \\
\hat{\mu}_{m_k,k} = \dfrac{\frac{1}{m_k \Delta t}\sum_{i=k-m_k}^{k-1} \Delta(\ln y_i) + \frac{s^2_{m_k,k}}{2\Delta t} + \frac{\hat{a}_{m_k,k}}{m_k}\left(\sum_{i=k-m_k}^{k-1} y_{i-1}\right)}{\hat{a}_{m_k,k}}, \\
\hat{\sigma}^2_{m_k,k} = \dfrac{s^2_{m_k,k}}{\Delta t}.
\end{cases}
\tag{2.18}
$$

Remark 2.3. We note that without loss of generality, the discrete-time data set $\{y_{-r+i} : i \in I_1(r-1)\}$ is assumed to be close to the true values of the solution process of the continuous-time dynamic process. In fact, this assumption is feasible in view of the uniqueness and continuous dependence of the solution process for stochastic functional or ordinary differential equation with respect to the initial data [24].

Remark 2.4. If the sample $\{y_i\}_{i=k-m_k-1}^{k-1}$ is a constant sequence, then it follows from (2.18) and the fact that $\Delta(\ln y_i) = 0$ and $s^2_{m_k,k} = 0$, that $\hat{\mu}_{m_k,k} \to \frac{1}{m_k} \sum_{i=k-m_k}^{k-1} y_{i-1}$. Also, it follows from (2.14) that $\hat{a}_{m_k,k} = 0$.

Remark 2.5. As we stated before, the theoretically estimated parameters a, μ, and σ^2 depend upon the time at which a data point is drawn. This is what we expected because of the fact that nonlinearity of the dynamic model together with environmental stochastic perturbations generates a non-stationary solution process. Using locally estimated parameters of the continuous-time dynamic system, we can find the average of the local parameters over the entire size of data set as follows:

$$\left\{ \bar{a} \;=\; \frac{1}{N}\sum_{i=0}^{N} a_{\hat{m}_i,i}, \quad \bar{\mu} = \frac{1}{N}\sum_{i=0}^{N} \mu_{\hat{m}_i,i}, \quad \overline{\sigma^2} = \frac{1}{N}\sum_{i=0}^{N} \sigma^2_{\hat{m}_i,i}. \right. \tag{2.19}$$

where $\bar{a}$, $\bar{\mu}$, and $\overline{\sigma^2}$ are referred to as aggregated parameter estimates of a, μ, and σ^2 over the given entire finite interval of time, respectively. Further detailed statistical analysis is outlined in Appendix B.

Remark 2.6. The discrete-time interconnected dynamic model for statistic process (DTIDMLSMVSP) (Lemma 2.1 [30]) and its transformation of data are utilized in (2.14), (2.15), (2.18), and (2.19) for updating statistic coefficients of equations in (2.11). This indeed accelerates the computation process. Furthermore, DTIDMLSMVSP plays a very significant role in the local discretization and model validation process.

2.7. Illustration 2: Dynamic Model for U.S. Treasury Bill Interest Rate and the U.S.-U.K. Foreign Exchange Rate

We also apply the above presented scheme for estimating parameters of a continuous-time model for U.S. Treasury Bill interest rate [44] and U.S.-U.K. foreign exchange rate [45] processes. By employing dynamic modeling process [23, 24], a continuous time dynamic model of interest rate process under random environmental perturbations is described in [30] as follows:

$$dy = (\beta y + \mu y^{\delta})dt + \sigma y^{\gamma} dW(t), \quad y(t_0) = y_0, \tag{2.20}$$

where $\beta, \mu, \delta, \sigma, \gamma \in \mathfrak{R}$; $y(t, t_0, y_0)$ is adapted, non-anticipating solution process with respect to $\mathcal{F}_t$; the initial process y_0 is $\mathcal{F}_{t_0}$-measurable and independent of $\{W(t), t \in [t_0, T]\}$; $W(t)$ is a standard Wiener process defined on a filtered probability space $(\Omega, \mathcal{F}, (\mathcal{F}_t)_{t\geq 0}, \mathbb{P})$.

Transformation of Stochastic Differential Equation (2.20): For (2.20), we consider the Lyapunov functions $V_1(t,y) = \frac{1}{2}y^2$ and $V_2(t,y) = \frac{1}{3}y^3$ as in (2.2). The Itô differentials of V_i, for $i = 1,2$, are given by

$$\begin{cases} dV_1 &= \left[y(\beta y + \mu y^{\delta}) + \frac{1}{2}\sigma^2 y^{2\gamma}\right]dt + \sigma y^{\gamma+1}dW(t), \\ dV_2 &= \left[y^2(\beta y + \mu y^{\delta}) + \sigma^2 y^{2\gamma+1}\right]dt + \sigma y^{\gamma+2}dW(t). \end{cases} \tag{2.21}$$

The Euler-type Numerical Schemes for (2.20) **and** (2.21) **[21, 30]**: Following the approach in Section 3 and illustration 2.6, the Euler discretized scheme ($\Delta t = 1$) for (2.20) is defined by

$$\begin{cases} \Delta y_i &= (\beta y_{i-1} + \mu y_{i-1}^{\delta}) + \sigma y_{i-1}^{\gamma}\Delta W(t_i), \\ \frac{1}{2}\Delta(y_i^2) &= y_{i-1}(\beta y_{i-1} + \mu y_{i-1}^{\delta}) + \frac{1}{2}\sigma^2 y_{i-1}^{2\gamma} + \sigma y_{i-1}^{\gamma+1}\Delta W(t_i), \\ \frac{1}{3}\Delta(y_i^3) &= y_{i-1}^2(\beta y_{i-1} + \mu y_{i-1}^{\delta}) + \sigma^2 y_{i-1}^{2\gamma+1} + \sigma y_{i-1}^{\gamma+2}\Delta W(t_i). \end{cases} \tag{2.22}$$

Generalized Moment Equations: Applying conditional expectation to (2.22) with respect to $\mathcal{F}_{i-1}$, we obtain

$$\begin{aligned} \mathbb{E}\left[\Delta y_i|\mathcal{F}_{i-1}\right] &= \beta y_{i-1} + \mu y_{i-1}^{\delta}, \\ \frac{1}{2}\mathbb{E}\left[\Delta(y_i^2)|\mathcal{F}_{i-1}\right] &= \beta y_{i-1}^2 + \mu y_{i-1}^{\delta+1} + \frac{1}{2}\sigma^2 y_{i-1}^{2\gamma}, \\ \frac{1}{3}\mathbb{E}\left[\Delta(y_i^3)|\mathcal{F}_{i-1}\right] &= \beta y_{i-1}^3 + \mu y_{i-1}^{\delta+2} + \sigma^2 y_{i-1}^{2\gamma+1}, \\ \mathbb{E}\left[(\Delta y_i - \mathbb{E}\left[\Delta y_i|\mathcal{F}_{i-1}\right])^2|\mathcal{F}_{i-1}\right] &= \sigma^2 y_{i-1}^{2\gamma}, \\ \frac{1}{4}\mathbb{E}\left[\left(\Delta(y_i^2) - \mathbb{E}\left[\Delta(y_i^2)\right]\right)^2|\mathcal{F}_{i-1}\right] &= \sigma^2 y_{i-1}^{2\gamma+2}. \end{aligned} \tag{2.23}$$

Remark 2.7. Orthogonality Condition Vector for (2.20) **and** (2.21)**:** Again, in the context of (2.20), (2.21), (2.22), and (2.23), the orthogonality condition vector [10, 30] with respect to continuous-time stochastic dynamic model (2.20) is as:

$$H(t_{i-1}, y(t_i), y(t_{i-1})) = \begin{pmatrix} \Delta y(t_i) - (\beta y(t_{i-1}) + \mu y^{\delta}(t_{i-1}))\Delta t_i \\ \frac{1}{2}\Delta(y^2(t_i)) - L(y^2(t_{i-1}))\Delta t_i \\ \frac{1}{3}\Delta(y^3(t_i)) - L(y^3(t_{i-1}))\Delta t_i \\ \left(\Delta y(t_i) - (\beta y(t_{i-1}) + \mu y^{\delta}(t_{i-1}))\Delta t_i\right)^2 - \sigma^2 y^{2\gamma}(t_{i-1})\Delta t_i \\ \left(\frac{1}{2}\Delta(y^2(t_i)) - L(y^2(t_{i-1}))\Delta t_i\right)^2 - \sigma^2 y^{2\gamma+2}(t_{i-1})\Delta t_i \end{pmatrix}, \tag{2.24}$$

where $L(y^2(t_{i-1}))\Delta t_i = \left(y(t_{i-1})\left(\beta y(t_{i-1}) + \mu y^{\delta}(t_{i-1})\right) + \frac{1}{2}\sigma^2 y^{2\gamma}(t_{i-1})\right)\Delta t_i$ and $L(y^3(t_{i-1}))\Delta t_i = \left(y^2(t_{i-1})\left(\beta y(t_{i-1}) + \mu y^{\delta}(t_{i-1})\right) + \sigma^2 y^{2\gamma+1}(t_{i-1})\right)\Delta t_i$. Moreover, unlike the orthogonality condition vector defined in the literature [8, 10, 38], this orthogonality condition vector is based on the discretization scheme (2.22) associated with nonlinear continuous-time stochastic differential equations (2.20) and (2.21).

Local Observation System of Algebraic Equations: Following the argument used in (2.14), for $k \in I_0(N)$, from Definitions 2.3-2.7 in [30] and using (2.23), we formulate a local observation/measurement process at t_k as an algebraic functions of m_k-local functions of restriction of the overall finite sample sequence $\{y_i\}_{i=-r}^{N}$ to m_k-point subpartition $P_k := t_{k-m_k} < t_{k-m_k+1} < ... < t_{k-1}$ as follows:

$$\begin{cases} \frac{1}{m_k}\sum\limits_{i=k-m_k}^{k-1} \mathbb{E}\left[\Delta y_i|\mathcal{F}_{i-1}\right] & = \beta\frac{\sum_{i=k-m_k}^{k-1} y_{i-1}}{m_k} + \mu\frac{\sum_{i=k-m_k}^{k-1} y_{i-1}^{\delta}}{m_k}, \\ \frac{1}{2m_k}\sum\limits_{i=k-m_k}^{k-1}\left[\mathbb{E}\left[\Delta(y_i^2)|\mathcal{F}_{i-1}\right] - \mathbb{E}\left[\left(\Delta y_i - \mathbb{E}\left[\Delta y_i|\mathcal{F}_{i-1}\right]\right)^2|\mathcal{F}_{i-1}\right]\right] & = \beta\frac{\sum_{i=k-m_k}^{k-1} y_{i-1}^2}{m_k} + \mu\frac{\sum_{i=k-m_k}^{k-1} y_{i-1}^{\delta+1}}{m_k}, \\ \frac{1}{m_k}\sum\limits_{i=k-m_k}^{k-1}\left[\frac{1}{3}\mathbb{E}\left[\Delta(y_i^3)|\mathcal{F}_{i-1}\right] - \sigma^2 y_{i-1}^{2\gamma+1}\right] & = \beta\frac{\sum_{i=k-m_k}^{k-1} y_{i-1}^3}{m_k} + \mu\frac{\sum_{i=k-m_k}^{k-1} y_{i-1}^{\delta+2}}{m_k}, \\ \frac{1}{m_k}\sum\limits_{i=k-m_k}^{k-1}\mathbb{E}\left[\left(\Delta y_i - \mathbb{E}\left[\Delta y_i|\mathcal{F}_{i-1}\right]\right)^2|\mathcal{F}_{i-1}\right] & = \sigma^2\frac{\sum_{i=k-m_k}^{k-1} y_{i-1}^{2\gamma}}{m_k}, \\ \frac{1}{4m_k}\sum\limits_{i=k-m_k}^{k-1}\mathbb{E}\left[\left(\Delta(y_i^2) - \mathbb{E}\left[\Delta(y_i^2)\right]\right)^2|\mathcal{F}_{i-1}\right] & = \sigma^2\frac{\sum_{i=k-m_k}^{k-1} y_{i-1}^{2\gamma+2}}{m_k}. \end{cases} \tag{2.25}$$

The solution $\sigma_{m_k,k}$ is given by

$$\sigma_{m_k,k} = \left[\frac{s_{m_k,k}^2}{\frac{1}{m_k}\sum\limits_{i=k-m_k}^{k-1} y_{i-1}^{2\gamma_{m_k,k}}}\right]^{1/2}, \tag{2.26}$$

and $\gamma_{m_k,k}$ satisfies the following nonlinear algebraic equation

$$s_{m_k,k}^2\sum_{i=k-m_k}^{k-1} y_{i-1}^{2\gamma_{m_k,k}+2} - \frac{1}{4}\mathbf{s}_{m_k,k}^2\sum_{i=k-m_k}^{k-1} y_{i-1}^{2\gamma_{m_k,k}} = 0, \tag{2.27}$$

where $s_{m_k,k}^2$ and $\mathbf{s}_{m_k,k}^2$ denote the local moving variance of Δy_i and $\Delta(y_i^2)$, respectively.

By the application of the Implicit Function Theorem [2], we conclude that for every non-constant m_k-local sequence $\{y(t_i)\}_{i=k-m_k}^{k-1}$, $\delta \neq 1$, there exist solution $\hat{\beta}_{m_k,k}$, $\hat{\mu}_{m_k,k}$, and $\hat{\delta}_{m_k,k}$ of system of algebraic equations (2.25) as a point estimates of β, μ and δ respectively, at time t_k, given by

$$\begin{cases} \hat{\mu}_{m_k,k} & = \dfrac{\frac{1}{m_k}\sum_{i=k-m_k}^{k-1}\Delta y_i\sum_{i=k-m_k}^{k-1} y_{i-1}^2 - \frac{1}{2}\left[\frac{1}{m_k}\sum_{i=k-m_k}^{k-1}\Delta(y_i^2) - s_{m_k,k}^2\right]\sum_{i=k-m_k}^{k-1} y_{i-1}}{\frac{1}{m_k}\left[\sum_{i=k-m_k}^{k-1} y_{i-1}^{\delta_{m_k,k}}\sum_{i=k-m_k}^{k-1} y_{i-1}^2 - \sum_{i=k-m_k}^{k-1} y_{i-1}^{1+\delta_{m_k,k}}\sum_{i=k-m_k}^{k-1} y_{i-1}\right]} \\ \hat{\beta}_{m_k,k} & = \dfrac{\sum_{i=k-m_k}^{k-1}\Delta y_i - \hat{\mu}_{m_k,k}\sum_{i=k-m_k}^{k-1} y_{i-1}^{\delta_{m_k,k}}}{\sum_{i=k-m_k}^{k-1} y_{i-1}}, \end{cases} \tag{2.28}$$

where $\delta_{m_k,k}$ satisfies the third equation in (2.25) described by

$$\frac{1}{3m_k}\sum_{i=k-m_k}^{k-1}\Delta(y_i^3)-\frac{\sigma^2_{m_k,k}}{m_k}\sum_{i=k-m_k}^{k-1}y_{i-1}^{2\gamma_{m_k,k}+1}-\beta_{m_k,k}\frac{\sum_{i=k-m_k}^{k-1}y_{i-1}^3}{m_k}-\mu_{m_k,k}\frac{\sum_{i=k-m_k}^{k-1}y_{i-1}^{\delta_{m_k,k}+2}}{m_k}=0. \tag{2.29}$$

We further note that the parameters of continuous-time dynamic process (2.20) are time-varying functions. This justifies the modifications needed for the development of continuous-time models of dynamic processes.

Remark 2.8. The presented illustrations exhibit the important features of the theoretical parameter estimation procedure [30]. The illustrations further clearly differentiate the Itô-Doob differential formula [24] based formation of orthogonality condition vectors in Remarks 2.2 and 2.7 and the algebraic manipulation and discretized scheme using the econometric specification based orthogonality condition vectors in [9, 11, 17].

Remark 2.9. The DTIDMLSMVSP and its transformation of data are utilized in (2.25), (2.26), (2.27), (2.28) and (2.29) for updating statistic coefficient of equations in (2.23). This indeed accelerates the computation process. Furthermore, DTIDMLSMVSP plays a very significant role in the local discretization and model validation errors.

3. Computational Algorithm

In this section, we outline theoretical computational components (5), (6) and (7) of LLGMM [30]. Again, for easy reference, we review the definitions of terms and expressions regarding computational, data organizational and simulation schemes. We introduce the idea of iterative data process and data simulation process time schedules in relation to the real time data observation/collection schedule. For the computational estimation of continuous time stochastic dynamic system state and parameters, it is essential to determine an admissible set of local conditional sample average and sample variance of local conditional sample in the context of a partition of time interval $[-\tau, T]$. Moreover, the discrete time dynamic model of conditional sample mean and sample variance statistic processes in Section 2 of [30] and the theoretical parameter estimation scheme in Section 3 coupled with the lagged adaptive expectation process motivate to outline a computational scheme in a systematic and coherent manner. A brief summary of the conceptual computational and simulation scheme is shown below.

3.1. Coordination of data observation, Iterative process, and Simulation schedules.

For easy reference, we present definitions 2.1-2.7 of iterative process and simulation time schedules discussed in Otunuga et al. [30]. Without loss of generality, we assume that the real data observation/collection partition schedule

P of $[-\tau, T]$ is defined in [30] by

$$P := \{t_i = -\tau + (r + i)\Delta t\}, \quad \text{for} \quad i \in I_{-r}(N), \tag{3.1}$$

where $I_i(k) = \{j \in \mathbb{Z} \ : \ i \leq j \leq k\}$, $r + N$ stands for the total size of data.

Definition 3.1. An iterative process time schedule in relation with a real data collection schedule is defined by

$$IP = \{F^{-r} t_i : \quad \text{for} \ \ t_i \in P\}, \tag{3.2}$$

where $F^{-r} t_i = t_{i-r}$, and F^{-r} is a forward shift operator [6], and r is a discrete version of time delays of τ defined in [30] by $r = \left[\left|\frac{\tau}{\Delta t_i}\right|\right] + 1$.

The simulation time depends on an order p of the time series model (2.16) of m_k-local conditional sample mean and variance processes.

Definition 3.2. Let P, F^{-r} and p be as defined in Definition 3.1. A simulation process time schedule in relation with a real data observation schedule is defined by

$$SP = \begin{cases} \{F^r t_i : \ \ \text{for} \ \ t_i \in P\}, \ \ \text{if} \ \ p \leq r \\ \{F^p t_i : \ \ \text{for} \ \ t_i \in P\}, \ \ \text{if} \ \ p > r. \end{cases} \tag{3.3}$$

Remark 3.1. We note that initial times of iterative and simulation processes are equal to the real data times t_r and t_p, respectively. Moreover, iterative and simulation processes time in (3.2) and (3.3), respectively, justify Remark 2.3. In short, t_i is a scheduled time clock for a collection of ith observation of the state of the system under investigation. The iterative and simulation process times are t_{i+r} and t_{i+p}, respectively.

3.2. Conceptual Computational Parameter Estimation Scheme [30]

For a conceptual computational dynamic system parameter estimation, we need to introduce a few concepts of local admissible sample/data observation size, m_k-local admissible conditional finite sequence at $t_k \in SP$, local finite sequence of parameter estimates at t_k.

Definition 3.3. For each $k \in I_0(N)$, we define a local admissible sample/data observation size m_k at $t_k \in SP$ in (3.3) as $m_k \in OS_k$, where

$$OS_k = \begin{cases} I_2(r + k - 1), \ \ \text{if } p \leq r, \\ I_2(p + k - 1), \ \ \text{if } p > r, \end{cases} \tag{3.4}$$

Moreover, OS_k is referred to as the local admissible set of lagged sample/data observation size at t_k; $OS_k \subseteq SP$ for $k \in I_0(N)$ and $OS_k \subseteq OS_{k+1}$ for $k \in I_0(N-1)$.

Definition 3.4. For each admissible $m_k \in OS_k$ in Definition 3.3, a m_k-local admissible lagged-adapted finite restriction sequence of conditional sample/data observation at t_k to subpartition P_k of P is defined by $\{\mathbb{E}[y_i|\mathcal{F}_{i-1}]\}_{i=k-m_k}^{k-1}$. Moreover, a m_k- class of admissible lagged-adapted finite sequences of conditional sample/data observation of size m_k at t_k is defined by

$$\mathcal{AS}_k = \{\{\mathbb{E}[y_i|\mathcal{F}_{i-1}]\}_{i=k-m_k}^{k-1} : \; m_k \in OS_k\} = \{\{\mathbb{E}[y_i|\mathcal{F}_{i-1}]\}_{i=k-m_k}^{k-1}\}_{m_k \in OS_k}, \tag{3.5}$$

for each $k \in I_0(N)$.

Without loss of generality, in the case of energy commodity model, for each $m_k \in OS_k$, we find corresponding m_k- local admissible adapted finite sequence of conditional sample/data observation at t_k, $\{\mathbb{E}[y_i|\mathcal{F}_{i-1}]\}_{i=k-m_k}^{k-1}$. Using this sequence and (2.18), we compute $\hat{a}_{m_k,k}$, $\hat{\mu}_{m_k,k}$ and $\hat{\sigma}^2_{m_k,k}$. This leads to a local admissible finite sequence of parameter estimates at t_k defined on OS_k as follows: $\left\{(\hat{a}_{m_k,k}, \hat{\mu}_{m_k,k}, \hat{\sigma}^2_{m_k,k})\right\}_{m_k \in OS_k} = \{(\hat{a}_{m_k,k}, \hat{\mu}_{m_k,k}, \hat{\sigma}^2_{m_k,k})\}_{m_k \in 2}^{r+k-1}$ or $\{(\hat{a}_{m_k,k}, \hat{\mu}_{m_k,k}, \hat{\sigma}^2_{m_k,k})\}_{m_k \in 2}^{p+k-1}$. It is denoted by

$$(\mathcal{A}_k, \mathbb{M}_k, \mathcal{S}_k) = \left\{(\hat{a}_{m_k,k}, \hat{\mu}_{m_k,k}, \hat{\sigma}^2_{m_k,k})\right\}_{m_k \in OS_k}, \tag{3.6}$$

for $k \in I_0(N)$.

3.3. Conceptual Computation of State Simulation Scheme: Energy Commodity Model

For the development of a conceptual computational scheme, we need to employ the method of induction. The presented simulation scheme is based on the idea of lagged adaptive expectation process [33]. An autocorrelation function (ACF) analysis [6, 8] performed on $s^2_{m_k,k}$ suggests that the discrete time interconnected dynamic model of local conditional sample mean and sample variance statistic in (2.8) of [30] is of order $p = 2$. Because of this, we need to identify an initial data. We begin with a given initial data y_{t_0}, $\{\hat{s}^2_{m_0,0}\}_{m_0 \in OS_0}$, $\{\hat{s}^2_{m_{-1},-1}\}_{m_{-1} \in OS_{-1}}$, and $\{\bar{S}^2_{m_{-1},-1}\}_{m_{-1} \in OS_{-1}}$.

Let $y^s_{m_k,k}$ be a simulated value of $\mathbb{E}[y_k|\mathcal{F}_{k-1}]$ at time t_k corresponding to a local admissible lagged-adapted finite sequence $\{\mathbb{E}[y_i|\mathcal{F}_{i-1}]\}_{i=k-m_k}^{k-1} \in \mathcal{AS}_k$ of conditional sample/data observation of size m_k at t_k defined in (3.5). This simulated value is derived from the discretized Euler scheme (2.10) by

$$y^s_{m_k,k} = y^s_{m_{k-1},k-1} + \hat{a}_{m_{k-1},k-1}(\hat{\mu}_{m_{k-1},k-1} - y^s_{m_{k-1},k-1})y^s_{m_{k-1},k-1}\Delta t + \hat{\sigma}_{m_{k-1},k-1} y^s_{m_{k-1},k-1}\Delta W_{m_k,k}. \tag{3.7}$$

Let

$$\{y^s_{m_k,k}\}_{m_k \in OS_k}, \quad k \in I_0(N), \tag{3.8}$$

be a m_k- local admissible sequence of simulated values corresponding to m_k-class $\mathcal{AS}_k$ of local admissible lagged-adapted finite sequences of conditional sample/data observation of size m_k at t_k in (3.5) for $k \in I_0(N)$.

3.4. Mean-Square Sub-Optimal Procedure

For each $k \in I_0(N)$, to find the best estimate of $\mathbb{E}[y_k|\mathcal{F}_{k-1}]$ at time t_k from a m_k -local admissible finite sequence $\{y^s_{m_k,k}\}_{m_k \in OS_k}$ of a simulated value of $\{\mathbb{E}[y_i|\mathcal{F}_{i-1}]\}$ defined in (3.8), we need to compute a local admissible finite sequence of quadratic mean square error corresponding to $\{y^s_{m_k,k}\}_{m_k \in OS_k}$. A quadratic mean square error is defined below.

Definition 3.5. A local quadratic mean square error of $\mathbb{E}[y_k|\mathcal{F}_{k-1}]$ relative to each member of the term of local admissible sequence $\{y^s_{m_k,k}\}_{m_k \in OS_k}$ of simulated values in (3.8) is defined by

$$\Xi_{m_k,k,y_k} = \left(\mathbb{E}[y_k|\mathcal{F}_{k-1}] - y^s_{m_k,k}\right)^2, \tag{3.9}$$

for $k \in I_0(N)$.

For any arbitrary small positive number ϵ and for each time t_k, to find the best estimate from the m_k-local admissible sequence $\{y^s_{m_k,k}\}_{m_k \in OS_k}$ of simulated values, we determine the following ϵ-sub-optimal admissible subset of set of m_k-size local admissible lagged sample size m_k at t_k (OS_k):

$$\mathcal{M}_k = \{m_k : \Xi_{m_k,k,y_k} < \epsilon \ \text{ for } \ m_k \in OS_k\}, \tag{3.10}$$

for $k \in I_0(N)$. There are three different cases that determine the ϵ-best sub-optimal sample size $\hat{m}_k$ at time t_k.

Case 1: If $m_k \in \mathcal{M}_k$ gives the minimum, then m_k is recorded as $\hat{m}_k$.

Case 2: If more than one value of $m_k \in \mathcal{M}_k$, then the largest of such m_k's is recorded as $\hat{m}_k$.

Case 3: If condition (3.10) is not met (the property that defines $\mathcal{M}_k$) at time t_k, (that is, $\mathcal{M}_k = \emptyset$), then the value of m_k where the minimum $\min_{m_k} \Xi_{m_k,k,y_k}$ is attained is recorded as $\hat{m}_k$. The $\epsilon-$ best sub-optimal estimates of the parameters $\hat{a}_{m_k,k}$, $\hat{\mu}_{m_k,k}$ and $\hat{\sigma}^2_{m_k,k}$ at the ϵ-best sub-optimal sample size $\hat{m}_k$ are also recorded as $a_{\hat{m}_k,k}$, $\mu_{\hat{m}_k,k}$ and $\sigma^2_{\hat{m}_k,k}$, respectively, for $k \in I_0(N)$.

Finally, the simulated value $y^s_{m_k,k}$ at time t_k with $\hat{m}_k$ is now recorded as the ϵ-best sub-optimal state estimate for $\mathbb{E}[y_k|\mathcal{F}_{k-1}]$ at time t_k and denoted by $y^s_{\hat{m}_k,k}$. Similar reasoning can be provided for the estimates of the parameters of the U.S. Treasury Bill interest rate and U.S.-U.K. foreign exchange rate model.

Remark 3.2. We augment a few more Conceptual Computational Comparison between the LLGMM and the existing OCBGMM (*Appendix C*) [30] as follows.

a: The LLGMM approach is focused on parameter and state estimation problems at each data collection/observation time t_k using the local lagged adaptive expectation process. In fact, LLGMM is discrete-time dynamic process. On the other hand, OCBGMM is centered on the state and parameter estimates using entire data that is to the left of the final data collection time $T_N = T$. Implied weakness in forecasting, as seen in the next section, is explicitly shown with the OCBGMM approach and the ensuing results.

b: We note that Remark 2.1 exhibits the interactions/interdependence between the first three components of LLGMM [30], namely (1) development of stochastic model for continuous-time dynamic process, (2) development of the discrete-time interconnected dynamic model for statistic process, (3) utilizing the Euler-type discretized scheme for nonlinear and non-stationary system of stochastic differential equations and their interactions. On the other hand, the OCBGMM is partially connected.

c: From the development of the computational algorithm section, we remark that the interdependence/ interconnectedness of the four remaining components of the LLGMM [30], "(4) employing lagged adaptive expectation process for developing generalized method of moment equations, (5) introducing conceptual computational parameter estimation problem, (6) formulating conceptual computational state estimation scheme, and (7) defining conditional mean square ϵ-sub optimal procedure" is clearly illustrated. Moreover, the above stated components as well as data are directly connected with the original continuous-time SDE. On the other hand, OCBGMM is composed of single size, single sequence, single estimates, single simulated value and single error. Hence, OCBGMM is "single shot approach" and highly dependent on its second component rather than the first component.

d: The LLGMM method [30] is a discrete-time dynamic system composed of seven interactive interdependent components. In fact, it is a dynamic non-parametric applied statistics method. On the other hand, the OCBGMM is static dynamic process of five almost isolated components.

e: Furthermore, LLGMM is a "two scale hierarchic" quadratic mean-square optimization process, but the optimization process of OCBGMM is "single-shot"

f: Although LLGMM performs in discrete-time, it operates like the original continuous-time dynamic process. The performance of the LLGMM approach is superior to the OCBGMM and IRGMM approaches.

g: The LLGMM method does not require a large size data set. In addition, as time t_k increases, it generates a larger size of lagged adapted data set thereby further stabilizing the state and parameter estimation procedure with finite size data set. On the other hand, the OCBGMM does not exhibit this flexibility.

h: Further comparative summary analysis is described in Sections 7 in the context of conceptual, computational and statistical settings, exhibiting the role, scope and performance of LLGMM.

Remark 3.3. We note that the choice of $p = 2$ was determined based on the statistical procedure known as the Autocorrelation Function Analysis (AFA) [6, 8].

4. LLGMM and Statistical Analysis

In this section, we apply the theoretical LLGMM algorithm [30] to four energy commodities, U.S. Treasury Bill interest rate and the U.S.-U.K. foreign exchange rate data sets. In addition, we investigate the parameter and state estimation, forecasting and confidence-interval problems in the context of stochastic dynamic models (2.8) and (2.20) for these data sets.

4.1. Application to Four Energy Commodity Data Sets:

In this section, we apply the above conceptual computational algorithm to the real time data sets, namely, daily Henry Hub natural gas data set for the period 01/04/2000-09/30/2004, daily crude oil data set for the period 01/07/1997 − 06/02/2008, daily coal data set for the period of 01/03/2000 − 10/25/2013, and weekly ethanol data set for the period of 03/24/2005 − 09/26/2013, [12, 13, 14, 48] in the context of stochastic dynamic model (2.8).

The descriptive statistics of data for the daily Henry Hub natural gas, daily crude oil data, daily coal data, and weekly ethanol data are recorded in Table 1 below.

Table 1: Descriptive Statistics for [12, 13, 14, 48]

Data Set Y	N	$\bar{Y}$	Std(Y)
Nat. Gas	1184 (days)	4.5504	1.5090)
Crude Oil	4165 (days)	54.0093	31.0248
Coal	3470 (days)	27.1441	17.8394
Ethanol	438 (weeks)	2.1391	0.4455

Graphical, Simulation and Statistical Results-Case 1: We consider three cases for initial discrete-time delay r. We then later show that as r increases, the root mean square error reduces, significantly. Here, we pick $r = 5$, $\Delta t = 1$, $\epsilon = 0.001$, and $p = 2$. The ϵ- best sub-optimal estimates of parameters a, μ and σ^2 at each real data times are exhibited in Table 2 below.

Table 2: Estimates $\hat{m}_k$, $\sigma^2_{\hat{m}_k,k}$, $\mu_{\hat{m}_k,k}$ and $a_{\hat{m}_k,k}$ for initial delay $r = 5$.

t_k	Natural gas				t_k	Crude oil				t_k	Coal				t_k	Ethanol			
	$\hat{m}_k$	$\sigma^2_{\hat{m}_k,k}$	$\mu_{\hat{m}_k,k}$	$a_{\hat{m}_k,k}$		$\hat{m}_k$	$\sigma^2_{\hat{m}_k,k}$	$\mu_{\hat{m}_k,k}$	$a_{\hat{m}_k,k}$		$\hat{m}_k$	$\sigma^2_{\hat{m}_k,k}$	$\mu_{\hat{m}_k,k}$	$a_{\hat{m}_k,k}$		$\hat{m}_k$	$\sigma^2_{\hat{m}_k,k}$	$\mu_{\hat{m}_k,k}$	$a_{\hat{m}_k,k}$
5	3	0.0001	2.2231	0.6011	5	3	0.0001	24.4100	0.0321	5	3	0.0001	11.5534	0.0142	5	2	0.0002	1.1767	0.5831
6	3	0.0002	2.2160	0.6122	6	3	0.0002	24.7165	0.0341	6	3	0.0000	11.2529	0.4109	6	5	0.0008	1.1717	0.5159
7	3	0.0002	2.2513	0.6087	7	4	0.0003	25.5946	0.0537	7	3	0.0001	9.9161	0.0165	7	4	0.0007	1.1707	1.4925
8	4	0.0002	2.2494	0.1628	8	5	0.0006	25.5550	0.0467	8	3	0.0002	11.4663	-0.0403	8	5	0.0008	1.1713	1.4791
9	4	0.0002	2.2658	-0.1497	9	4	0.0006	25.5695	0.0499	9	3	0.0005	10.5922	-0.0843	9	5	0.0006	1.1709	2.1406
10	4	0.0003	2.1371	0.1968	10	4	0.0004	25.4787	0.0221	10	4	0.0009	8.9379	0.0714	10	4	0.0004	1.1900	0.8621
11	4	0.0004	2.5071	-0.2781	11	3	0.0001	25.7742	0.0100	11	4	0.0023	8.9051	0.1784	11	3	0.0025	1.1900	0.3719
12	4	0.0000	2.2550	0.3545	12	3	0.0002	26.9477	-0.0157	12	3	0.0015	9.0169	0.0855	12	3	0.0004	1.2188	0.5368
13	4	0.0005	2.5122	0.6246	13	3	0.0001	25.8786	-0.0112	13	3	0.0020	8.6231	0.0739	13	5	0.0004	1.1120	12.2917
14	4	0.0015	2.4850	0.5604	14	5	0.0005	22.1834	0.0049	14	2	0.0001	10.0100	0.0564	14	5	0.0007	1.1669	-0.9289
15	3	0.0007	2.5378	0.4846	15	5	0.0004	23.5425	0.0010	15	5	0.0067	9.5281	0.0741	15	5	0.0014	0.7492	-0.0879
16	3	0.0007	2.5715	0.7737	16	4	0.0002	23.8500	0.0000	16	4	0.0058	6.1821	0.0694	16	5	0.0011	1.7968	0.3087
17	5	0.0011	2.5688	0.5984	17	4	0.0002	23.8486	0.0502	17	4	0.0015	8.8087	0.0404	17	5	0.0002	1.8484	-0.1901
18	4	0.0010	2.5831	0.5423	18	5	0.0004	23.2913	-0.0113	18	4	0.0035	9.0681	0.0652	18	5	0.0003	1.1650	-0.1611
19	5	0.0007	2.5893	0.4256	19	3	0.0000	24.4715	0.1282	19	3	0.0040	9.0752	0.1527	19	5	0.0022	1.8943	0.1502
20	5	0.0006	2.6100	0.0683	20	3	0.0004	24.3878	0.0415	20	3	0.0049	9.0801	0.1405	20	5	0.0047	1.8144	0.2073
21	5	0.0007	2.3171	0.2893	21	5	0.0003	24.3336	0.2067	21	4	0.0043	8.9898	0.0946	21	4	0.001	1.8400	0.0464
22	4	0.0015	2.7043	0.6983	22	4	0.0002	23.9993	0.0200	22	5	0.0054	8.9148	0.0036	22	3	0.0020	3.7350	0..1628
23	3	0.0009	2.6590	0.8316	23	4	0.0001	24.1909	-0.0894	23	4	0.0018	8.6771	0.0884	23	3	0.0008	1.9905	0.1599
24	3	0.0010	2.6917	0.1822	24	3	0.0002	25.0812	-0.0252	24	5	0.0035	8.7586	0.0985	24	3	0.0018	1.9006	-3.4926
25	4	0.0017	2.5620	0.2201	25	3	0.0002	22.2942	0.0064	25	5	0.0006	8.4779	-0.1155	25	4	0.0234	2.4827	0.1837
...	...	...	..	...	...	...	...	..	...	...	...	...	..	..	...	...	...	...	...
...	...	...	..	...	...	...	...	..	...	...	...	...	..	..	...	...	...	...	...
1145	4	0.0003	5.7203	0.1225	2440	5	0.0003	58.431	0.0141	2865	3	0.001	37.657	0.0397	375	3	0.0008	2.1456	1.1005
1146	3	0.0003	5.6651	0.2031	2441	5	0.0003	57.205	0.0084	2866	3	0.0006	37.73	0.0468	376	4	0.0012	2.0689	0.2666
1147	3	0.0002	5.6601	0.3133	2442	4	0.0001	57.554	0.0165	2867	5	0.0014	39.6	0.0087	377	3	0.0009	2.0538	0.4339
1148	5	0.0006	5.6909	0.216	2443	5	0.0003	57.871	0.0168	2868	3	0.0006	38.769	0.0331	378	3	0.0008	2.054	0.7726
1149	3	0.0003	5.6982	0.2404	2444	5	0.0003	60.441	0.0023	2869	5	0.0019	38.272	0.0245	379	4	0.0007	2.0551	0.7588
1150	5	0.0006	5.6108	0.1362	2445	5	0.0003	38.954	-0.0006	2870	3	0.0014	37.627	0.0234	380	3	0.0003	2.0692	4.5252
1151	5	0.0006	5.61	0.1089	2446	4	0.0006	59.659	0.0165	2871	3	0.0004	37.753	-0.243	381	5	0.0021	1.995	-0.4407
1152	5	0.0006	5.4383	0.06272	2447	4	0.001	59.548	0.016	2872	4	0.0008	36.11	0.0101	382	5	0.0025	1.3252	-0.048
1153	4	0.0003	5.4307	0.1755	2448	4	0.0007	58.964	0.0115	2873	5	0.0015	33.823	0.0042	383	5	0.0023	0.82891	-0.04
1154	5	0.0005	5.4155	0.1569	2449	4	0.0005	58.415	0.0166	2874	4	0.0009	35.221	0.0183	384	4	0.0025	2.5937	0.3073
1155	3	0.0004	5.3742	-2.275	2450	5	0.0003	58.61	0.0193	2875	5	0.0011	33.381	0.0084	385	3	0.0064	2.6054	0.6097
1156	5	0.0006	5.4405	0.1392	2451	4	0.0004	59.244	0.0091	2876	4	0.0007	34.6	0.0228	386	5	0.0044	2.5947	0.4157
1157	4	0.0003	5.4423	0.2339	2452	5	0.0003	58.955	0.0143	2877	3	0.001	34.463	0.0441	387	3	0.0035	2.595	0.354
1158	4	0.0008	5.4276	0.1712	2453	4	0.0004	59.508	0.0179	2878	5	0.0009	34.583	0.0334	388	3	0.0018	2.6054	0.6561
1159	5	0.0006	5.3958	0.1309	2454	4	0.0003	59.978	0.0193	2879	5	0.0008	34.63	0.0443	389	5	0.0043	2.5992	0.3862
1160	3	0.0002	5.3557	-0.1882	2455	5	0.0003	59.957	0.0199	2880	4	0.0005	35.221	0.0207	390	3	0.0009	2.5812	0.3334
1161	3	0.0003	5.5081	-0.0696	2456	4	0.0005	59.849	0.0163	2881	5	0.0007	35.249	0.0196	391	4	0.0013	2.6299	-0.3594
1162	4	0.0003	4.908	0.0381	2457	5	0.0004	59.441	0.0095	2882	3	0.0003	35.583	0.1566	392	4	0.0013	2.6776	-0.2827
1163	4	0.0002	5.0635	0.1038	2458	4	0.0003	58.479	0.0103	2883	4	0.0004	36.036	0.0224	393	4	0.0011	1.5114	0.0394
1164	3	0.0002	5.082	0	2459	4	0.0002	57.917	0.0158	2884	3	0.0005	36.276	0.0373	394	3	0.0006	2.2927	0.5982
1165	4	0.0002	5.1099	-0.2756	2460	4	0.0005	56.122	0.0062	2885	4	0.0004	36.195	0.0374	395	5	0.0035	2.3275	0.3191

Table 2 shows the ϵ- best sub-optimal local admissible sample size $\hat{m}_k$ and the parameters $a_{\hat{m}_k,k}$, $\sigma^2_{\hat{m}_k,k}$, and $\mu_{\hat{m}_k,k}$ for four energy commodity price data at time t_k. This is based on $p \leq r$ and $r = 5$. Here, the range of the ϵ-best sub-optimal local admissible sample size $\hat{m}_k$ for any time $t_k \in [5, 25] \bigcup [1145, 1165]$, $t_k \in [5, 25] \bigcup [2440, 2460]$, $t_k \in [5, 25] \bigcup [2865, 2885]$, and $t_k \in [5, 25] \bigcup [375, 395]$ for natural gas, crude oil, coal and ethanol data, respectively, is

$$2 \leq \hat{m}_k \leq 5. \tag{4.1}$$

Remark 4.1. From (4.1), we draw the following conclusions:

a: From (3.4) and Definition 3.3 (OS_k), at each time t_k, for the four energy price data sets, the ϵ-best sub-optimal local admissible sample size $\hat{m}_k$ is attained on the subset $\{2, 3, 4, 5\}$ of (OS_k). Hence, the ϵ-best sub-optimal local state and parameter estimates are obtained in at most four iterates rather than $k + r - 1$.

b: The basis for the conclusion (a) is due to the fact that the ϵ-best sub-optimization process described in Subsections 3.3 and 3.4 stabilizes the local state and parameter estimations at each time t_k.

c: From (a) and (b), we further remark that, in practice, the entire local lagged admissible set OS_k of size m_k at time t_k is not fully utilized. In fact, for any $m_k \in OS_k$ and $m_k > \hat{m}_k$ such that as m_k approached $k + r - 1$, the corresponding state and parameters relative to m_k approach the ϵ-best sub-optimal local state and parameter estimates relative to the ϵ-best sub-optimal local admissible sample size $\hat{m}_k$ at time t_k. This is not surprising because of the nature of the state hereditary process, that is, as the size of the time-delay m_k increases, the influence of the past state history decreases.

d: From (c), we further conclude that the second (DTIDMLSMVSP) and the fourth (local lagged adaptive process) component of the LLGMM [30] are stabilizing agents. This justifies the introduction of the term, namely, conceptual computational state and parameter estimation scheme. In fact, these components play a role in not only the local ϵ-best suboptimal quadratic error reduction, but also local error stabilization problem depending on the choice of $\epsilon > 0$.

e: The conclusions (a), (b), (c) and (d) are independent of "large" data size and stationary conditions.

In the following, the graphs of $a_{\hat{m}_k,k}$ for natural gas, crude oil, coal and ethanol are exhibited in Figures 1 (a), (b), (c) and (d), respectively.

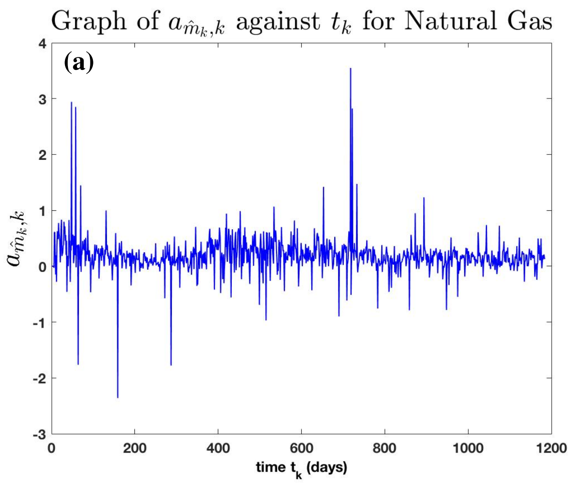

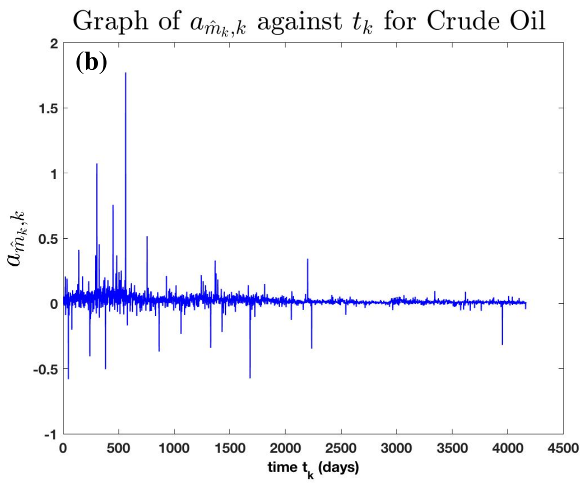

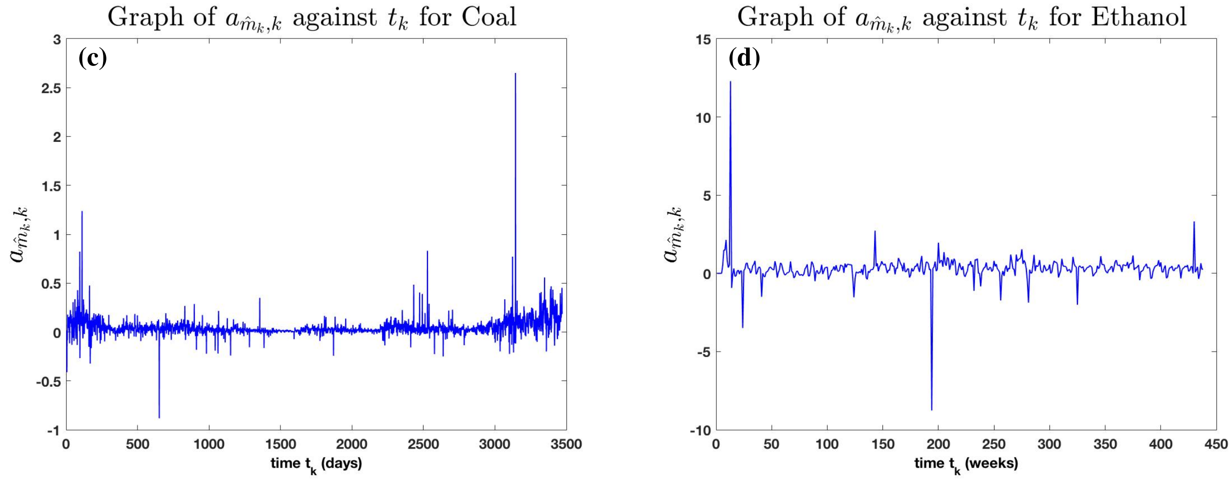

Figure 1: The graphs of mean reverting rate $a_{\hat{m}_k,k}$ with time t_k using initial delay $r = 5$.

Figure 1: **(a), (b), (c) and (d)** are the graphs of $a_{\hat{m}_k,k}$ (with respect to (2.8)) against time t_k for the daily Henry Hub natural gas data [14] , daily crude oil data [13], daily coal data [12], and weekly ethanol data [48], respectively. Each sketch exhibits the rate at which the data sets are reverting to the mean level.

Furthermore, we show the graphs of $\mu_{\hat{m}_k,k}$ for each of the data set.

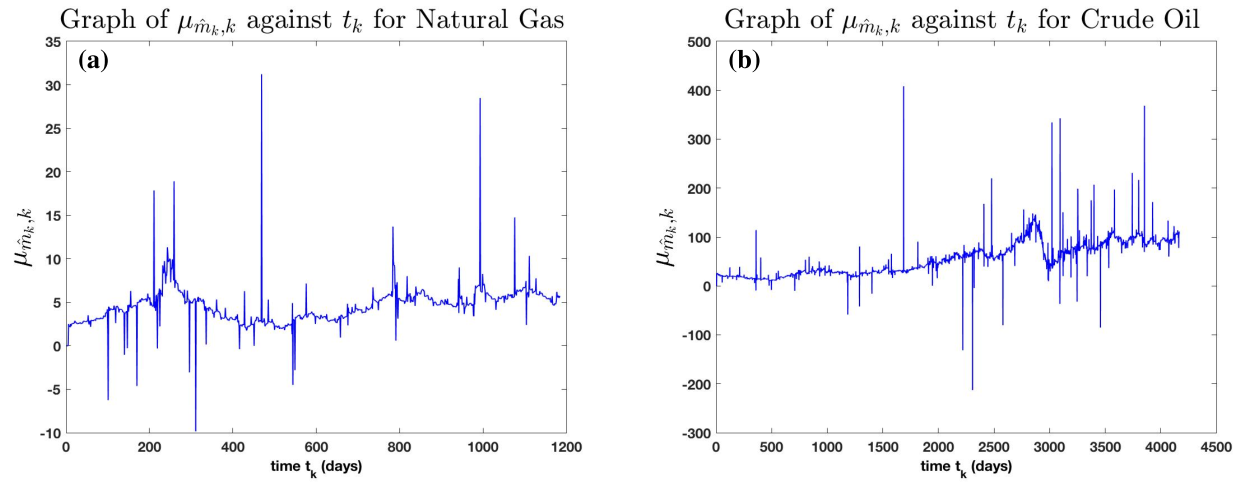

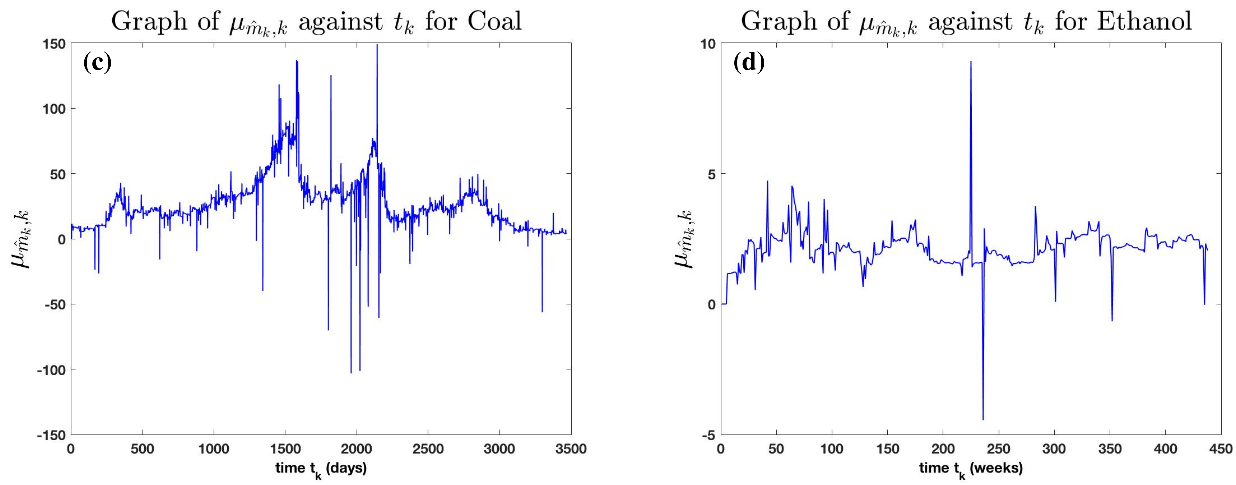

Figure 2: The graphs of mean level $\mu_{\hat{m}_k,k}$ with time t_k using initial delay $r = 5$

Figure 2: **(a), (b), (c) and (d)** are the graphs of $\mu_{\hat{m}_k,k}$ (with respect to (2.8)) against time t_k for the daily Henry Hub natural gas [14], daily crude oil [13], daily coal [12], and weekly ethanol data [48], respectively. The sample mean value of the real data y_k for natural gas, crude oil, coal and ethanol data are given by 4.5385, 54.0093, 27.1441 and 2.1391, respectively. It can be seen from Figure 2: **(a)**, **(b)**, **(c)** and **(d)** that the graph of $\mu_{\hat{m}_k,k}$ for the Henry Hub natural gas, crude oil, coal and ethanol data moves around the mean value 4.5385, 54.0093, 27.1441 and 2.1391, respectively. This analysis shows that the parameter $\mu_{\hat{m}_k,k}$ is close to the respective mean value of the data at time t_k. We also note that $\{\mu_{\hat{m}_i,i}\}_{i=0}^{N}$ and $\{a_{\hat{m}_i,i}\}_{i=0}^{N}$ are discrete-time ϵ- best sub-optimal simulated random samples generated by the scheme described at the beginning of Section 4.1

Figures 3 (a), (b), (c) and (d) show the graph of $s^2_{\hat{m}_k,k}$ for natural gas, crude oil, coal and ethanol, respectively.

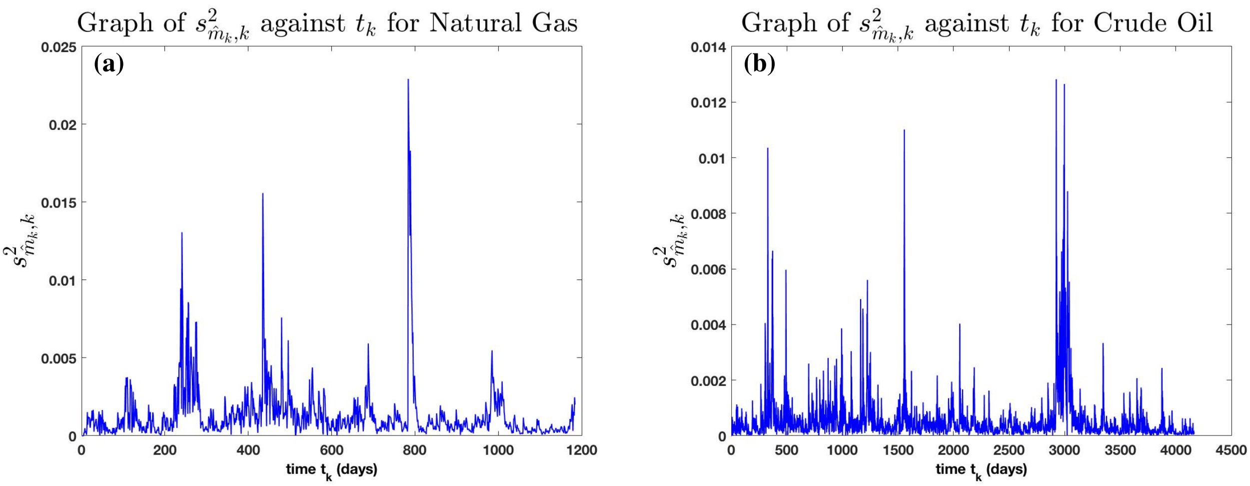

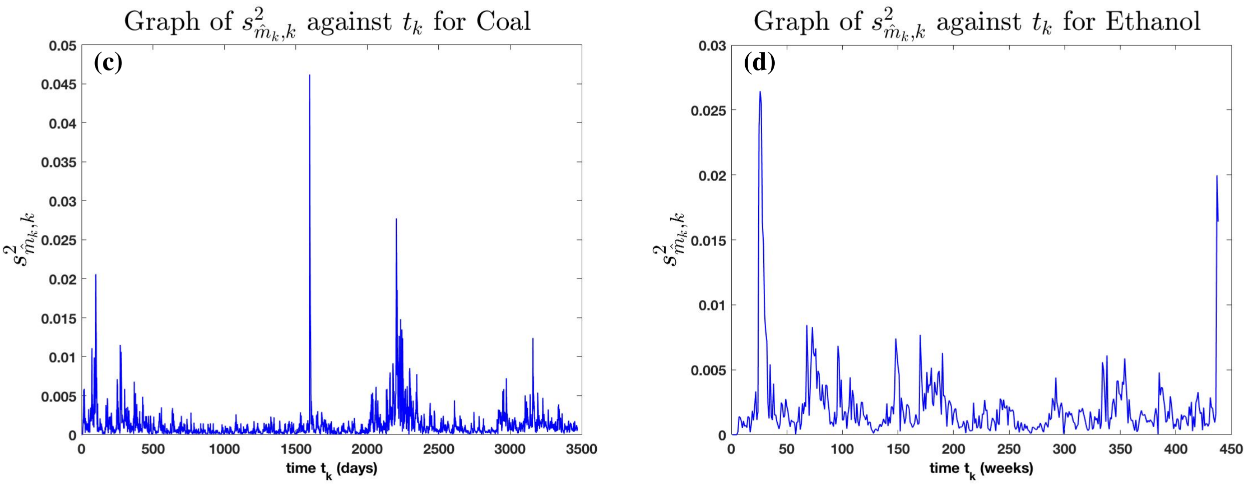

Figure 3: Moving Variance $s^2_{\hat{m}_k,k}$ against t_k with initial delay $r = 5$.

Figure 3: **(a), (b), (c) and (d)** are graphs of $s^2_{\hat{m}_k,k}$ (with respect to (2.8)) against time t_k with initial delay $r = 5$ for the daily Henry Hub natural gas data [14] , daily crude oil data [13], daily coal data [12], and weekly ethanol data [48], respectively. We found these estimates using the discrete time dynamic model (2.16) (see Lemma 2.1 in [30]) with $p = 2$. This is based on the autocorrelation and partial autocorrelation function described in [6, 8]. Using the third part of (2.18), the volatility square at time t_k can be calculated.

In Table 3, the real and LLGMM simulated price values for the four energy commodities: natural gas, crude oil, coal and ethanol are exhibited in columns 2-3, 6-7, 10-11, and 14-15, respectively. The absolute error of each of the energy commodity's simulated value is shown in columns 4, 8, 12, and 16.

Table 3: Real, Simulation using LLGMM method, and absolute error of simulation with starting delay $r = 5$.

t_k	Natural gas			t_k	Crude oil			t_k	Coal			t_k	Ethanol		
	Real y_k	Simulated $y^s_{\hat{m}_k,k}$ (LLGMM)	$\lvert Error \rvert$ $\lvert y_k - y^s_{\hat{m}_k,k} \rvert$		Real	Simulated $y^s_{\hat{m}_k,k}$ (LLGMM)	$\lvert Error \rvert$ $\lvert y_k - y^s_{\hat{m}_k,k} \rvert$		Real	Simulated $y^s_{\hat{m}_k,k}$ (LLGMM)	$\lvert Error \rvert$ $\lvert y_k - y^s_{\hat{m}_k,k} \rvert$		Real	Simulated $y^s_{\hat{m}_k,k}$ (LLGMM)	$\lvert Error \rvert$ $\lvert y_k - y^s_{\hat{m}_k,k} \rvert$
5	2.216	2.216	0	5	25.200	25.200	0	5	10.560	10.560	0	5	1.190	1.190	0
6	2.260	2.253	0.007	6	25.100	25.077	0.023	6	10.240	10.436	0.196	6	1.150	1.174	0.024
7	2.244	2.241	0.003	7	25.950	25.606	0.344	7	10.180	10.325	0.145	7	1.180	1.180	0.000
8	2.252	2.249	0.003	8	25.450	25.494	0.044	8	9.560	10.072	0.512	8	1.160	1.148	0.012
9	2.322	2.329	0.007	9	25.400	25.411	0.011	9	8.750	8.338	0.412	9	1.190	1.196	0.006
10	2.383	2.376	0.007	10	25.100	24.981	0.119	10	9.060	9.072	0.012	10	1.190	1.209	0.019
11	2.417	2.417	0.000	11	24.800	24.763	0.037	11	8.880	9.084	0.204	11	1.225	1.186	0.039
12	2.559	2.534	0.025	12	24.400	24.301	0.099	12	9.440	9.581	0.141	12	1.220	1.217	0.003
13	2.485	2.554	0.069	13	23.850	24.862	1.012	13	10.310	9.739	0.571	13	1.290	1.250	0.040
14	2.528	2.525	0.003	14	23.850	23.961	0.111	14	9.810	9.633	0.177	14	1.410	1.320	0.090
15	2.616	2.615	0.001	15	23.850	24.010	0.160	15	9.060	9.197	0.137	15	1.470	1.392	0.078
16	2.523	2.478	0.045	16	23.900	24.071	0.171	16	8.750	8.806	0.056	16	1.530	1.461	0.069
17	2.610	2.638	0.028	17	24.500	24.554	0.054	17	8.820	8.879	0.059	17	1.630	1.545	0.085
18	2.610	2.606	0.004	18	24.800	24.795	0.005	18	9.560	9.326	0.234	18	1.750	1.743	0.007
19	2.610	2.614	0.004	19	24.150	24.165	0.015	19	8.820	8.749	0.071	19	1.750	1.858	0.108
20	2.699	2.726	0.027	20	24.200	23.971	0.229	20	8.820	8.774	0.046	20	1.840	1.886	0.046
21	2.759	2.748	0.011	21	24.000	24.028	0.028	21	8.690	8.867	0.177	21	1.895	1.916	0.021
22	2.659	2.638	0.021	22	23.900	23.886	0.014	22	8.630	8.519	0.111	22	1.950	2.034	0.084
23	2.742	2.737	0.005	23	23.050	23.253	0.203	23	8.690	8.693	0.003	23	1.974	2.033	0.059
24	2.562	2.561	0.001	24	22.300	22.586	0.286	24	8.940	8.952	0.012	24	2.700	2.011	0.69
25	2.495	2.487	0.008	25	22.450	22.418	0.032	25	9.310	9.374	0.064	25	2.515	2.332	0.179
...	...	....	...	...	...	...	....	...	...	...	...	...	...	...	...
...	....	....	...	....	...	....	....	...	...	...	...	...	...	...	...
1145	5.712	5.709	0.003	2440	57.350	57.298	0.052	2865	29.310	29.065	0.245	375	2.073	2.019	0.054
1146	5.588	5.592	0.004	2441	56.740	56.650	0.090	2866	28.680	28.619	0.061	376	2.020	2.003	0.017
1147	5.693	5.650	0.043	2442	57.550	57.613	0.063	2867	26.770	28.408	1.638	377	2.073	2.094	0.021
1148	5.791	5.786	0.005	2443	59.090	59.152	0.062	2868	27.450	27.480	0.03	378	2.065	2.076	0.011
1149	5.614	5.458	0.156	2444	60.270	58.926	1.344	2869	27.000	27.250	0.250	379	2.055	2.061	0.006
1150	5.442	5.460	0.018	2445	60.750	59.675	1.075	2870	26.670	26.544	0.126	380	2.209	2.169	0.040
1151	5.533	5.571	0.038	2446	58.410	59.408	0.998	2871	26.510	26.497	0.013	381	2.440	2.208	0.232
1152	5.378	5.397	0.019	2447	58.720	58.917	0.197	2872	26.480	26.463	0.017	382	2.517	2.220	0.297
1153	5.373	5.374	0.001	2448	58.640	58.502	0.138	2873	25.150	25.781	0.631	383	2.718	2.362	0.356
1154	5.382	5.420	0.038	2449	57.870	58.721	0.851	2874	25.570	25.615	0.045	384	2.541	2.687	0.146
1155	5.507	5.501	0.006	2450	59.130	58.985	0.145	2875	25.880	25.948	0.068	385	2.566	2.607	0.041
1156	5.552	5.551	0.001	2451	60.110	60.087	0.023	2876	25.240	25.451	0.211	386	2.626	2.549	0.077
1157	5.310	5.272	0.038	2452	58.940	58.858	0.082	2877	25.000	24.649	0.351	387	2.587	2.606	0.019
1158	5.338	5.348	0.010	2453	59.930	59.390	0.540	2878	25.080	24.984	0.096	388	2.628	2.624	0.004
1159	5.298	5.353	0.055	2454	61.180	60.283	0.897	2879	25.050	25.158	0.108	389	2.587	2.556	0.031
1160	5.189	5.207	0.018	2455	59.660	59.939	0.021	2880	25.890	25.835	0.055	390	2.536	2.546	0.010
1161	5.082	5.087	0.005	2456	58.590	58.49	0.100	2881	25.230	25.211	0.019	391	2.420	2.425	0.005
1162	5.082	5.207	0.125	2457	58.280	58.624	0.344	2882	25.940	25.727	0.213	392	2.247	2.245	0.002
1163	5.082	4.783	0.299	2458	58.790	59.188	0.398	2883	25.260	25.347	0.087	393	2.223	2.196	0.027
1164	4.965	4.849	0.116	2459	56.23	55.442	0.788	2884	25.250	25.276	0.026	394	2.390	2.381	0.009
1165	4.767	4.733	0.034	2460	55.900	56.055	0.155	2885	26.060	25.660	0.400	395	2.380	2.398	0.018

Remark 4.2. We have used the estimated parameters $a_{\hat{m}_k,k}$, $\mu_{\hat{m}_k,k}$, and $\sigma^2_{\hat{m}_k,k}$, in Table 2 to simulate the daily prices of natural gas, crude oil, coal, and ethanol. For this purpose, we pick $\epsilon = 0.001$. For each time t_k, we estimate the simulated prices $y^s_{\hat{m}_k,k}$. Among the set of admissible set values m_k, the value that gives the minimum $\mathcal{M}_k$ is recorded as $\hat{m}_k$. If condition (3.10) is not satisfied at time t_k, the value of m_k where the minimum $\min\limits_{m_k} \Xi_{m_k,k,y_k}$ is attained, is recorded as $\hat{m}_k$. The ϵ- best sub-optimal estimates of the parameters $\hat{a}_{m_k,k}$, $\hat{\mu}_{m_k,k}$ and $\hat{\sigma}^2_{m_k,k}$ at $\hat{m}_k$ are also recorded as $a_{\hat{m}_k,k}$, $\mu_{\hat{m}_k,k}$ and $\sigma^2_{\hat{m}_k,k}$; the value of $y^s_{m_k,k}$ at time t_k corresponding to $\hat{m}_k$, $a_{\hat{m}_k,k}$, $\mu_{\hat{m}_k,k}$ and $\sigma^2_{\hat{m}_k,k}$ is also recorded as the $\epsilon-$ best sub-optimal simulated value $y^s_{\hat{m}_k,k}$ of y_k.

Next, we show the graphs of the simulated data using the LLGMM method for each commodity in Figure 4.

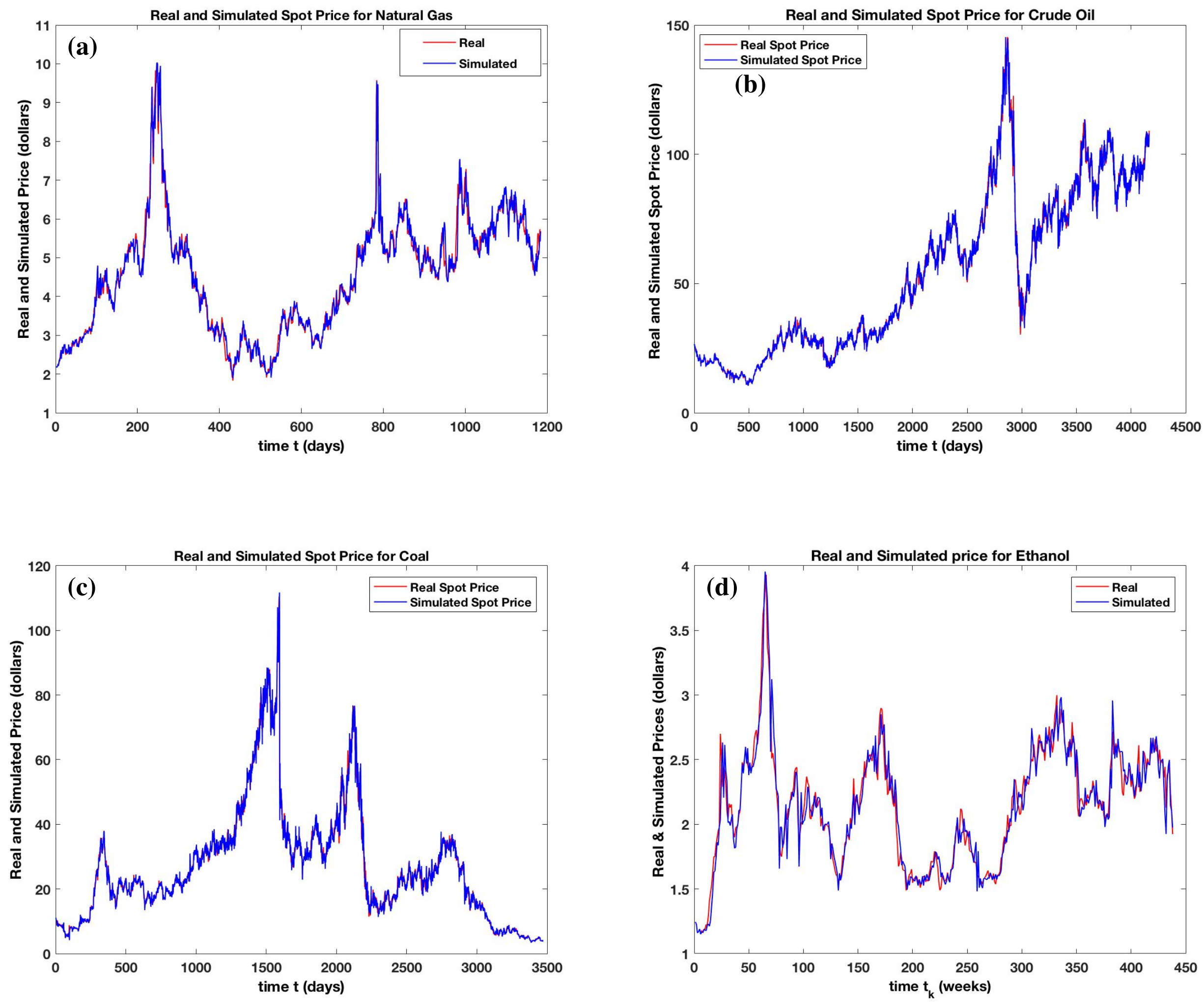

Figure 4: Real and Simulated Prices using initial delay $r = 5$.

Figures 4: **(a), (b), (c) and (d)** under the application of the LLGMM approach show the graphs of the real and simulated spot prices for the daily Henry Hub natural gas [14] , daily crude oil [13], daily coal [12], and weekly ethanol data [48], respectively. The red line represents the real data y_k while the blue line represents the simulated value $y^s_{\hat{m}_k,k}$.

Graphical, Simulation and Statistical Results-Case 2: For better simulation results in Figure 4, we increase the magnitude of time delay r. We pick $r = 10$, $\Delta t = 1$, $\epsilon = 0.001$, and $p = 2$. The $\epsilon-$ best sub-optimal estimates of parameters a, μ and σ^2 at each real data times are exhibited in $Appendix\ A.1$, Table $A.13$. In Table $A.14$, the real and LLGMM simulated price values of each of the four energy commodities: natural gas, crude oil, coal and ethanol are exhibited in columns 2-3, 6-7, 10-11, and 14-15, respectively. The absolute error of each of the energy commodity's simulated value is shown in columns 4, 8, 12, 16, respectively.

The following graphs exhibit the simulation using the LLGMM approach for natural gas, crude oil, coal and ethanol data with an initial time delay $r = 10$:

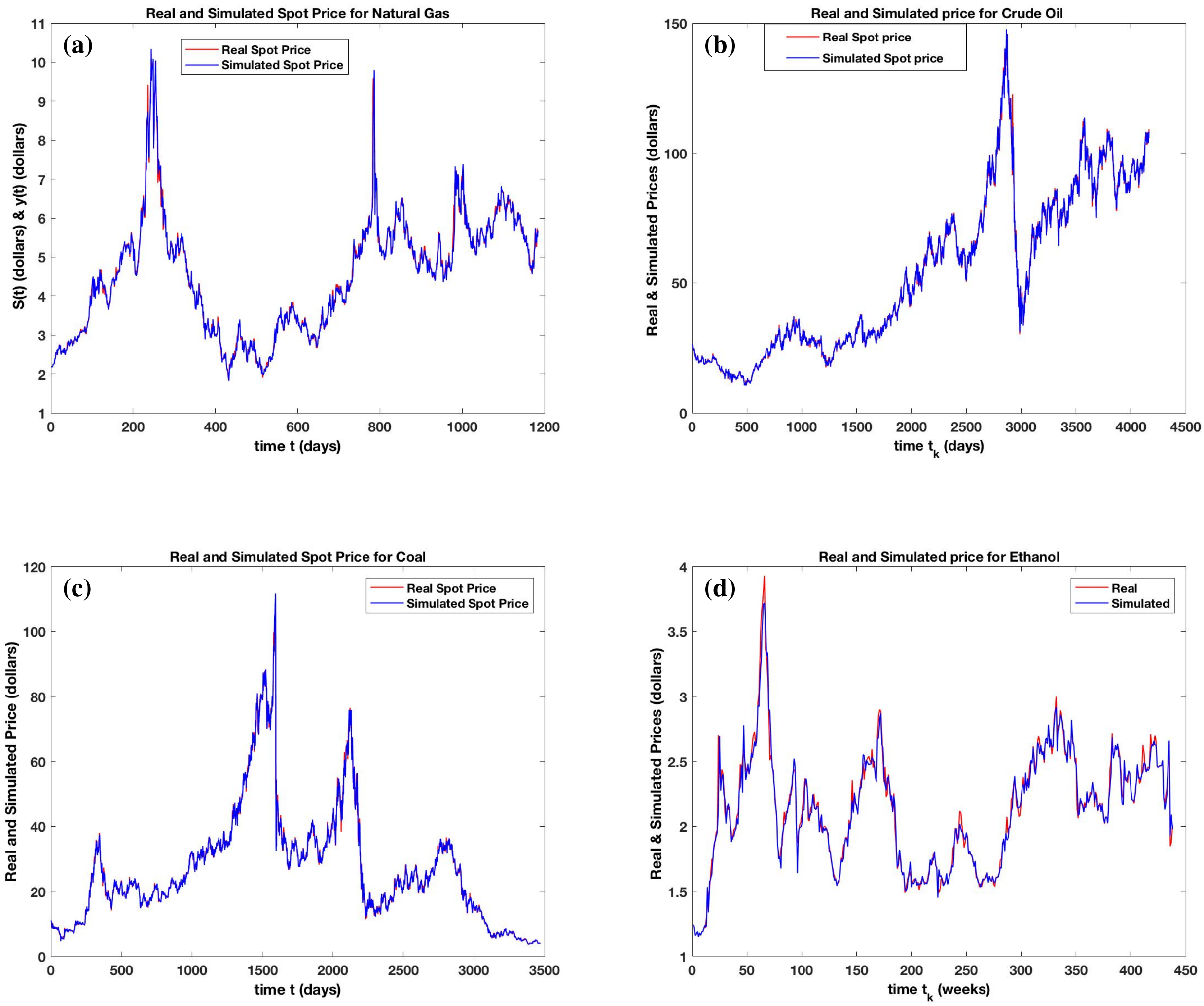

Figure 5: Real and Simulated Prices for initial delay $r = 10$.

Figures 5: **(a), (b), (c) and (d)** show the graphs of the real and simulated spot prices for the daily Henry Hub natural gas data [14], daily crude oil data [13], daily coal data [12], and weekly ethanol data [48], respectively using $r = 10$. The red line represents the real data y_k while the blue line represent the simulated value $y^s_{\hat{m}_k,k}$. The root mean square error of the simulation for the natural gas, crude oil, coal and ethanol data are given by 0.1004, 0.5401, 0.8879 and 0.0618, respectively.

Graphical, Simulation and Statistical Results-Case 3: Again, we pick $r = 20$, $\Delta t = 1$, $\epsilon = 0.001$, and $p = 2$, the $\epsilon-$ best sub-optimal estimates of parameters a, μ and σ^2 at each real data times are recorded in *Appendix A*.2, Table *A*.15. In *Appendix A*.2, Table *A*.16, the real and the LLGMM simulated price values of natural gas, crude oil, coal and ethanol are exhibited in columns 2-3, 6-7, 10-11, and 14-15, respectively. The absolute error of each of the energy commodity's simulated value is shown in columns 4, 8, 12, 16, respectively. The following graphs exhibit the simulation using the LLGMM method for natural gas, crude oil, coal and ethanol data with an initial discrete-time delay $r = 20$:

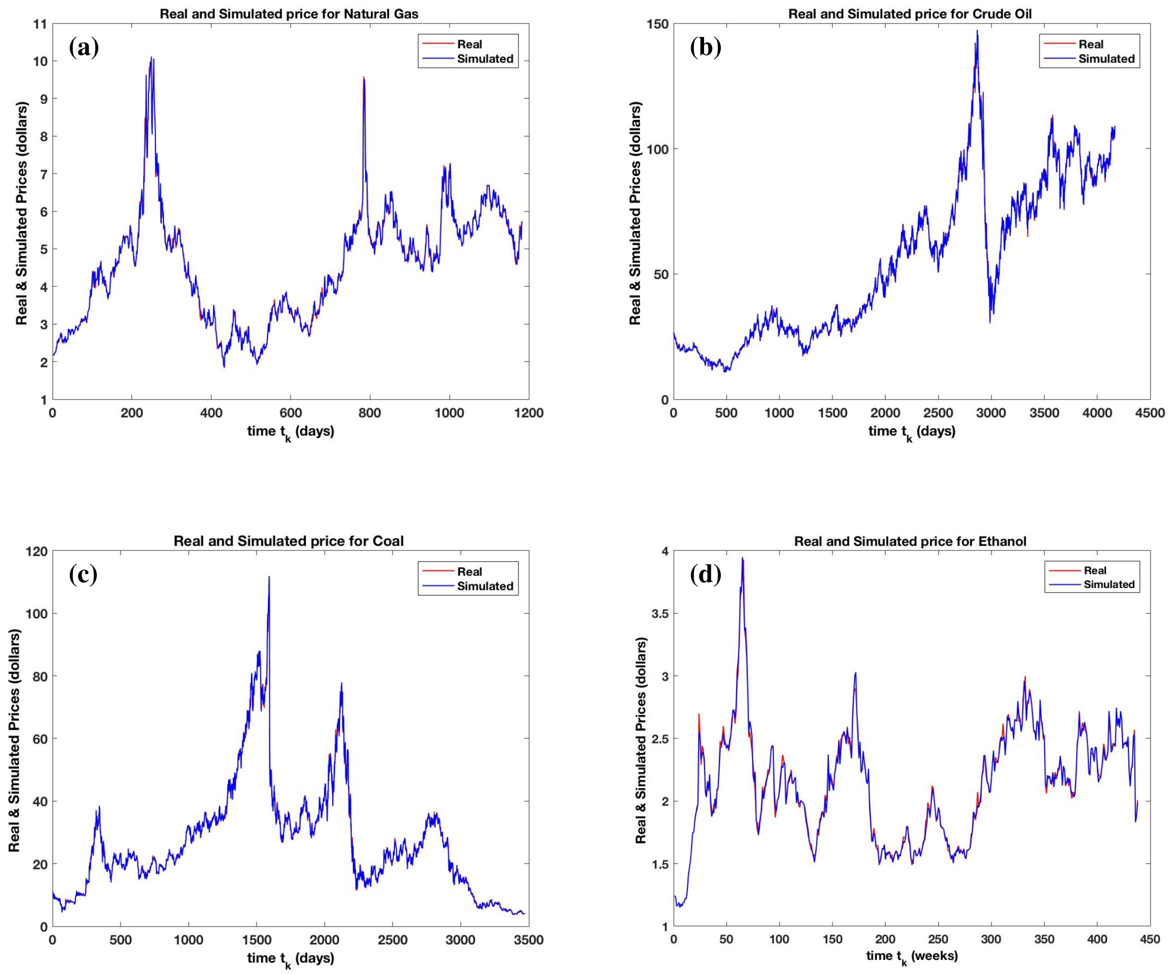

Figure 6: Real and Simulated Prices for initial delay $r = 20$.

Figures 6: **(a), (b), (c) and (d)** for $r = 20$ show the graphs of the real and simulated spot prices for the daily Henry Hub natural gas data [14], daily crude oil data [13], daily coal data [12], and weekly ethanol data [48], respectively. The red line represents the real data y_k while the blue line represent the simulated value $y^s_{\hat{m}_k,k}$.

Goodness-of-fit Measures: We find the goodness-of-fit measures for four energy commodities: natural gas, crude oil, coal and ethanol. This is achieved by using the goodness-of-fit measures described in [11]:

$$\begin{cases} \widehat{RAMSE} & = \left[\frac{1}{N}\sum\limits_{t=1}^{N}\frac{1}{S}\sum\limits_{s=1}^{S}\left(y_t^{(s)}-y_t\right)^2\right]^{\frac{1}{2}}, \\ \widehat{AMAD} & = \frac{1}{N}\sum\limits_{t=1}^{N}\operatorname*{median}_{s}\left(|y_t^s-\operatorname*{median}_{l}\left(y_t^l\right)|\right), \\ \widehat{AMB} & = \frac{1}{N}\sum\limits_{t=1}^{N}\left(|\operatorname*{median}_{s}\left(y_t^s\right)-y_t|\right), \end{cases} \tag{4.2}$$

where $\left\{y_t^{(s)}\right\}_{t=1,2,...,N}^{s=1,2,...,S}$ is a double sequence of simulated values at the data collected/observed time $t = 1, 2, ..., N$; $\widehat{RAMSE}$ is the root mean square error of the simulated path, $\widehat{AMAD}$ measures the variability and $\widehat{AMB}$ measures the average median bias. The goodness-of-fit measures are computed using $S = 100$ pseudo-data sets. The comparison of the goodness-of-fit measures $\widehat{RAMSE}$, $\widehat{AMAD}$ and $\widehat{AMB}$ for the four energy commodities are recorded in Table 4.

Remark 4.3. As the $\widehat{RAMSE}$ decreases, the state estimates approach the true value of the state. As the value of $\widehat{AMAD}$ increases, the influence of the random environmental fluctuations on the state dynamic process increases. In addition, if the value of $\widehat{RAMSE}$ decreases and the value of $\widehat{AMAD}$ increases, then the method of study possesses a greater degree of ability for state and parameter estimation accuracy and greater degree of ability to measure the variability of random environmental perturbations on the state dynamic of system. Moreover, as the $\widehat{RAMSE}$ decreases, $\widehat{AMAD}$ increases and the $\widehat{AMB}$ decreases, the method of study increases its performance under the three goodness of fit measures in a coherent way. On the other hand, as the $\widehat{RAMSE}$ increases, the state estimates tend to move away from the true value of the state. As the value of $\widehat{AMAD}$ decreases, the influence of the random environmental fluctuations on state dynamic process decreases. In addition, if the value of $\widehat{RAMSE}$ increases and the value of $\widehat{AMAD}$ decreases, then the method of study possesses a lesser degree of ability for state and parameter estimation accuracy and lesser degree of ability to measure the variability of random environmental perturbations on the state dynamic of system. Moreover, as the $\widehat{RAMSE}$ increases, $\widehat{AMAD}$ decreases and the $\widehat{AMB}$ increases, the method of study decreases its performance under the three goodness-of-fit measures in a coherent manner.

The Comparison of Goodness-of-fit Measures: The following table exhibits the Goodness-of-fit Measures for the energy commodities natural data, crude oil, coal, and ethanol data using the initial delays $r = 5$, $r = 10$, and $r = 20$.

Table 4: Goodness-of-fit Measures for the cases: $r = 5$, $r = 10$, and $r = 20$.

Goodness of-fit Measure	$r = 5$				$r = 10$				$r = 20$			
	Natural gas	**Crude oil**	**Coal**	**Ethanol**	**Natural gas**	**Crude oil**	**Coal**	**Ethanol**	**Natural gas**	**Crude oil**	**Coal**	**Ethanol**
$\widehat{RAMSE}$	**0.1801**	**1.1122**	**1.2235**	**0.1001**	**0.1004**	**0.5401**	**0.8879**	**0.0618**	**0.0674**	**0.4625**	**0.4794**	**0.0375**
$\widehat{AMAD}$	**1.1521**	**24.6476**	**9.4160**	**0.3409**	**1.1330**	**24.5376**	**9.4011**	**0.3233**	**1.1318**	**24.5010**	**9.4009**	**0.3213**
$\widehat{AMB}$	**1.1372**	**27.2707**	**12.8370**	**0.3566**	**1.1371**	**27.2708**	**12.8369**	**0.3566**	**1.1371**	**27.2707**	**12.8370**	**0.3566**

Remark 4.4. From Tables 3, $A.14$ and $A.16$, it is clear that as r increases the absolute error decreases. Furthermore, the comparison of the Goodness-of-fit measures in Table 4 for the energy commodities using the initial delays $r = 5$, $r = 10$, and $r = 20$ shows that as the delay r increases, the root mean square error decreases, significantly; $\widehat{AMAD}$, the average median absolute deviation decreases very slowly, and $\widehat{AMB}$, the average median bias remains unchanged.

Remark 4.5. All the codes for the parameter estimation, simulations and forecasting are written and tested using Matlab program. Due to the online control nature of m_k in our model, it is worth mentioning that the execution times for each of the four commodities depend on the robustness of the data.

4.2. Application to U.S. Treasury Bill Interest Rate and U.S.-U.K. Foreign Exchange Rate Data Sets:

In this subsection, we apply the conceptual computational algorithm discussed in Sections 3 and 4 to estimate the parameters in equation (2.20) in the context of the U.S. Treasury Bill interest rate (U.S. TBYIR) [44] and the U.S.-U.K. foreign exchange rate (U.S.-U.K. FER) [45] data collected on Forex database.

Graphical, Simulation and Statistical Results: Using $\epsilon = 0.001$, $r = 20$, and $p = 2$, the $\epsilon-$ best sub-optimal estimates of parameters β, μ, δ, σ and γ for each U.S. Treasury Bill and U.S.-U.K. Foreign Exchange rate data sets are exhibited in Tables 5 and 6, respectively.

Table 5: Estimates for $\hat{m}_k, \beta_{\hat{m}_k,k}, \mu_{\hat{m}_k,k}, \delta_{\hat{m}_k,k}, \sigma_{\hat{m}_k,k}, \gamma_{\hat{m}_k,k}$ for U.S. Treasury Bill interest rate data.

t_k	Interest Rate					
	$\hat{m}_k$	$\beta_{\hat{m}_k,k}$	$\mu_{\hat{m}_k,k}$	$\delta_{\hat{m}_k,k}$	$\sigma_{\hat{m}_k,k}$	$\gamma_{\hat{m}_k,k}$
21	2	1.5199	-7.0332	1.46	0.0446	0.9078
22	2	1.2748	-5.919	1.46	0.0941	1.5
23	10	2.9904	-13.928	1.46	0.0576	1.5
24	12	1.8604	-8.6515	1.46	0.0895	1.5
25	6	2.1606	-10.076	1.46	0.1064	1.5
26	20	0.0199	-0.0372	1.46	0.1097	1.3872
27	16	-0.0274	0.1991	1.46	0.1066	1.4348
28	4	-0.1841	0.9753	1.46	0.1345	1.2081
29	19	0.3261	-1.3952	1.46	0.1855	0.7006
30	12	0.2707	-1.1525	1.46	0.1624	1.4187
31	13	0.543	-2.4097	1.46	0.2571	1.4986
32	11	0.5357	-2.4098	1.46	0.1962	-0.0695
33	11	0.4723	-2.1258	1.46	0.3494	0.097
34	11	-0.3697	1.4705	1.46	1.4014	1.4983
35	4	-0.7862	3.3703	1.46	0.3488	1.4993
36	6	-0.3375	1.3041	1.46	0.2914	1.4711
37	5	0.3541	-2.0609	1.46	0.2676	1.4972
38	14	0.2368	-1.1239	1.46	0.3201	1.4961
39	8	1.1109	-5.5453	1.46	0.6811	-0.7462
40	4	1.9032	-9.1187	1.46	1.1055	0.1008
41	11	0.4364	-2.1327	1.46	0.3532	1.4994
42	4	0.2942	-1.3004	1.46	0.4885	1.4975
43	5	0.4012	-1.9198	1.46	0.3418	1.5
44	3	0.2605	-1.2108	1.46	0.4133	1.4705
45	5	0.4213	-2.0086	1.46	0.3324	1.4992
....	....	....	.....	....	....	.....
....	....	....	.....	....	....	.....
420	12	3.8416	-18.331	1.46	0.1187	1.4906
421	12	2.8918	-13.821	1.46	0.6961	1.386
422	12	0.5602	-2.6281	1.46	0.3759	1.1741
423	7	0.5825	-2.7201	1.46	0.1753	1.4935
424	7	0.7397	-3.4486	1.46	0.1687	0.5396
425	7	0.2488	-1.1148	1.46	0.1819	0.6161
426	7	0.8447	-3.9535	1.46	0.4182	0.7124
427	11	-0.2202	1.098	1.46	0.2013	0.6577
428	12	-0.1169	0.6256	1.46	0.1779	0.6063
429	9	0.1464	-0.6472	1.46	0.3672	1.2589
430	9	0.0343	-0.117	1.46	0.3637	0.7374
431	9	0.1785	-0.6832	1.46	0.1395	0.5804
432	19	-0.0031	0.1015	1.46	0.1932	1.1832
433	8	0.1651	-0.6463	1.46	0.1745	0.5374
434	19	0.4102	-1.6622	1.46	0.121	0.3774
435	8	0.2941	-1.1608	1.46	0.1085	1.0262
436	19	0.3694	-1.4911	1.46	0.1547	1.4945
437	14	1.6473	-6.6877	1.46	0.2198	-0.0071
438	5	1.417	-5.7323	1.46	0.1406	-0.1462
439	17	1.3024	-5.3352	1.46	0.133	0.2225
440	9	0.2839	-1.191	1.46	0.1929	0.0883
441	17	0.2053	-0.8785	1.46	0.2007	-0.1338
442	17	-0.4585	1.6754	1.46	0.4803	0.944
443	7	-0.2917	0.8858	1.46	0.5227	-0.236
444	9	-0.023	-0.2999	1.46	0.5836	-0.2083
445	13	-0.3263	1.2217	1.46	0.2632	-0.1684

Table 6: Estimates for $\hat{m}_k$, $\beta_{\hat{m}_k,k}$, $\mu_{\hat{m}_k,k}$, $\delta_{\hat{m}_k,k}$, $\sigma_{\hat{m}_k,k}$, $\gamma_{\hat{m}_k,k}$ for U.S.-U.K. Foreign Exchange Rate.

t_k	U.S.-U.K. Foreign Exchange Rate					
	$\hat{m}_k$	$\beta_{\hat{m}_k,k}$	$\mu_{\hat{m}_k,k}$	$\delta_{\hat{m}_k,k}$	$\sigma_{\hat{m}_k,k}$	$\gamma_{\hat{m}_k,k}$
21	2	-0.1282	0.1406	1.4892	0.0235	-1.4529
22	3	8.3385	-7.7988	1.4892	0.0256	1.4954
23	2	3.1279	-2.9205	1.4892	0.0286	1.4995
24	20	0.22	-0.1976	1.4892	0.0298	1.4948
25	18	3.0772	-2.8778	1.4892	0.016	1.4741
26	4	3.8605	-3.6034	1.4892	0.0147	1.3925
27	13	3.7355	-3.4973	1.4892	0.0395	1.4959
28	16	2.436	-2.2773	1.4892	0.0315	-0.7142
29	17	1.8545	-1.7299	1.4892	0.0159	-1.4613
30	3	6.4061	-5.9636	1.4892	0.0324	-2.4907
31	12	1.0648	-0.9689	1.4892	0.0242	1.47
32	15	0.4861	-0.4244	1.4892	0.0285	1.5
33	18	2.9505	-2.7502	1.4892	0.0267	1.4943
34	5	3.8981	-3.635	1.4892	0.0984	1.4807
35	4	0.4644	-0.4841	1.4892	0.1052	1.4884
36	3	0.753	-0.7159	1.4892	0.0474	1.4954
37	3	0.719	-0.682	1.4892	0.0472	1.4995
38	3	-0.7094	0.6544	1.4892	0.0482	1.4948
39	5	1.221	-1.1708	1.4892	0.0649	1.4741
40	9	6.7537	-6.4315	1.4892	0.0395	1.4959
41	9	1.0019	-0.9439	1.4892	0.0566	1.4962
42	11	5.5279	-5.2617	1.4892	0.0309	1.499
43	5	5.3829	-5.1253	1.4892	0.0529	0.1514
44	10	5.2433	-4.9934	1.4892	0.0483	0.8817
45	10	5.2445	-4.9945	1.4892	0.0305	1.3425
⋮	⋮	....	....	....	....	.....
155	2	10.779	-10.219	1.4892	0.0167	0.8188
156	14	2.4641	-2.3297	1.4892	0.0227	0.8437
157	4	3.2423	-3.0622	1.4892	0.0184	1.4906
158	6	3.1716	-3.0016	1.4892	0.0204	0.4736
159	7	6.2013	-5.8656	1.4892	0.0163	0.6027
160	8	9.3459	-8.8311	1.4892	0.0207	0.6834
161	4	5.3512	-5.0566	1.4892	0.027	0.4978
162	16	-1.3298	1.2689	1.4892	0.0289	0.3431
163	12	4.7287	-4.4662	1.4892	0.0206	1.2122
164	18	6.22	-5.8772	1.4892	0.0184	1.0666
165	19	13.13	-12.394	1.4892	0.021	1.4906
166	18	7.1076	-6.6994	1.4892	0.0211	1.386
167	5	3.2762	-3.0824	1.4892	0.0255	1.1741
168	11	3.0507	-2.8403	1.4892	0.0296	1.4935
169	10	0.9617	-0.8742	1.4892	0.0234	0.5396
170	19	2.0934	-1.9275	1.4892	0.027	0.6161
171	5	0.0174	-0.0078	1.4892	0.0275	0.7124
172	7	3.2551	-3.0304	1.4892	0.0244	0.6577
173	19	0.909	-0.8452	1.4892	0.0258	0.6063
174	19	0.8669	-0.807	1.4892	0.0219	1.2589
175	10	1.9332	-1.7976	1.4892	0.0189	0.7374
176	10	13.928	-12.966	1.4892	0.0235	0.5804
177	6	8.7675	-8.1583	1.4892	0.0232	1.1832
178	9	1.3481	-1.2544	1.4892	0.0198	0.5374
179	14	0.9565	-0.8852	1.4892	0.0232	0.3774
180	8	0.7656	-0.5372	1.4892	0.0132	0.2771

Tables 5 and 6 show the ϵ- best sub-optimal local admissible sample size $\hat{m}_k$ and the corresponding parameter estimates $\beta_{\hat{m}_k,k}$, $\mu_{\hat{m}_k,k}$, $\delta_{\hat{m}_k,k}$, $\sigma_{\hat{m}_k,k}$, and $\gamma_{\hat{m}_k,k}$ for the U.S. Treasury Bill interest rate (U.S.-TBYIR) and U.S.-U.K. foreign exchange rate (U.S.-U.K. FER) data at each time t_k, respectively. This is based on $p \leq r$, and the initial real data time-delay $r = 20$, that is, the data schedule time $t_r = t_{20}$. Furthermore, note that the range of the ϵ-best sub-optimal local admissible sample size for the U.S. TBYIR and U.S.-U.K. FER data for time $t_k \in [21, 45] \bigcup [420, 445]$ and $t_k \in [21, 45] \bigcup [155, 180]$, respectively, is $2 \leq \hat{m}_k \leq 20$. All comments (Remark 4.1) made with regard to Table 2 remains valid with regard to Tables 5 and 6 in the context of the U.S. Treasury Bill interest rate and the U.S.-U.K. foreign exchange rate data at time t_k and the LLGMM approach.

We show the graphs of $\beta_{\hat{m}_k,k}$, $\mu_{\hat{m}_k,k}$, $\delta_{\hat{m}_k,k}$, $\sigma_{\hat{m}_k,k}$, and $\gamma_{\hat{m}_k,k}$ for both monthly U.S. TBYIR and U.S.-U.K. FER.

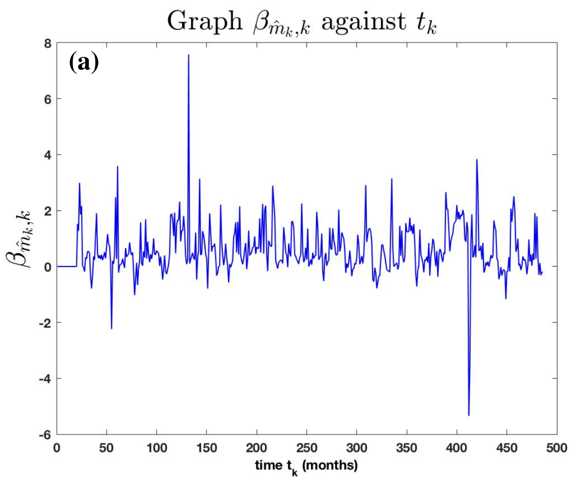

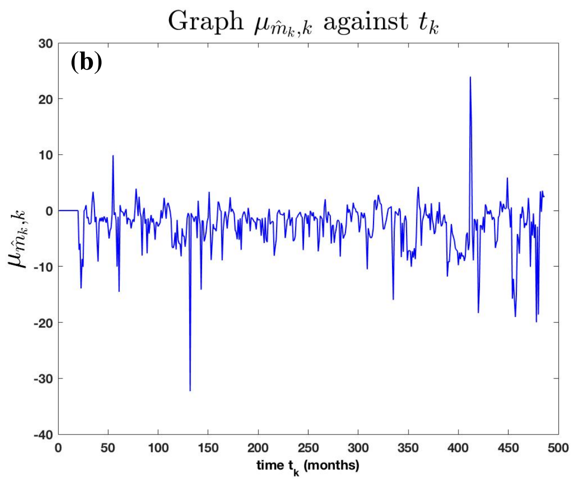

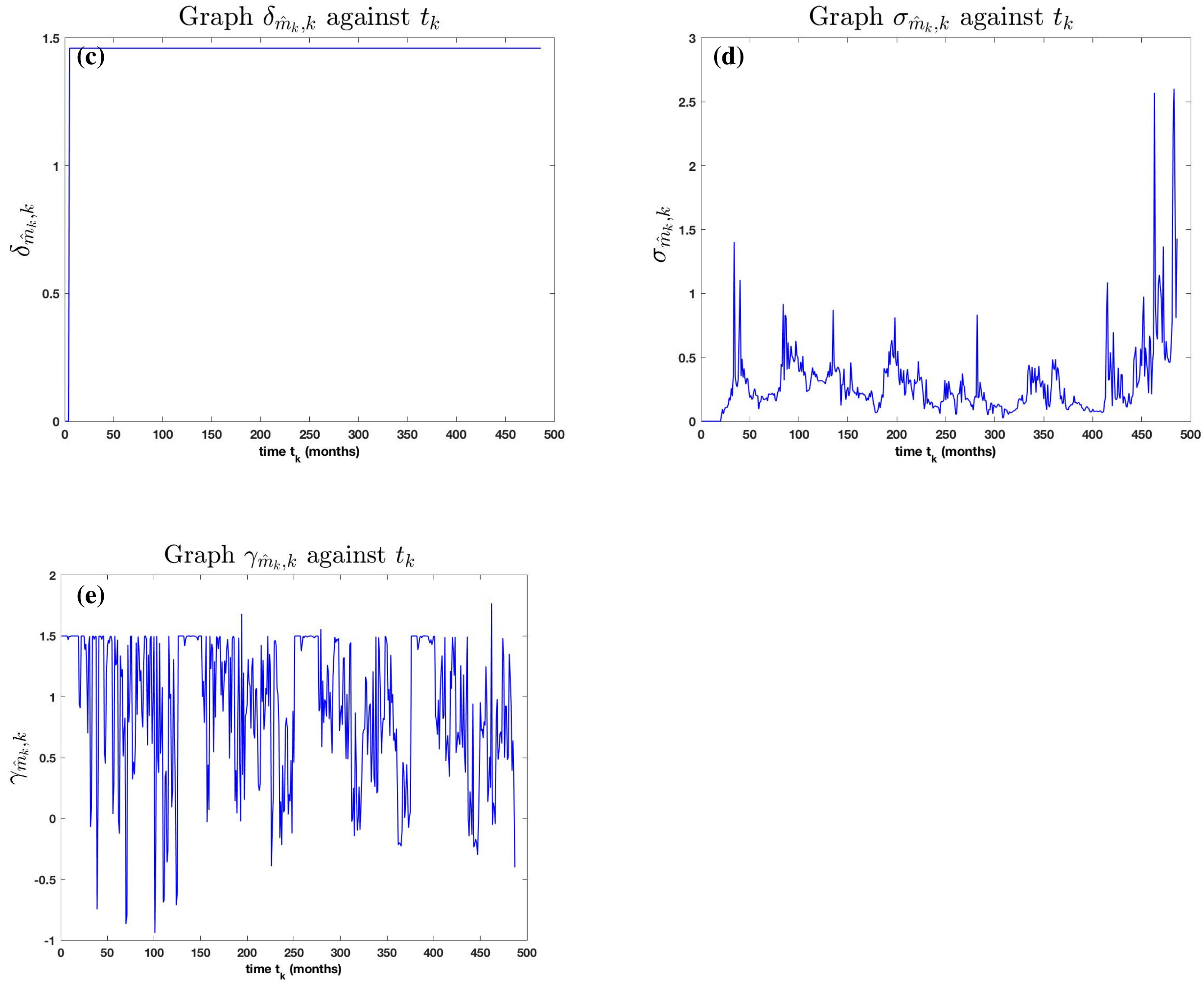

Figure 7: $\beta_{\hat{m}_k,k}$, $\mu_{\hat{m}_k,k}$, $\delta_{\hat{m}_k,k}$, $\sigma_{\hat{m}_k,k}$, and $\gamma_{\hat{m}_k,k}$ for U.S. TYBIR using $r = 20$.

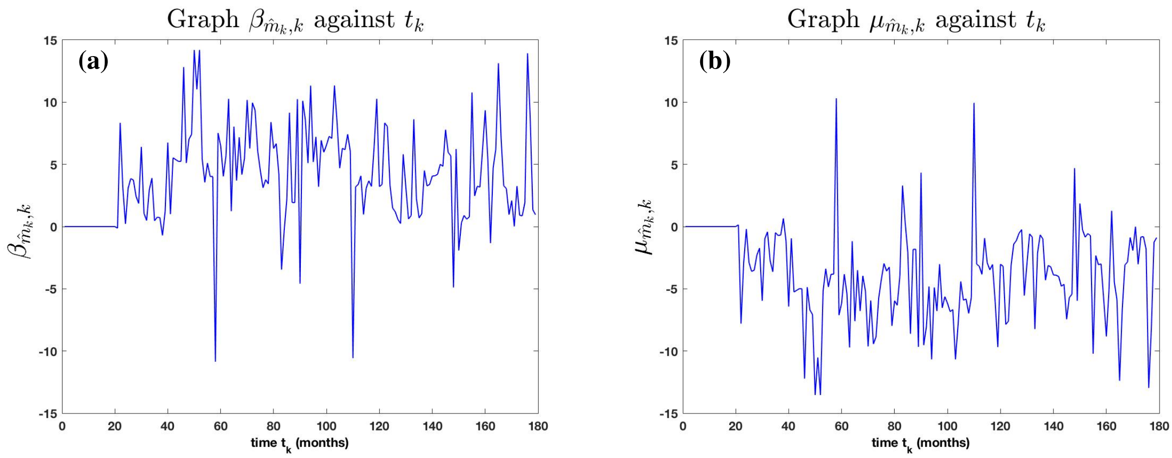

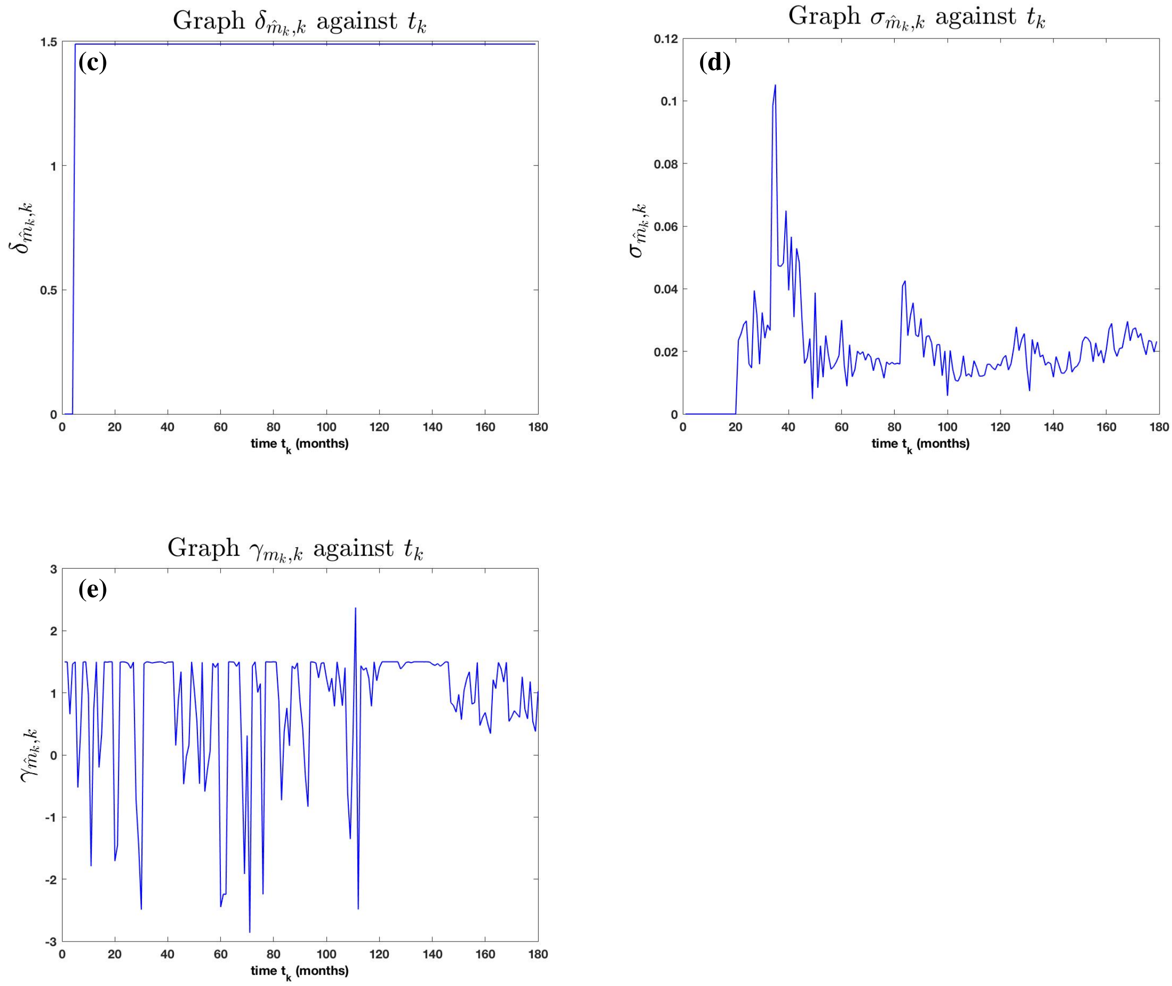

Figure 8: $\beta_{\hat{m_k},k}$, $\mu_{\hat{m_k},k}$, $\delta_{\hat{m_k},k}$, $\sigma_{\hat{m_k},k}$, and $\gamma_{\hat{m_k},k}$ for U.S.-U.K. FER using r = 20.

Figures 7-8: **(a), (b), (c), (d) and (e)** are graphs of parameters in model (2.20) for U.S. TYBIR and U.S.-U.K. FER, respectively.

The following graphs show simulated path for the U.S. Treasury Bill interest rate and U.S.-U.K. FER with r = 20.

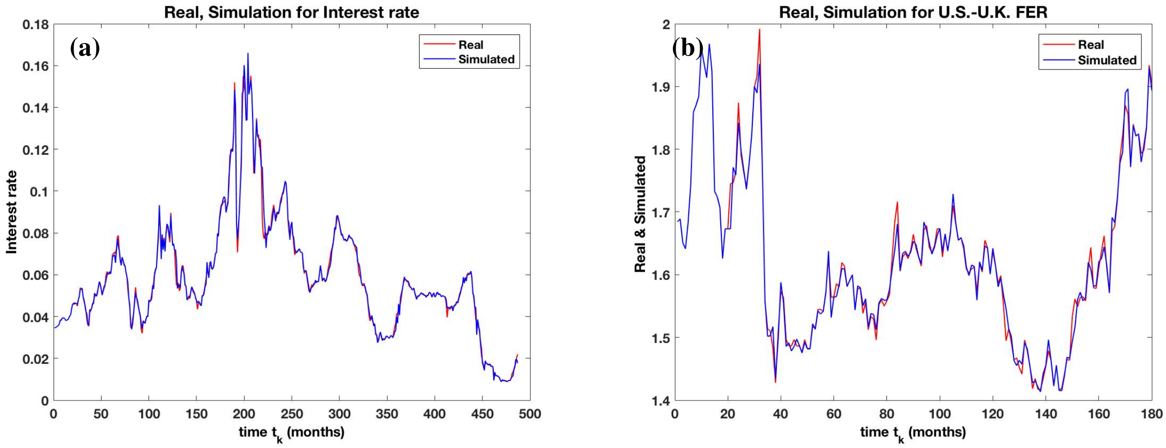

Figure 9: Real and Simulated value for Interest rate and U.S.-U.K. foreign exchange rate using $r = 20$.

Figures 9(a) and (b) show the real and simulated path for U.S. TBYIR and U.S.-U.K. FER, respectively.

Comparison of Goodness-of-fit Measures for U.S. TBYIR and U.S.-U.K. FER using $r = 20$: The following table compares the Goodness-of-fit Measures for the U.S. TBYIR and U.S.-U.K. FER data using $r = 20$.

Table 7: Goodness-of-fit Measures for the U.S. TBYIR and U.S.-U.K. FER data using $r = 20$.

Goodness of-fit Measure	$r = 20$	
	U.S. TBYIR	U.S.-U.K. FER
$\widehat{RAMSE}$	0.0024	0.0137
$\widehat{AMAD}$	0.0148	0.0718
$\widehat{AMB}$	0.0165	0.1033

5. Forecasting

In this section, we outline the application of the LLGMM approach to robust forecasting and the confidence interval problems. Moreover, this approach does not require a large data size as well as any type of stationary conditions [6]. First, we shall sketch an outline of the forecasting problem. The $\epsilon-$ best sub-optimal simulated value $y^s_{\hat{m}_k,k}$ at time t_k is used to define a forecast $y^f_{\hat{m}_k,k}$ for y_k at a lead time t_k for each of the energy commodity model, the U.S. TBYIR and U.S.-U.K. FER.

5.1. Forecasting for Energy Commodity Model

In the context of Illustration 1 (Section 2.6), we begin forecasting from a lead time t_k. Using the data up to time t_{k-1}, we compute $\hat{m}_i$, $\sigma^2_{\hat{m}_i,i}$, $a_{\hat{m}_i,i}$ and $\mu_{\hat{m}_i,i}$ for $i \in I_0(k-1)$. We assume that we have no information about the real data $\{y_i\}_{i=k}^{N}$. Under these considerations, imitating the computational procedure outlined in Sections 3 and 4 and using (2.18), we find the estimate of the forecast $y^f_{\hat{m}_k,k}$ at time t_k by employing the following discrete-time iterative process

$$y^f_{\hat{m}_k,k} = y^s_{\hat{m}_{k-1},k-1} + a_{\hat{m}_{k-1},k-1} y^s_{\hat{m}_{k-1},k-1}(\mu_{\hat{m}_{k-1},k-1} - y^s_{\hat{m}_{k-1},k-1})\Delta t + \sigma_{\hat{m}_{k-1},k-1} y^s_{\hat{m}_{k-1},k-1} \Delta W(t_k), \tag{5.1}$$

where the estimates $\sigma^2_{\hat{m}_{k-1},k-1}$, $a_{\hat{m}_{k-1},k-1}$ and $\mu_{\hat{m}_{k-1},k-1}$ are defined in (2.18) with respect to the known past data up to the time t_{k-1}. We note that $y^f_{\hat{m}_k,k}$ is the ϵ-sub-optimal estimate for y_k at time t_k .

To determine $y^f_{\hat{m}_{k+1},k+1}$, we need $\sigma^2_{\hat{m}_k,k}$, $a_{\hat{m}_k,k}$ and $\mu_{\hat{m}_k,k}$. Since we only have information of real data up to time t_{k-1}, we use the forecasted estimate $y^f_{\hat{m}_k,k}$ as the estimate of y_k at time t_k, and to estimate $\sigma^2_{\hat{m}_k,k}$, $a_{\hat{m}_k,k}$ and $\mu_{\hat{m}_k,k}$. Hence, we can write $a_{\hat{m}_k,k}$ as $a_{\hat{m}_k,k} \equiv a_{\hat{m}_k, y_{k-\hat{m}_k+1}, y_{k-\hat{m}_k+2}, \ldots, y_{k-1}, y^f_{m_k,k}}$. We can also re-write $\mu_{\hat{m}_k,k} \equiv \mu_{\hat{m}_k, y_{k-\hat{m}_k+1}, y_{k-\hat{m}_k+2}, \ldots, y_{k-1}, y^f_{\hat{m}_k,k}}$. To find $y^f_{\hat{m}_{k+2},k+2}$, we use the estimates $a_{\hat{m}_{k+1},k+1} \equiv a_{\hat{m}_{k+1}, y_{k-\hat{m}_k+2}, y_{k-\hat{m}_k+3}, \ldots, y_{k-1}, y^f_{\hat{m}_k,k}, y^f_{\hat{m}_{k+1},k+1}}$, $\mu_{\hat{m}_{k+1},k+1} \equiv \mu_{\hat{m}_{k+1}, y_{k-\hat{m}_k+2}, y_{k-\hat{m}_k+3}, \ldots, y_{k-1}, y^f_{\hat{m}_k,k}, y^f_{\hat{m}_{k+1},k+1}}$. Continuing this process in this manner (using principle of Mathematical Induction, [23]), we use the estimates $a_{\hat{m}_{k+i-1},k+i-1} \equiv a_{\hat{m}_{k+i-1}, y_{k-\hat{m}_k+i}, y_{k-\hat{m}_k+i+1}, \ldots, y_{k-1}, y^f_{\hat{m}_k,k}, y^f_{\hat{m}_{k+1},k+1}, \ldots, y^f_{\hat{m}_{k+1},k+i-1}}$, $\mu_{\hat{m}_{k+i-1},k+i-1} \equiv \mu_{\hat{m}_{k+i-1}, y_{k-\hat{m}_k+i}, y_{k-\hat{m}_k+i+1}, \ldots, y_{k-1}, y^f_{\hat{m}_k,k}, y^f_{\hat{m}_{k+1},k+1}, \ldots, y^f_{\hat{m}_{k+1},k+i-1}}$ to estimate $y^f_{\hat{m}_{k+i},k+i}$

5.2. Prediction/Confidence Interval for Energy Commodities

In order to be able to assess the future certainty, we also discuss the prediction/confidence interval. We define the $100(1-\alpha)\%$ confidence interval for the forecast of the state $y^f_{\hat{m}_i,i}$ at time t_i, $i \geq k$, as $y^f_{\hat{m}_i,i} \pm z_{1-\alpha/2}\left(s^2_{\hat{m}_{i-1},i-1}\right)^{1/2} y^f_{\hat{m}_{i-1},i-1}$, where $\left(s^2_{\hat{m}_{i-1},i-1}\right)^{1/2} y^f_{\hat{m}_{i-1},i-1}$ is the estimate for the sample standard deviation for the forecasted state derived from the following iterative process

$$y^f_{\hat{m}_k,k} = y^f_{\hat{m}_{k-1},k-1} + a_{\hat{m}_{k-1},k-1} y^f_{\hat{m}_{k-1},k-1}(\mu_{\hat{m}_{k-1},k-1} - y^f_{\hat{m}_{k-1},k-1})\Delta t + \sigma_{\hat{m}_{k-1},k-1} y^f_{\hat{m}_{k-1},k-1} \Delta W(t_k). \tag{5.2}$$

It is clear that the 95 % confidence interval for the forecast at time t_i is

$$\left(y^f_{\hat{m}_i,i} - 1.96\left(s^2_{\hat{m}_{i-1},i-1}\right)^{1/2} y^f_{\hat{m}_{i-1},i-1}, y^f_{\hat{m}_i,i} + 1.96\left(s^2_{\hat{m}_{i-1},i-1}\right)^{1/2} y^f_{\hat{m}_{i-1},i-1}\right)$$

where the lower and upper end of the interval denotes the lower and upper bound of the state estimate, respectively.

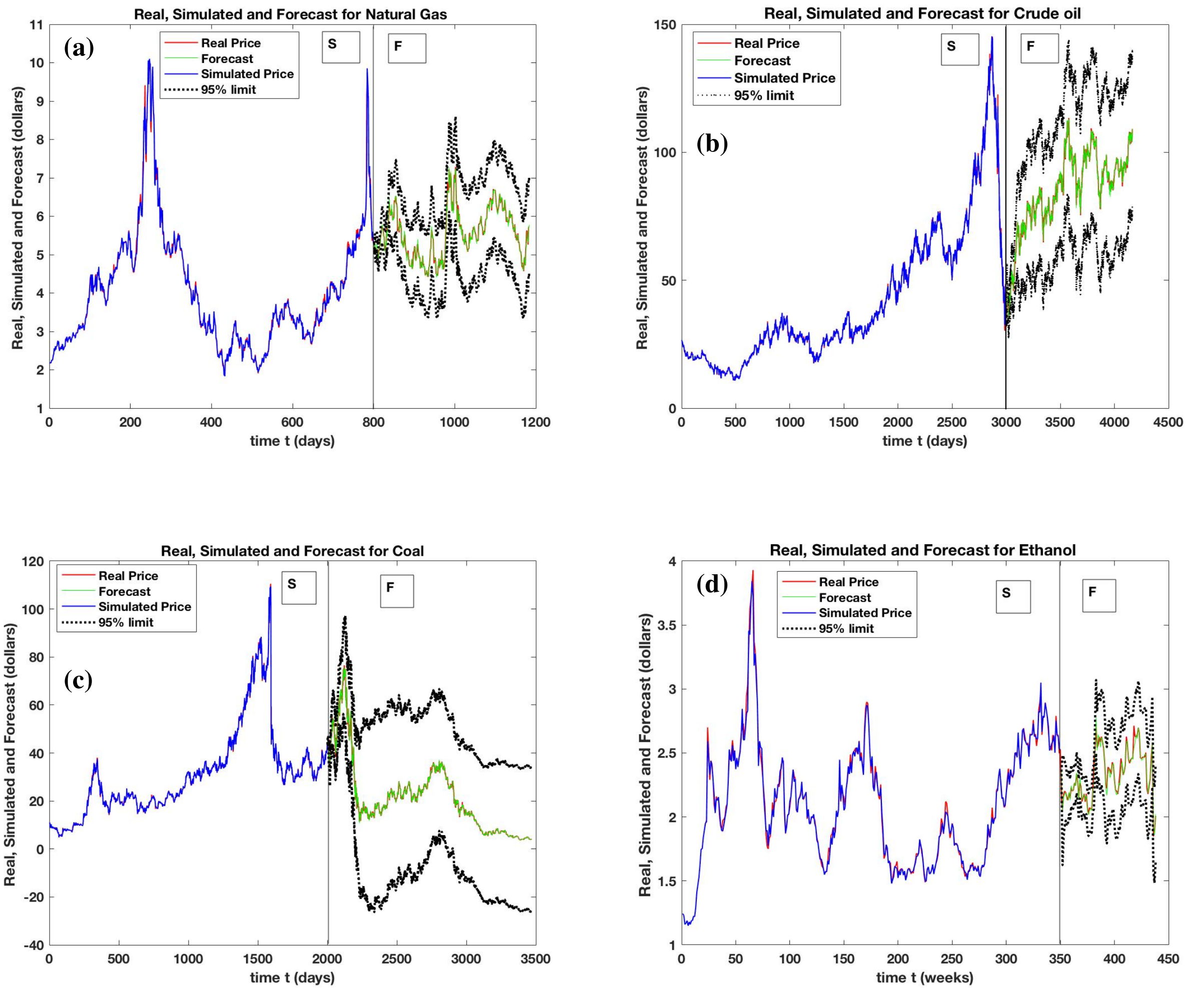

Figure 10: Real, Simulated and Forecasted values using initial delay $r = 20$.

Figures 10: **(a), (b), (c) and (d)** show the graphs of the forecast and 95% confidence limit for the daily Henry Hub natural gas [14], daily crude oil [13], daily coal [12], and weekly ethanol data [48], respectively. Moreover, Figure 10: **(a)**, **(b)**, **(c)** and **(d)** show two regions: the simulation region S and the forecast region F. For the simulation region S, we plot the real price data in red color and the simulated price data in blue color. For the forecast region F, we plot the real price in red color, the forecast price in green and the 95% confidence estimate of the forecast (as explained in Section 5.1) in black dots. The upper and lower simulated sketches in Figures 10 **(a), (b), (c) and (d)** corresponds to the upper and lower ends of the 95% confidence interval, respectively.

5.2.1. Sample forecasting error for energy commodities: $r = 20$

In this subsection, utilizing the procedure described in Subsection 5.1, we consider ten samples of forecast for each four energy commodities for each lead time greater than or equal to corresponding initial lead times. We draw scattered plots of deviations of the ten sample forecasts from corresponding real and 95% forecast price for each lead time. These plots would exhibit the degree of stability and reliability of LLGMM approach. In addition, it would shed a light on the behavior of long-range forecasting. For the four energy commodities, namely, natural gas, crude oil, coal and ethanol, we choose the following initial lead-time forecast times and the lead-time domains as: 08/01/2004 to 12/13/2004 for natural gas, from lead time 06/03/2008 to 08/12/2008 for crude oil, from lead time 10/28/2013 to 01/08/2014 for coal and from lead time 10/03/2013 to 09/11/2014 for ethanol data.

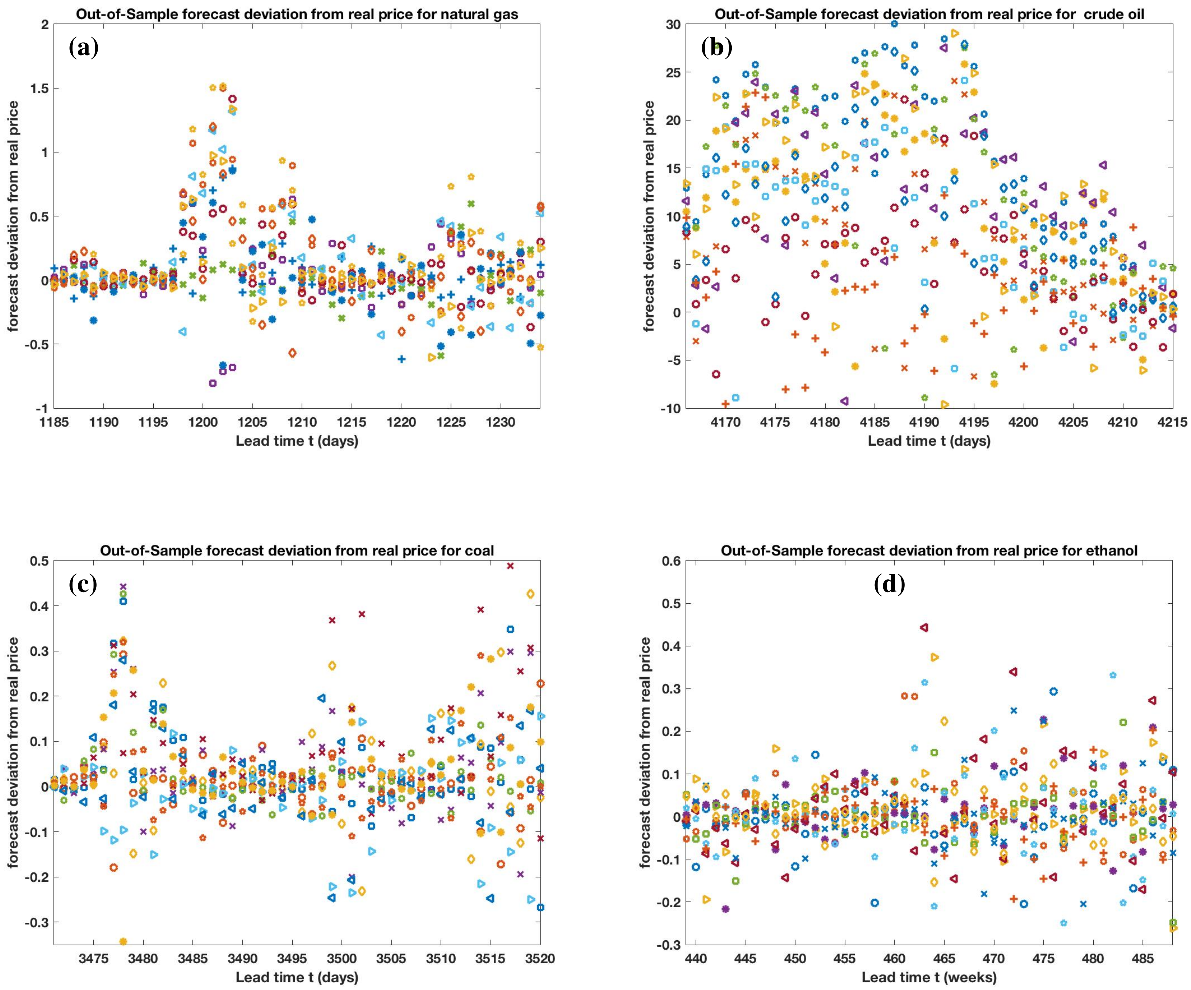

Figure 11: Out-Of-Sample Forecast deviation from future price for energy commodities using $r = 20$.

Figures 11 **(a), (b), (c) and (d)** exhibit scattered plots of 10 out-of-sample forecast errors/deviation from real/future price for the daily Henry Hub natural gas, daily crude oil, daily coal, and weekly ethanol data with lead times 08/01/2004, 06/03/2008, 10/28/2013 and 10/03/2013, respectively. The 10 scattered sample error points for each lead time are identified by blue, red, orange, purple circles ($\circ$), dots ($\bullet$), triangles ($\triangleright$ and $\triangleleft$), diamond ($\diamond$), mark (x). It is easily noticeable that at least 8/9 are within one unit absolute deviations with 70-80% lead time domain.

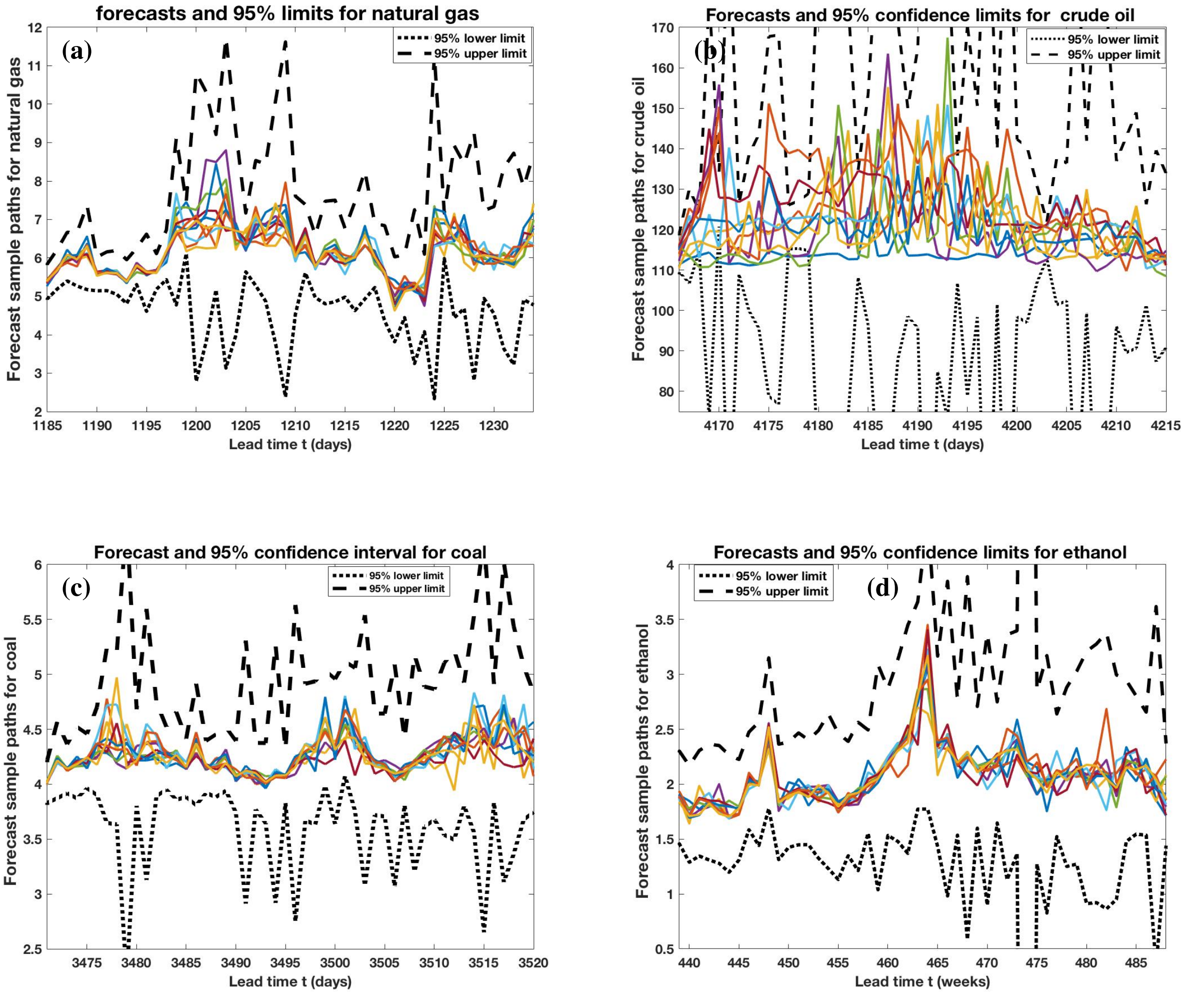

Figure 12: Ten samples forecast and 95% confidence forecast with bounds for energy commodities using $r = 20$.

Figures 12 **(a), (b), (c) and (d)** show the 95% confidence and 10 forecast sample path trajectories coupled with 95% confidence upper and lower sample bound trajectories for the daily Henry Hub natural gas, daily crude oil, daily coal, and weekly ethanol data with lead times 08/01/2004, 06/03/2008, 10/28/2013 and 10/03/2013, respectively. 10 sample and the 95% sample forecasts are represented by black, blue, red, etc. colors. It is obvious that all 11 sample forecast paths are within the 95% upper and lower bounds. In short, the 95% confidence interval is robust with respect to a sample of 10 forecast realizations. 95% interval estimate is highly reliable and stable in the sense of longer lead times.

5.2.2. Sensitivity of forecast estimates to perturbations in model parameters for energy commodity: $r = 20$

In this subsection, we demonstrate the influence of the state dynamic parametric variations with respect to a nominal forecasting dynamic process (5.1) for each of the four energy commodities. We introduce random parametric perturbations in the ϵ-sub-optimal parameters $a_{\hat{m}_k,k}$, $\mu_{\hat{m}_k,k}$ and $\sigma_{\hat{m}_k,k}$ as follows

$$a_{\hat{m}_k,k,\nu_1} \equiv a_{\hat{m}_k,k} = a_{\hat{m}_k,k} + \nu_1 e_1, \quad \mu_{\hat{m}_k,k,\nu_2} \equiv \mu_{\hat{m}_k,k} = \mu_{\hat{m}_k,k} + \nu_2 e_2, \tag{5.3}$$

where e_i, $i = 1, 2, 3$ are independent standard normal random variables and ν_i, $i = 1, 2, 3$ characterize the magnitudes (noise intensities) of the random fluctuations. A dynamic process corresponding to the ϵ-sub-optimal parameters $a_{\hat{m}_k,k}$ and $\mu_{\hat{m}_k,k}$ is referred as nominal price dynamic process of (5.1) or (5.2). A price dynamic process corresponding to parameters described in (5.3) is referred to perturbation of (5.1) or (5.2). This, together with (5.1)-(5.2) are now used to estimate the forecast value.

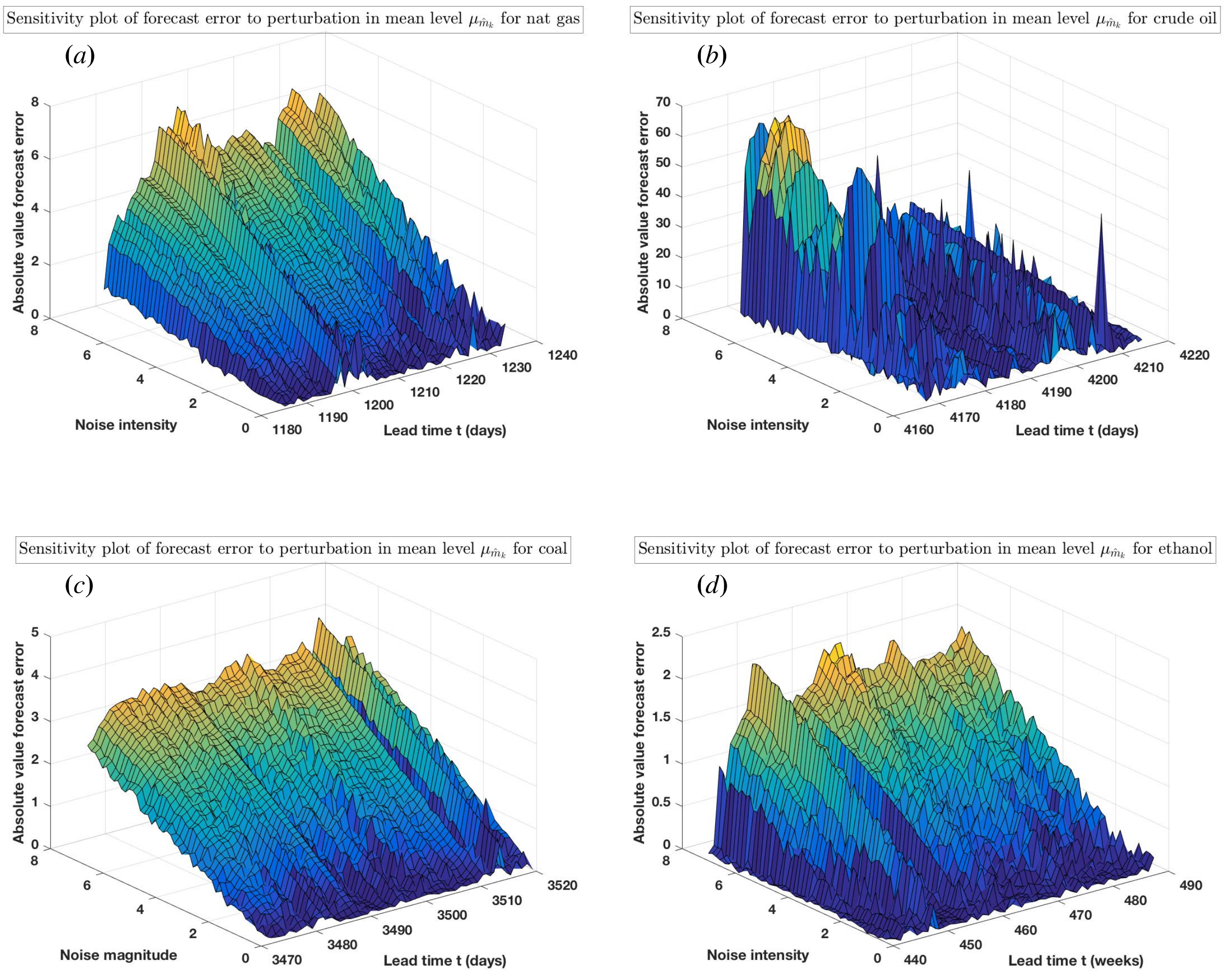

Figure 13: Forecast error sensitivity analysis of the mean level nominal parameter $\mu_{\hat{m}_k,k,\nu_2}$ using initial delay $r = 20$.

Figures 13 **(a), (b), (c) and (d)** exhibit the absolute value of the sample forecast error/deviation of parametric perturbation in the mean level $\mu_{\hat{m}_k,k,\nu_2}$ from the corresponding nominal parameter (the ϵ-sub-optimal parameters $\mu_{\hat{m}_k,k}$) for the natural gas, crude oil, coal and ethanol data, respectively. These plots show how the absolute value of the sample forecast error changes with respect to the sample nominal forecast and noise intensity introduced in the mean level $\mu_{\hat{m}_k,k,\nu_2}$ as described in (5.3) for each energy commodity. The lead time for each forecast is the same as that presented in Subsubsection 5.2.1. It is clear from the sample path trajectories' plots that as the noise intensity in the mean level parameter $\mu_{\hat{m}_k,k,\nu_2}$ increases, the color of the graph changes from blue to yellow. Here, a dark blue color represents region with very low absolute value of the error; a light blue error represents region with low error; a light yellow color represents region with high magnitude error and a dark yellow color represents regions with very high error.

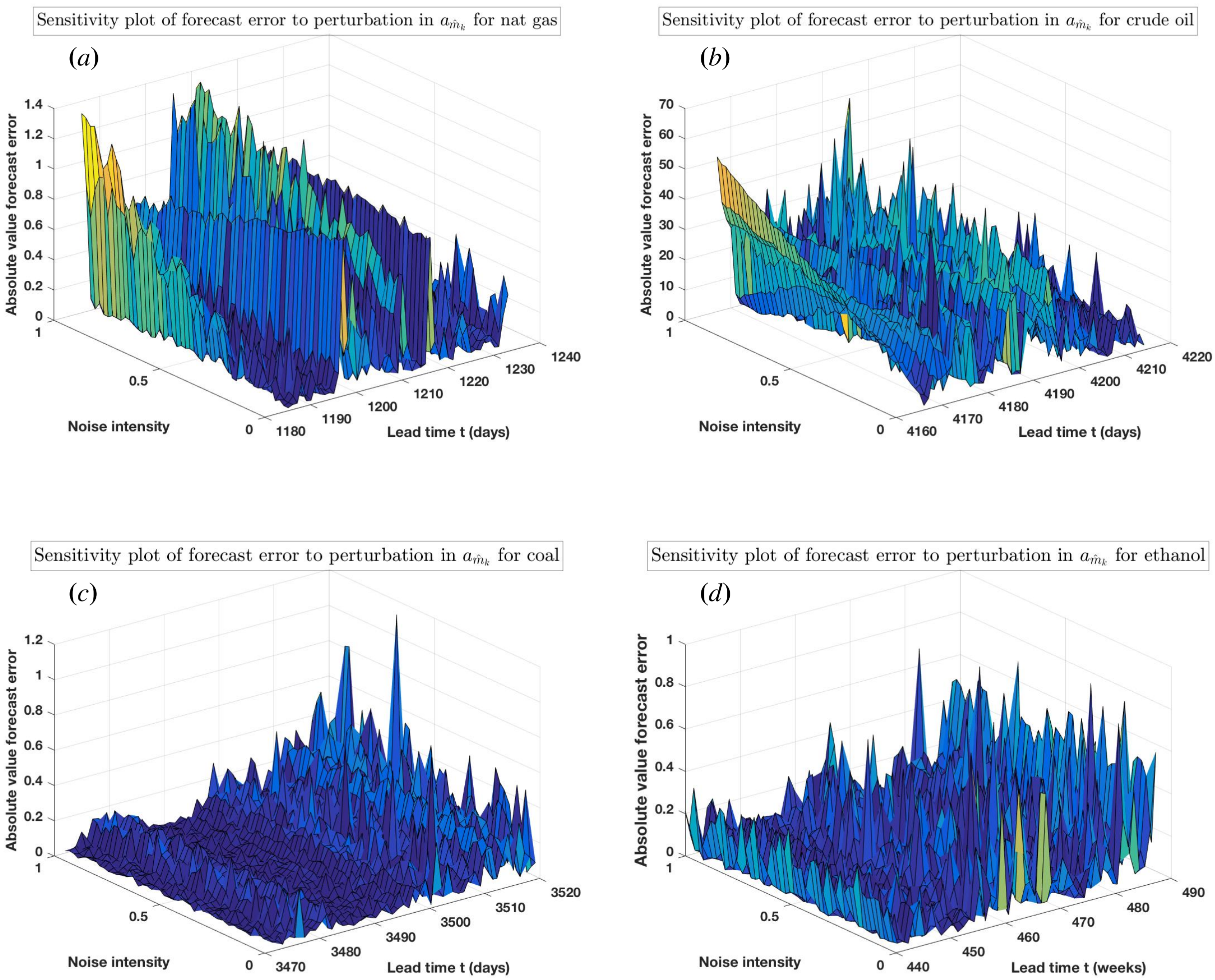

Figure 14: Forecast error sensitivity analysis in the mean reverting rate $a_{\hat{m}_k,k,\nu_1}$ (the nominal parameter) using initial delay $r = 20$.

Figures 14 (a), (b), (c) **and** (d) show the sensitivity of the energy commodity price out-of-sample-forecast error to perturbation in the mean reverting rate $a_{\hat{m}_k,k,\nu_1}$ for the natural gas, crude oil, coal and ethanol data, respectively. By definition, the mean reverting rate, $a_{\hat{m}_k,k,\nu_1}$, is the rate by which price shocks dissipate and the variable reverts towards the mean. They show how the out-of-sample-forecast error changes with respect to out-of-sample-time and noise intensity introduced in the mean reverting rate $a_{\hat{m}_k,k,\nu_1}$ as described in (5.3) for each energy commodity.

5.3. *Prediction/Confidence Interval for U.S. Treasury Bill Interest Rate and U.S.-U.K. Foreign Exchange Rate*

Following the procedure presented in Section 5.1, we show the graph of the real, simulated, forecast and 95 % confidence limit (with respect to (2.20)) for the U.S. TBYIR and U.S.-U.K. FER for the initial delay $r = 20$.

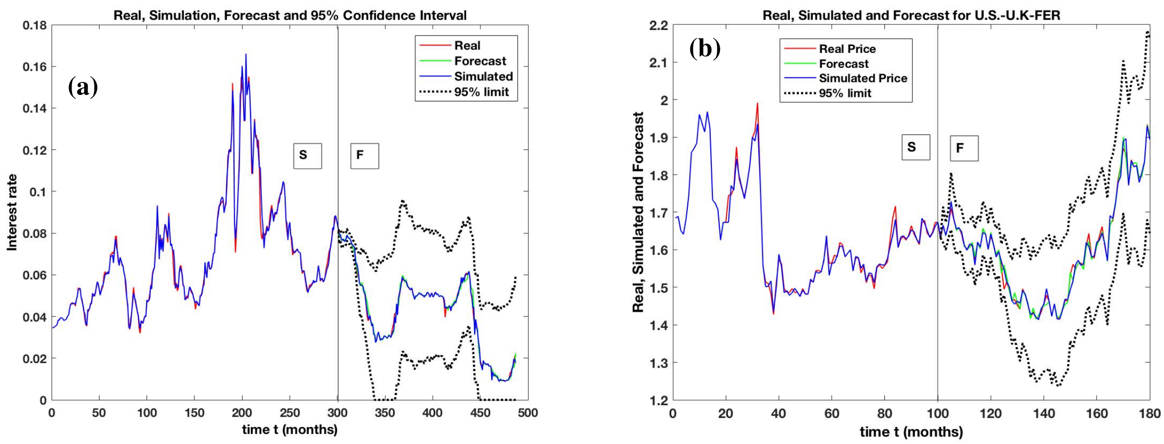

Figure 15: Real, Simulated, Forecast and 95% Confidence Limit for U.S. TBYIR and U.S.-U.K.-FER Data.

Figure 15(a) shows the real, simulated, forecast and 95% confidence limit for the Interest rate data and Figure 15(b) shows the real, simulated, forecast and 95% confidence level for the U.S.-U.K. FER.

5.3.1. *Sensitivity of forecast estimates to perturbations in model parameters for USTBYIR and U.S.-U.K. FER:* $r = 20$

Similar to the approach discussed in Subsection 5.2.2, we give the sensitivity of forecast estimates to perturbation plot for the U.S. Treasury Bill Interest Rate and U.S.-U.K. FER.

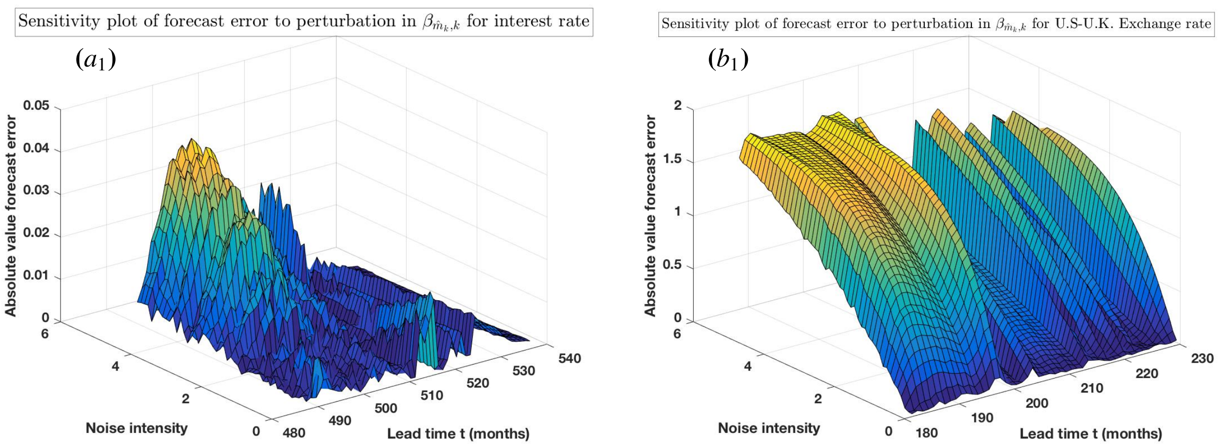

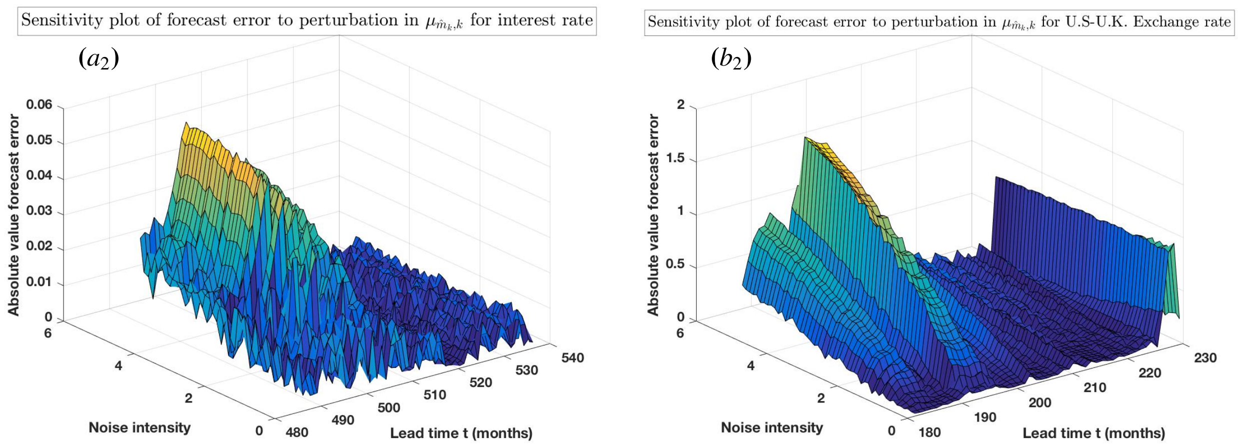

Figure 16: Forecast error sensitivity analysis in $\beta_{\hat{m}_k,k}$ and $\mu_{\hat{m}_k,k}$ (the nominal parameter) for USTBYIR: $r = 20$.

Figures 16 (a_1) **and** (b_1) show both the sensitivity analysis of the absolute value of sample forecast errors corresponding to the perturbed and nominal parameter $\beta_{\hat{m}_k,k}$ for the U.S. Treasury Bill interest rate and the U.S.-U.K.-FER, respectively. Figures 16 (a_2) **and** (b_2) show both the sensitivity analysis of the absolute value of sample forecast errors corresponding to the perturbed and nominal parameter $\mu_{\hat{m}_k,k}$ for the U.S. Treasury Bill interest rate and the U.S.-U.K.-FER, respectively.

6. The byproduct of the LLGMM approach

The second component, DTIDMLSMVSP (2.16) of the LLGMM [30] in Section 2 plays role: (a) to initiate ideas for the usage of discrete-time interconnected dynamic approach parallel to the continuous-time dynamic process, (b) to speed-up the computation time, (c) to significantly reduce the state error estimates, and also (d) as an alternative approach to the GARCH(1,1) model [4, 5] as well as comparable results with ex post volatility results of Chan et al [9]. Furthermore, LLGMM directly generates (Remark 2.5, Section 3) a GMM based method. In this section, we briefly discuss these comparison in the context of four energy commodity, U.S. TBYIR and U.S.-U.K. FER data.

6.1. Comparison between DTIDMLSMVSP and GARCH Model

In this subsection, we briefly compare the applications of DTIDMLSMVSP (2.16) and GARCH in the context of four energy commodities. We compare the estimates $s^2_{\hat{m}_k,k}$ with the estimate derived from the usage of a GARCH(1,1) model described in [4] and defined by

$$\begin{aligned} z_t|\mathcal{F}_{t-1} &\sim \mathcal{N}(0, h_t), \\ h_t &= \alpha_0 + \alpha_1 h_{t-1} + \beta_1 z^2_{t-1}, \ \ \alpha_0 > 0, \ \alpha_1, \beta_1 \geq 0. \end{aligned} \tag{6.1}$$

The parameters α_0, α_1, and β_1 of the GARCH(1,1) conditional variance model (6.1) for the four commodities natural gas, crude oil, coal, and ethanol are estimated. The estimates of the parameters are given in Table 8 below.

Table 8: Parameter estimates for GARCH(1,1) Model (6.1).

Data Set	α_0	α_1	β_1
Natural Gas	6.863×10^{-5}	0.853	0.112
Crude Oil	9.622×10^{-5}	0.917	0.069
Coal	3.023×10^{-5}	0.903	0.081
Ethanol	4.152×10^{-4}	0.815	0.019

We later show a side by side comparison of $s^2_{\hat{m}_k,k}$ [30] and the volatility described by GARCH(1,1) model (6.1) with coefficients in Table 8.

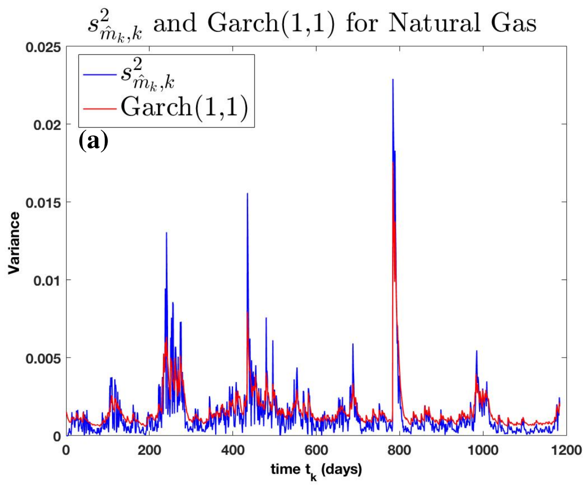

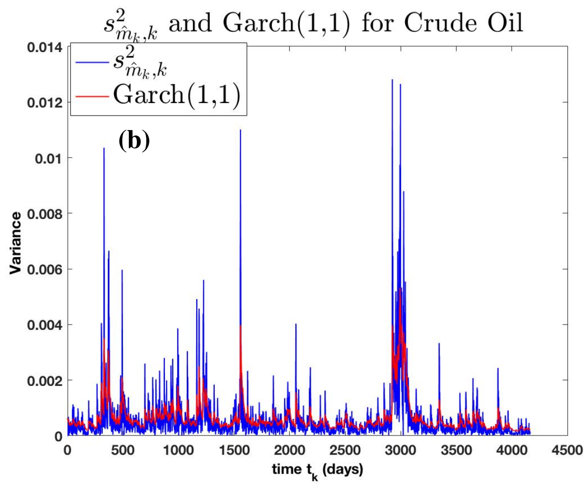

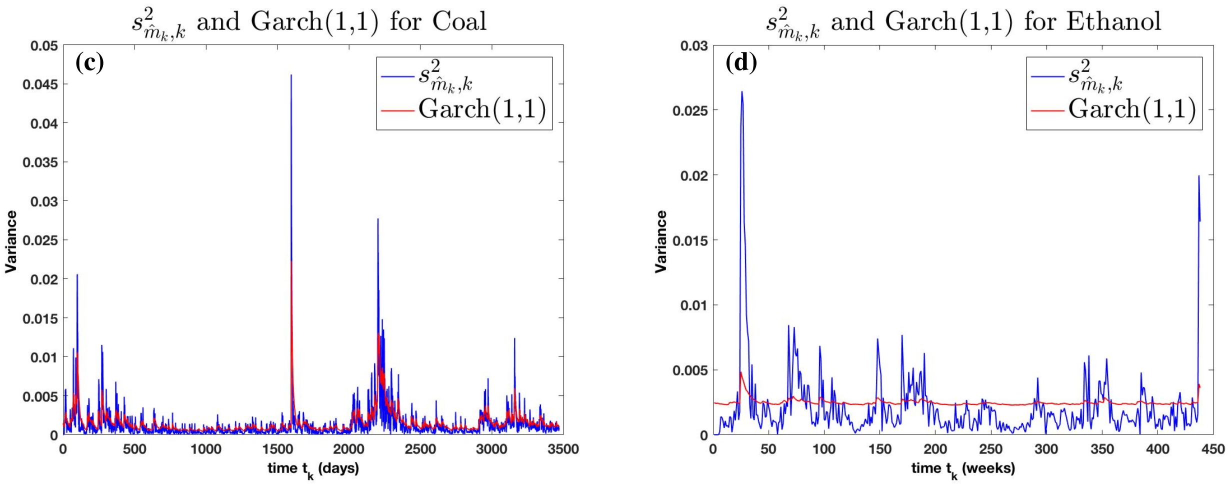

Figure 17: $s^2_{\hat{m}_k,k}$ and GARCH(1,1) .

Figure 17: **(a), (b), (c)** and **(d)** show comparison of the volatility graphs using $s^2_{\hat{m}_k,k}$ and GARCH(1,1) model (6.1) for the daily Henry Hub natural gas [14], daily crude oil [13], daily coal [12] and weekly ethanol data [48], respectively. The blue and red lines show the graphs of estimates using $s^2_{\hat{m}_k,k}$ and GARCH(1,1) model, respectively. The GARCH model does not estimate volatility as heavily evidenced in Figure 17 **(d)**. In fact, it demonstrated insensitivity.

We also compare Figure 4 with simulations using the GARCH(1,1) model (6.1) as the conditional variance below.

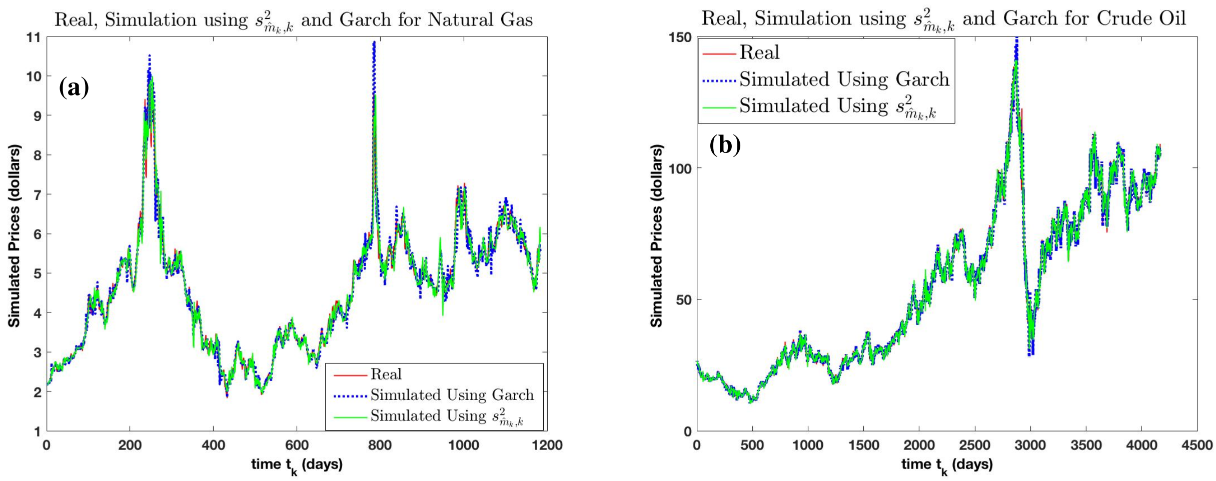

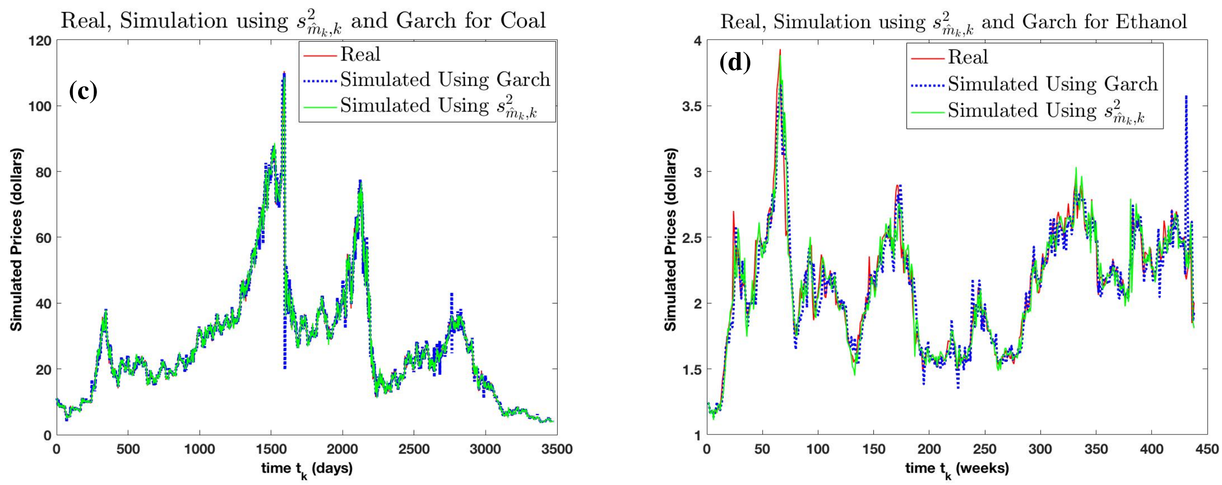

Figure 18: Simulation derived by using $s^2_{\hat{m}_k,k}$ and GARCH(1,1)

Figure 18: **(a), (b), (c) and (d)** are graphs of the simulations using $s^2_{\hat{m}_k,k}$ and GARCH(1,1) model (6.1) to estimate the volatility process for the daily Henry Hub natural gas [14] , daily crude oil [13], daily coal [12], and weekly ethanol data [48], respectively. The blue dotted line shows the graph of estimates for the simulations using GARCH(1,1) model to simulate the volatility, the green dotted line is simulated estimates described in Figure 4, and the red line shows the real data. It can be seen that the GARCH model fails to capture most of the spikes in the data. Moreover, the GARCH model creates significant errors by over-and-under estimating the variance. These spikes were perfectly captured in Figure 4 where we use the discrete-time dynamic model of local sample variance statistics process [30] to estimate the volatility process described by GARCH (1,1) model (6.1). This illustrates the significance of dynamic statistic model (2.16) (Lemma 2.1of [30]) that performs better than the GARCH (1,1) volatility model.

6.2. *Comparison of DTIDMLSMVSP [30] with the work of Chan et al [9]:*

In this subsection, using the U.S. TBYIR and U.S.-U.K. FER data, the comparison between the DTIDMLSMVSP and ex post volatility of Chan et al [9] is made.

According to the work of Chan et al [9], we define the ex post volatility by the absolute value of the change in U.S. TBYIR data. Likewise, we define simulated volatility by the square root of the conditional variance implied by the estimates of the model (2.20). Using (2.20), we calculate our simulated volatility as $\sigma_{\hat{m}_k,k}\left(y^s_{\hat{m}_k,k}\right)^{\delta_{\hat{m}_k,k}}$. Figure 19 below shows the comparison between ex post volatility and simulated volatility. We compare our result with the result of Chan et al [9] and conclude that our method performs better than their method.

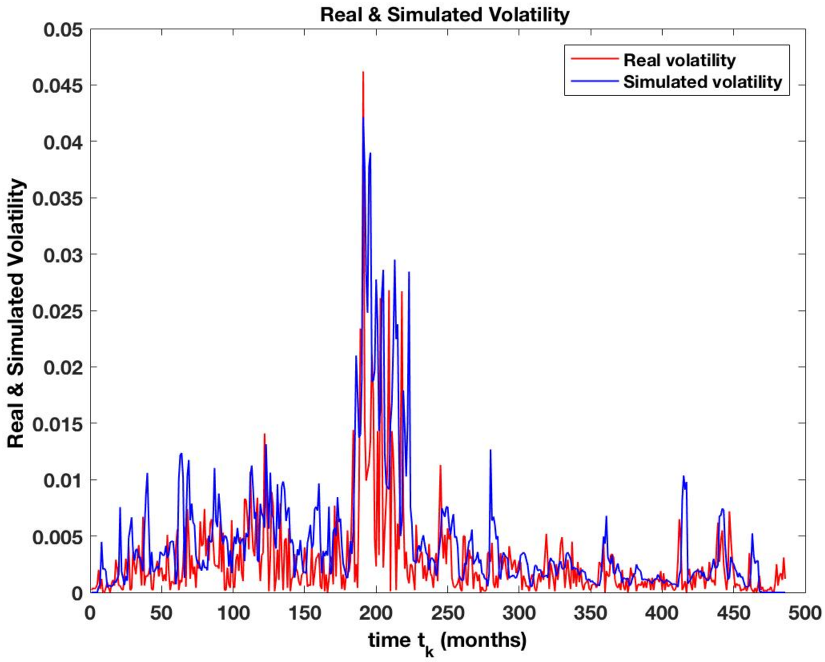

Figure 19: Ex Post Volatility and Simulated Volatility for Interest Rate.

Figure 19 shows the Ex post volatility and simulated volatility for the U.S. Treasury Bill interest rate data [44]. We compare our work in Figure 19 (using DTIDMLSMVSP [30]) with Figure 1 of Chan et al [9]. Their model does not clearly estimate the volatility. It demonstrated insensitivity in the sense that it was unable to capture most of the spikes in the interest rate ex post volatility data.

7. Comparisons of LLGMM with Existing and Newly Developed OCBGMM

In this Section, we briefly compare LLGMM and OCBGMM in the frame-work of the conceptual, computational, mathematical and statistical results coupled with role, scope and applications. For this purpose, to better appreciate and understand the comparative work, we utilize the state and parameter estimation problems for the stochastic dynamic model of interest rate that has been studied extensively [9, 11] in the frame-work of orthogonality condition vector based generalized method of moments (OCBGMM). We recall that the LLGMM approach is based on seven interactive components (Section 1). On the other hand, the existing OCBGMM (GMM [9] and IRGMM [11]) approach and its extensions are based on five components (Section 3, [30]). We further remark that the basis for the formation of orthogonality condition parameter vectors (OCPV) in the LLGMM (Section 3) and OCBGMM (GMM/IRGMM) are different. In fact, in the existing OCBGMM (GMM/IRGMM [9, 11]), the orthogonality condition vectors are formed on the basis of algebraic manipulation coupled with econometric specification-based discretization scheme

(OCPV-Algebraic) rather than stochastic calculus and a continuous-time stochastic dynamic model independent based (OCPV-Analytic). This motivates to extend a couple of OCBGMM-based state and parameter estimation methods.

In this section, using the stochastic calculus based formation of the OCPV-Analytic in the context of the continuous-time stochastic dynamic model (Section 2), we develop two new OCBGMM based methods for the state and parameter estimation problems. The proposed OCBGMM methods are direct extensions of the existing OCBGMM method and its extension IRGMM [9, 11] in the context of the OCPV. Because of this difference and for the sake of comparison, the newly developed OCBGMM and the existing OCBGMM methods are referred to as the OCBGMM-Analytic and OCBGMM-Algebraic, respectively. In particular, the GMM [9] and IRGMM [11] with OCPV-algebraic are denoted as GMM-Algebraic and IRGMM-Algebraic and corresponding extensions under the OCPV-Analytic as GMM-Analytic and IRGMM-Analytic, respectively. Furthermore, using LLGMM based method, the aggregated generalized method of moments (AGMM) (2.19) introduced in Subsection 2.6 and described in *Appendix B* is also compared along with the above stated methods, namely, GMM-Algebraic, GMM-Analytic, IRGMM-Algebraic, and IRGMM-Analytic.

A comparative analysis of the results of GMM-Algebraic, GMM-Analytic, IRGMM-Algebraic, IRGMM-Analytic and Aggregated Generalized Method of Moment (AGMM) methods with the LLGMM for the state and parameter estimation problems of the interest rate and energy commodities stochastic dynamic models are briefly outlined in *Appendix B*, *Appendix C*.2, and *Appendix D*. First, based on the material in Sections 1, 2, and 3, we briefly summarize the comparison between the LLGMM and OCBGMM methods.

7.1. Theoretical Comparison Between LLGMM and OCBGMM

Based on the foundations of the analytical, conceptual, computational, mathematical, practical, statistical and theoretical motivations in the context of the material in Sections 2, 3, 4, 5 and 6, we summarize the comparison between the applications of innovative LLGMM [30] approach with the existing and newly developed LLGMM based OCBGMM methods. The comparative results are presented in tables in *Appendix C* in a systematic manner.

7.2. Comparisons of LLGMM and existing methods: Stochastic Interest rate model

The continuous-time interest rate process is described by a nonlinear Itô-Doob-type stochastic differential equation:

$$dy = (\alpha + \beta y)dt + \sigma y^{\gamma} dW(t). \tag{7.1}$$

An energy commodity stochastic dynamic model described in (2.8) in Subsection 2.6 is a modified generalized version of (7.1). These models would be utilized to further compare the role, scope and merit of the LLGMM and

OCBGMM methods in the frame-work of the graphical, computational and statistical results and its applications to forecasting and prediction with certain degree of confidence.

Remark 7.1. The continuous-time interest rate model (7.1) was chosen so that we can compare our LLGMM method with OCBGMM method described in [9] and [11]. Our proposed model for the continuous-time interest rate model is described in (2.20). We will later compare the results derived using model (7.1) with the results using (2.20) in Subsections 2.7 and 4.2.

In order to fulfil the objectives of the comparison, we need to construct the necessary tools outlined in Section 2.

Descriptive Statistic for Time-series Data Set: First, we consider one-month risk free rates from the Monthly Interest rate data sets for the period of June 30, 1964 to December 31, 2004.

Table 9: Statistics for the interest rate data for June 30, 1964 to December 31, 2004

Variable	N	Mean	Std dev	ρ_1	ρ_2	ρ_3	ρ_4	ρ_5	ρ_6
y_t	487	0.0592	0.0276	0.9809	0.9508	0.9234	0.8994	0.8764	0.8519
Δy_t	486	-0.00003	0.0050	0.3305	-0.0919	-0.1048	-0.0351	0.0403	-0.1877

Mean, standard deviations, and autocorrelations of monthly U.S. Treasury Bill interest rate data. ρ_j denotes the autocorrelation coefficient of order j, N represents the total number of observations used in this study.

The Orthogonality Condition Vector for (7.1)**:** In the following, we first present the orthogonality condition parameter vectors (OCPV) for the GMM-Algebraic, GMM-Analytic, IRGMM-Algebraic, and IRGMM-Analytic methods. These orthogonality vectors are then used for the state and parameter estimation problems. For this, we need to follow the procedure (Section 2) for obtaining the analytic orthogonality condition parameter vector (OCPV-Analytic).

We consider the Lyapunov functions $V_1(t, y) = \frac{1}{2}y^2$ and $V_2(t, y) = \frac{1}{3}y^3$. The Itô differentials of V_1 and V_2 with respect to (7.1) are:

$$\begin{cases} d\left(\frac{1}{2}y^2\right) &= \left[\alpha y + \beta y^2 + \frac{1}{2}\sigma^2 y^{2\gamma}\right] dt + \sigma y^{\gamma+1} dW(t) \\ d\left(\frac{1}{3}y^3\right) &= \left[\alpha y^2 + \beta y^3) + \sigma^2 y^{2\gamma+1}\right] dt + \sigma y^{\gamma+2} dW(t). \end{cases} \tag{7.2}$$

The components of orthogonality condition vector (OCPV-Analytic) are listed below:

$$\begin{cases} \Delta y_t - (\mathbb{E}\left[y_t|\mathcal{F}_{t-1}\right] - y_{t-1}) \\ \frac{1}{2}\Delta\left(y_t^2\right) - \frac{1}{2}\left(\mathbb{E}\left[y_t^2|\mathcal{F}_{t-1}\right] - y_{t-1}^2\right) \\ \frac{1}{3}\Delta\left(y_t^3\right) - \frac{1}{3}\left(\mathbb{E}\left[y_t^3|\mathcal{F}_{t-1}\right] - y_{t-1}^3\right) \\ \mathbb{E}\left[(\Delta y_t - \mathbb{E}\left[\Delta y_t|\mathcal{F}_{t-1}\right])^2 |\mathcal{F}_{t-1}\right] - \sigma^2 y_{t-1}^{2\gamma}\Delta t, \end{cases} \tag{7.3}$$

where

$$\begin{cases} \mathbb{E}\left[y_t|\mathcal{F}_{t-1}\right] - y_{t-1} & = & (\alpha+\beta y)\Delta t \\ \frac{1}{2}\left(\mathbb{E}\left[y_t^2|\mathcal{F}_{t-1}\right] - y_{t-1}^2\right) & = & \left[\alpha y_{t-1} + \beta y_{t-1}^2 + \frac{1}{2}\sigma^2 y_{t-1}^{2\gamma}\right]\Delta t \\ \frac{1}{3}\left(\mathbb{E}\left[y_t^3|\mathcal{F}_{t-1}\right] - y_{t-1}^3\right) & = & \left[\alpha y_{t-1}^2 + \beta y_{t-1}^3 + \sigma^2 y_{t-1}^{2\gamma+1}\right]\Delta t \\ \mathbb{E}\left[\left(\Delta y_t - \mathbb{E}\left[\Delta y_t|\mathcal{F}_{t-1}\right]\right)^2|\mathcal{F}_{t-1}\right] & = & \sigma^2 y_{t-1}^{2\gamma}\Delta t. \end{cases} \tag{7.4}$$

On the other hand, using discrete-time econometric specifications coupled with algebraic manipulations, the components of orthogonality condition parameter vector (OCPV-Algebraic) [9, 18, 30] are as follows:

$$\begin{cases} y_t - y_{t-1} - (\alpha+\beta y)\Delta t \\ y_{t-1}\left(y_t - y_{t-1} - (\alpha+\beta y)\Delta t\right) \\ \left(y_t - y_{t-1} - (\alpha+\beta y)\Delta t\right)^2 - \sigma^2 y_{t-1}^{2\gamma} \\ y_{t-1}\left[\left(y_t - y_{t-1} - (\alpha+\beta y)\Delta t\right)^2 - \sigma^2 y_{t-1}^{2\gamma}\right] \end{cases} \tag{7.5}$$

Now, we are ready to apply the GMM-Algebraic, IRGMM-Algebraic, GMM-Analytic and IRGMM-Analytic methods.

Parameter Estimates of (7.1) **using LLGMM and OCBGMM Methods:** Following the construction in Remark 2.5, we define the average $\bar{\alpha}, \bar{\beta}, \bar{\sigma}$, and $\bar{\gamma}$ by

$$\left\{ \bar{\alpha} = \frac{1}{N}\sum_{k=1}^{N}\alpha_{\hat{m}_k,k}, \quad \bar{\beta} = \frac{1}{N}\sum_{k=1}^{N}\beta_{\hat{m}_k,k}, \quad \bar{\sigma} = \frac{1}{N}\sum_{k=1}^{N}\sigma_{\hat{m}_k,k}, \quad \bar{\gamma} = \frac{1}{N}\sum_{k=1}^{N}\gamma_{\hat{m}_k,k}, \right. \tag{7.6}$$

where the parameters $\alpha_{\hat{m}_k,k}$, $\beta_{\hat{m}_k,k}$, $\sigma_{\hat{m}_k,k}$, and $\gamma_{\hat{m}_k,k}$ are estimated in Table $C.27$ at time t_k using LLGMM method. Imitating the argument used in *Appendix B*, the parameters and state are also estimated. These parameter estimates are recorded in the row of AGMM approach in Table 10.

We also estimate the parameters in (7.1) by following the computational procedure described in [9] and applying it to both the GMM-algebraic and GMM-analytic frame-work. Similarly, following the computational procedure described in [11], the parameter estimates in (7.1) are determined under the IRGMM-algebraic and IRGMM-analytic approaches. These parameter estimates are recorded in rows of GMM-algebraic, GMM-analytic, IRGMM-algebraic and IRGMM-analytic approaches, respectively, in Table 10.

Comparison of Goodness-of-fit Measures: In order to statistically compare the different estimation techniques, we estimate the statistics $\widehat{RAMSE}$, $\widehat{AMAD}$, and $\widehat{AMB}$ defined in (4.2).

The goodness-of-fit measures are computed using $S = 100$ pseudo-data sets of the same sample size, and the real data set, $N = 487$ months. The $t-$statistics of each parameter estimate is in parenthesis in Table 10, the smallest value of $\widehat{RAMSE}$ for all method is italicized. The goodness-of-fit measures $\widehat{RAMSE}$, $\widehat{AMAD}$ and $\widehat{AMB}$ are recorded under the columns 6, 7, and 8, respectively.

Table 10: Comparison of Parameter estimates of model (7.1) and the goodness-of-fit measures $\widehat{RAMSE}$, $\widehat{AMAD}$ and $\widehat{AMB}$ using GMM-Algebraic, GMM-Analytic, IRGMM-Algebraic, IRGMM-Analytic, AGMM and LLGMM methods.

Method	α	β	σ	γ	$\widehat{RAMSE}$	$\widehat{AMAD}$	$\widehat{AMB}$
GMM-Algebraic	0.0017	-0.0308	0.4032	1.5309	0.0424	0.0098	0.0195
	(1.53)	(-1.33)	(1.55)	(3.21)			
GMM-Analytic	0.0009	-0.0153	0.0184	0.4981	0.0315	0.0161	0.0190
	(1.06)	(-0.90)	(1.25)	(1.73)			
IRGMM-Algebraic	0.0020	-0.0410	0.207	1.3031	0.03186	0.00843	0.01972
	(0.32)	(-0.21)	(0.25)	(1.02)			
IRGMM-Analytic	0.0084	-0.1436	0.1075	1.3592	0.0278	0.0028	0.01968
	(0.44)	(-0.40)	(0.22)	(1.01)			
AGMM	0.0084	-0.1436	0.1075	1.3592	0.0288	0.0047	0.0207
	(0.41)	(-0.33)	(0.25)	(0.98)			
LLGMM					*0.0027**	0.0146	0.0178

Table 10 shows a comparison of parameter estimates of model (7.1) and the goodness-of-fit measures $\widehat{RAMSE}$, $\widehat{AMAD}$ and $\widehat{AMB}$ under the usage of GMM-Algebraic, GMM-Analytic, IRGMM-Algebraic, IRGMM-Analytic, AGMM and LLGMM methods. The LLGMM estimates are derived using initial discrete-time delay $r = 20$, $p = 2$ and $\epsilon = 0.001$. Among these stated methods, the LLGMM method generates the smallest $\widehat{RAMSE}$ value. In fact, the $\widehat{RAMSE}$ value for the LLGMM is smaller than one tenth of any other $\widehat{RAMSE}$ values. Moreover, second, third and fourth smaller $\widehat{RAMSE}$ values are due to the IRGMM-Analytic, AGMM and GMM-Analytic methods, respectively. This exhibits the superiority of the LLGMM method over all other methods. We further observe that the LLGMM approach yields the smallest $\widehat{AMB}$ in comparison with the OCBGMM approaches. The GMM-Analytic, IRGMM-Analytic and IRGMM-Algebraic rank the second, third and fourth smaller values, respectively. The high value of $\widehat{AMAD}$ for the LLGMM method signifies that LLGMM captures the influence of random environmental fluctuations on the dynamic of interest rate process. We further note that the first, second, third and fourth smaller $\widehat{AMB}$ values are due to the LLGMM, GMM-Analytic, GMM-Algebraic and IRGMM-Analytic methods, respectively. These statements can be confirmed by comparing fluctuations in LLGMM simulation in Figure $C.22$ with other simulations in Figures $C.23$-$C.26$. Again, from Remark 4.3, the smallest $\widehat{RAMSE}$, higher $\widehat{AMAD}$ and smallest $\widehat{AMB}$ value under the LLGMM method exhibits superior performance under the three goodness-of-fit measures. We also notice that the performance of stochastic calculus based-OCPV-Analytic methods (GMM-Analytic, IRGMM-Analytic and AGMM) is better than the performance of OCPV-Algebraic based methods (GMM-Algebraic and IRGMM-Algebraic). In short, this suggests that the OCPV-Analytic based GMM methods are superior to the OCPV-Algebraic based GMM methods.

Table 11: Parameter estimates and goodness of fit tests for month risk free rates for periods 06/1964 – 12/1981 and 01/1982 – 12/2004

Orthogonality Condition	06/1964 – 12/1981	01/1982 – 12/2004
	$\widehat{RAMSE}$	$\widehat{RAMSE}$
GMM-Algebraic	0.0468	0.0377
GMM-Analytic	0.0315	0.0347
IRGMM-Algebraic	0.0307	0.0326
IRGMM-Analytic	0.0200	0.0215
LLGMM	0.0030*	0.0017*

Table 11 shows the goodness-of-fit measures $\widehat{RAMSE}$ using GMM-Algebraic, GMM-Analytic, IRGMM-Algebraic, IRGMM-Analytic and LLGMM methods for two separate sub-periods: 06/1964-12/1981 and 01/1982-12/2004. Among all methods, the LLGMM method generates the smallest $\widehat{RAMSE}$ value for each subperiods. Moreover, the goodness-of-fit measure $\widehat{RAMSE}$ regarding the LLGMM method is less than one sixth, and one twelfth of any other $\widehat{RAMSE}$ value, respectively. In fact, the ranking of IRGMM-Analytic, IRGMM-Algebraic, GMM-Analytic and GMM-Algebraic methods are second, third, fourth and fifth place, respectively.

In the following, using the LLGMM method and three goodness of fit measures, we validate dynamic models (2.20) and (7.1) in the context of real data set.

7.3. *Comparison of Goodness of fit Measures of model (2.20) with model (7.1) using LLGMM method*

As stated in Remark 7.1, we compare the Goodness of fit Measures $\widehat{RAMSE}$, $\widehat{AMAD}$, and $\widehat{AMB}$ using the U.S. Treasury Bill interest rate data and the LLGMM applied to the model validation problems of two proposed continuous-time dynamic models of U.S. Treasury Bill interest rate process described by (2.20) and (7.1). The LLGMM state estimates of (2.20) and (7.1) are computed under the same initial discrete-time delay $r = 20$, $p = 2$ and $\epsilon = 0.001$. The results are recorded in the following table.

Table 12: Comparison of Goodness of fit Measure of model (2.20) with model (7.1)

LLGMM	$\widehat{RAMSE}$	$\widehat{AMAD}$	$\widehat{AMB}$
Model (2.20)	*0.0024**	0.0145	0.0178
Model (7.1)	0.0027	0.0146	0.0178

Table 12 shows that the Goodness of fit Measures $\widehat{RAMSE}$, $\widehat{AMAD}$, and $\widehat{AMB}$ of the LLGMM method using both models (7.1) and (2.20) are very close. Model (2.20) appears to have the least $\widehat{RAMSE}$ value. This shows that the model (2.20) is a better dynamic model for U.S. Treasure Bill interest rate prices than model (7.1) under the LLGMM application, since it has a lower root mean square error. The $\widehat{AMAD}$ value using (7.1) is larger than the value using (2.20). This suggests that the influence of the random environmental fluctuations on state dynamic model (7.1) is higher than using the model (2.20). The $\widehat{AMB}$ value derived using both models appeared to be the same, indicating that both models give the same average median bias estimates. Based on this statistical analysis, we conclude that (2.20) is most realistic continuous-time stochastic dynamic model for the short-term riskless rate model. Model (2.20) includes many well-known interest rate models such as CKLS diffusion model [9] as a special case (with $\delta = 0$).

APPENDIX AND SUPPLEMENTAL MATERIALS

For $\Delta t = 1$, $\epsilon = 0.001$, $p = 2$, the $\epsilon-$ best sub-optimal estimates of parameters a, μ and σ^2 in (2.8) for four energy commodity data sets using $r = 10$ and $r = 20$ are outlined in $Appendix\ A$. The AGMM approach generated by the idea in Remark 2.5 is fully outlined, applied and compared with four energy data sets in $Appendix\ B$. A detailed comparison regarding the theoretical, graphical and performance of the LLGMM and OCBGMM methods are presented in $Appendix\ C$. In addition, a comparison of LLGMM with a few nonparametric statistical methods is also outlined in $Appendix\ D$

Appendix A. State and Parameter Estimates of daily Natural gas, daily Crude oil, daily Coal, and weekly Ethanol data for initial delays $r = 10$ and $r = 20$

An initial choice of r and p in Section 3 plays a very significant role in computational coordination, parameter and state estimation and state simulation. The ACF [6, 8] is used to determine the value p. An initial discrete-time delay r is used based on the increasing sequential choice $r = 5, 10, 20$ for the best graphical simulation result. The results are outlined in $Appendix\ A.1$ and $Appendix\ A.2$.

Appendix A.1. State and Parameter Estimates for daily Natural gas, Crude oil, Coal, and weekly Ethanol data using initial delay $r = 10$

Table A.13: Estimates $\hat{m}_k$, $\sigma^2_{\hat{m}_k,k}$, $\mu_{\hat{m}_k,k}$ and $a_{\hat{m}_k,k}$ for initial delay $r = 10$.

t_k	Natural gas				t_k	Crude oil				t_k	Coal				t_k	Ethanol			
	$\hat{m}_k$	$\sigma^2_{\hat{m}_k,k}$	$\mu_{\hat{m}_k,k}$	$a_{\hat{m}_k,k}$		$\hat{m}_k$	$\sigma^2_{\hat{m}_k,k}$	$\mu_{\hat{m}_k,k}$	$a_{\hat{m}_k,k}$		$\hat{m}_k$	$\sigma^2_{\hat{m}_k,k}$	$\mu_{\hat{m}_k,k}$	$a_{\hat{m}_k,k}$		$\hat{m}_k$	$\sigma^2_{\hat{m}_k,k}$	$\mu_{\hat{m}_k,k}$	$a_{\hat{m}_k,k}$
11	8	0.0003	2.0015	0.1718	11	4	0.0003	24.3532	0.0100	11	6	0.0015	8.5931	0.0245	11	6	0.0009	1.1830	0.8082
12	6	0.0003	2.1346	0.0131	12	4	0.0001	25.8537	-0.0157	12	10	0.0011	9.2573	0.0208	12	6	0.0009	1.2087	0.3843
13	7	0.0004	2.5701	0.0630	13	3	0.0003	25.8786	-0.0152	13	2	0.0029	7.6663	-0.0520	31	9	0.0013	4.0236	0.0040
14	9	0.0007	2.6746	0.0461	14	10	0.0010	24.0633	0.0084	14	5	0.0053	9.7962	0.0481	14	2	0.0009	1.1073	0.0509
15	7	0.0012	2.4425	0.4071	15	10	0.0009	22.7352	0.0025	15	10	0.0041	9.4047	0.0496	15	9	0.0024	1.0755	-0.1896
16	3	0.0013	2.5549	0.4621	16	4	0.0002	23.8665	0.0423	16	5	0.0050	9.4886	0.0694	16	2	0.0025	2.8800	0.0289
17	8	0.0015	2.5576	0.1934	17	7	0.0005	24.0777	0.0194	17	10	0.0048	9.1694	0.0598	17	9	0.0023	0.9139	-0.1012
18	8	0.0014	2.5628	0.2495	18	9	0.0008	24.2210	0.0138	18	4	0.0016	9.0681	0.1119	18	2	0.0018	0.7387	-0.0826
19	7	0.0015	2.5705	0.3522	19	7	0.0006	24.1147	0.0268	19	4	0.0043	9.0152	0.1527	19	7	0.0017	2.0655	0.0896
20	9	0.0011	2.5943	0.2946	20	6	0.0004	24.2748	0.0256	20	3	0.0039	9.0801	0.1613	20	8	0.0023	2.2742	0.0690
21	9	0.0010	2.6947	0.0775	21	7	0.0005	24.2175	0.0258	21	3	0.0030	8.7421	0.0946	21	7	0.0014	2.4094	0.0554
22	9	0.0010	2.6464	0.1883	22	4	0.0002	23.9993	0.0317	22	8	0.0085	8.8853	0.0944	22	6	0.0029	2.0457	0.1327
23	3	0.0009	2.7139	0.6983	23	10	0.0008	23.8479	0.0130	23	3	0.0010	8.6669	0.1055	23	7	0.0016	2.0441	0.1332
24	10	0.0013	2.6421	0.2966	24	10	0.0009	24.7657	-0.0087	24	6	0.0060	8.7592	0.0967	24	9	0.0020	1.3966	-0.2082
25	9	0.0018	2.6387	0.2382	25	4	0.0001	21.8903	0.0115	25	7	0.0064	8.8440	0.0908	25	6	0.0200	2.4981	0.1465
26	2	0.0015	2.5223	0.6595	26	4	0.0003	22.2871	0.0258	26	8	0.0067	8.8464	0.0895	26	7	0.0173	2.3356	0.1927
27	4	0.0018	2.5464	0.3474	27	10	0.0011	35.7200	-0.0010	27	3	0.0012	9.0667	0.1633	27	9	0.0143	2.3860	0.1416
28	3	0.0008	2.5780	0.2807	28	4	0.0003	22.1582	0.0391	28	8	0.0053	8.9557	0.0539	28	8	0.0138	2.3919	0.2196
29	2	0.0011	2.6588	-0.1271	29	6	0.0004	22.2194	0.0401	29	4	0.0007	9.0561	0.1246	29	7	0.0152	2.4087	0.3983
30	7	0.0031	2.5610	0.3718	30	7	0.0005	22.2596	0.0394	30	8	0.0041	8.9685	0.1025	30	10	0.0106	2.3164	0.2386
...	...	...	...	...	...	...	...	...	...	...	...	...	...	...	...	...	...	...	...
...	...	...	...	...	...	...	...	...	...	...	...	...	...	...	...	...	...	...	...
1145	4	0.0002	5.7203	0.1225	2440	6	0.0004	58.4990	0.0149	2865	4	0.0001	29.6070	0.0339	375	5	0.0008	2.1469	0.9842
1146	4	0.0003	5.6485	0.0951	2441	6	0.0004	57.7330	0.0070	2866	6	0.0005	29.3520	0.0213	376	4	0.0009	2.0689	0.2666
1147	4	0.0003	5.6704	0.2152	2442	8	0.0006	58.1010	0.0086	2867	7	0.0008	29.8620	-0.0231	377	6	0.0011	2.0999	0.2756
1148	7	0.0007	5.7138	0.1245	2443	8	0.0006	58.2670	0.0105	2868	3	0.0002	27.4300	0.0253	378	7	0.0014	2.0924	0.2551
1149	4	0.0004	5.6800	0.2544	2444	6	0.0004	60.6030	0.0027	2869	7	0.0016	26.8240	0.0056	379	10	0.0044	2.0941	0.2867
1150	6	0.0007	5.6331	0.1455	2445	6	0.0003	70.6110	0.0005	2870	3	0.0010	27.0540	0.0542	380	5	0.0007	2.0731	0.8434
1151	4	0.0007	5.5648	0.0971	2446	7	0.0003	58.6010	0.0072	2871	6	0.0009	26.7590	0.0182	381	6	0.0017	2.0214	-0.4677
1152	10	0.0026	5.5382	0.0588	2447	9	0.0009	58.7720	0.0077	2872	3	0.0006	26.4340	0.0220	382	6	0.0024	1.4504	-0.0549
1153	5	0.0006	5.4049	0.1000	2448	4	0.0006	58.9640	0.0115	2873	3	0.0004	26.6850	-0.1453	383	6	0.0017	1.6343	-0.0794
1154	5	0.0004	5.4155	0.1569	2449	10	0.0011	58.4730	0.0073	2874	9	0.0023	25.9970	0.0131	384	10	0.0057	2.7780	0.0309
1155	8	0.0010	5.4718	0.0725	2450	4	0.0003	58.5010	0.0344	2875	3	0.0014	25.5990	0.0532	385	8	0.0039	2.7055	0.0750
1156	7	0.0007	5.4528	0.1645	2451	3	0.0003	59.6250	0.0077	2876	4	0.0010	25.5580	0.0543	386	6	0.0018	2.6000	0.3021
1157	8	0.0009	5.4395	0.2011	2452	5	0.0003	58.9550	0.0143	2877	10	0.0027	25.2940	0.0067	387	8	0.0031	2.6118	0.1997
1158	5	0.0007	5.4183	0.1614	2453	10	0.0014	59.3090	0.0137	2878	6	0.0012	25.3300	0.0391	388	6	0.0027	2.6058	0.6130
1159	7	0.0008	5.3905	0.1281	2454	10	0.0013	59.4310	0.0108	2879	9	0.0019	25.2960	0.0155	389	8	0.0035	2.5973	0.4169
1160	9	0.0011	5.3367	0.0973	2455	10	0.0012	59.2480	0.0133	2880	9	0.0017	25.4620	0.0264	390	5	0.0024	2.5947	0.5364
1161	8	0.0008	4.9339	0.0155	2456	9	0.0010	59.3460	0.0112	2881	7	0.0012	25.3400	0.0369	391	5	0.0019	2.6500	-0.2801
1162	8	0.0007	5.0020	0.0210	2457	6	0.0005	59.2690	0.0106	2882	9	0.0018	25.4310	0.0416	392	5	0.0017	2.6321	-0.3394
1163	7	0.0004	5.0947	0.0732	2458	4	0.0002	58.4790	0.0103	2883	7	0.0011	25.3550	0.0445	393	6	0.0020	3.0563	-0.0442
1164	5	0.0001	4.9554	0.0671	2459	3	0.0004	58.4160	0.0976	2884	9	0.0016	25.3400	0.0445	394	9	0.0055	2.4093	0.0868
1165	9	0.0009	4.0877	0.0148	2460	10	0.0014	57.0380	0.0026	2885	4	0.0005	25.5440	0.0675	395	4	0.0027	2.3140	0.4706

Table $A.13$ shows the ϵ- best sub-optimal local admissible sample size $\hat{m}_k$ and the parameter estimates $a_{\hat{m}_k,k}$, $\mu_{\hat{m}_k,k}$ and $\sigma^2_{\hat{m}_k,k}$ for four energy commodities price at time t_k. This is based on the value of p and the initial real data time delay $r = 10$. We further note that the range of the ϵ-best sub-optimal local admissible sample size $\hat{m}_k$ for any time $t_k \in [11, 30] \bigcup [1145, 1165]$, $t_k \in [11, 30] \bigcup [2440, 2460]$, $t_k \in [11, 30] \bigcup [2865, 2885]$, and $t_k \in [11, 30] \bigcup [375, 395]$ for natural gas, crude oil, coal and ethanol data, respectively, is $2 \leq \hat{m}_k \leq 10$. Moreover, all comments (Remark 4.1) that are made with regard to Table 2 regarding the four energy commodities remain valid with regard to Table $A.13$

Table A.14: Real, Simulation using LLGMM method, and absolute error of simulation using starting delay $r = 10$

t_k	Natural gas			t_k	Crude oil			t_k	Coal			t_k	Ethanol		
	Real y_k	Simulated $y^s_{\hat{m}_k,k}$ (LLGMM)	$\lvert Error \rvert$ $\lvert y_k - y^s_{\hat{m}_k,k} \rvert$		Real	Simulated $y^s_{\hat{m}_k,k}$ (LLGMM)	$\lvert Error \rvert$ $\lvert y_k - y^s_{\hat{m}_k,k} \rvert$		Real	Simulated $y^s_{\hat{m}_k,k}$ (LLGMM)	$\lvert Error \rvert$ $\lvert y_k - y^s_{\hat{m}_k,k} \rvert$		Real	Simulated $y^s_{\hat{m}_k,k}$ (LLGMM)	$\lvert Error \rvert$ $\lvert y_k - y^s_{\hat{m}_k,k} \rvert$
10	2.3830	2.3830	0.0000	10	25.1000	25.1000	0.0000	10	9.0600	9.0600	0.0000	10	1.1900	1.1900	0.0000
11	2.4170	2.4179	0.0009	11	24.8000	25.0181	0.2181	11	8.8800	8.8800	0.0000	11	1.2250	1.2249	0.0001
12	2.5590	2.4935	0.0655	12	24.4000	24.3221	0.0779	12	9.4400	9.4216	0.0184	12	1.2200	1.2425	0.0225
13	2.4850	2.4949	0.0099	13	23.8500	23.7260	0.1240	13	10.3100	10.0621	0.2479	13	1.2900	1.2278	0.0622
14	2.5280	2.5123	0.0157	14	23.8500	24.4203	0.5703	14	9.8100	9.8058	0.0042	14	1.4100	1.5339	0.1239
15	2.6160	2.6158	0.0002	15	23.8500	23.8174	0.0326	15	9.0600	8.8075	0.2525	15	1.4700	1.3390	0.1310
16	2.5230	2.5233	0.0003	16	23.9000	23.8845	0.0155	16	8.7500	8.4774	0.2726	16	1.5300	1.5745	0.0445
17	2.6100	2.6314	0.0214	17	24.5000	24.0924	0.4076	17	8.8200	8.7839	0.0361	17	1.6300	1.5996	0.0304
18	2.6100	2.5852	0.0248	18	24.8000	24.3340	0.4660	18	9.5600	9.3610	0.1990	18	1.7500	1.6320	0.1180
19	2.6100	2.6130	0.0030	19	24.1500	24.1566	0.0066	19	8.8200	8.6667	0.1533	19	1.7500	1.7495	0.0005
20	2.6990	2.6728	0.0262	20	24.2000	24.5277	0.3277	20	8.8200	8.7833	0.0367	20	1.8400	1.8586	0.0186
21	2.7590	2.7601	0.0011	21	24.0000	23.7803	0.2197	21	8.6900	8.5498	0.1402	21	1.8950	1.8874	0.0076
22	2.6590	2.6427	0.0163	22	23.9000	24.1935	0.2935	22	8.6300	8.7065	0.0765	22	1.9500	1.9257	0.0243
23	2.7420	2.7365	0.0055	23	23.0500	23.0564	0.0064	23	8.6900	8.7620	0.0720	23	1.9740	1.9548	0.0192
24	2.5620	2.5610	0.0010	24	22.3000	23.2208	0.9208	24	8.9400	8.9706	0.0306	24	2.7000	2.1431	0.5569
25	2.4950	2.5455	0.0505	25	22.4500	23.1640	0.7140	25	9.3100	8.8231	0.4869	25	2.5150	2.6941	0.1791
26	2.5400	2.5245	0.0155	26	22.3500	22.7275	0.3775	26	8.9400	8.9945	0.0545	26	2.2900	2.2753	0.0147
27	2.5920	2.5996	0.0076	27	21.7500	21.5907	0.1593	27	8.9400	8.9676	0.0276	27	2.4400	2.3645	0.0755
28	2.5700	2.5849	0.0149	28	22.1000	22.0868	0.0132	28	9.1300	9.1741	0.0441	28	2.4150	2.4019	0.0131
29	2.5410	2.5403	0.0007	29	22.4000	22.4301	0.0301	29	9.1900	9.1766	0.0134	29	2.3000	2.2440	0.0560
30	2.6180	2.6151	0.0029	30	22.5000	22.6614	0.1614	30	8.5700	8.4567	0.1133	30	2.1000	2.2048	0.1048
...	...	....	...	...	...	...	....	...	...	...	...	...	...	...	...
...	....	....	...	....	...	....	....	...	...	...	...	...	...	...	...
1145	5.712	5.7533	0.0413	2440	57.35	57.762	0.412	2865	29.31	29.518	0.2083	375	2.073	2.0662	0.0068
1146	5.588	5.5892	0.0012	2441	56.74	56.743	0.0028	2866	28.68	28.495	0.1851	376	2.02	2.0267	0.0067
1147	5.693	5.7143	0.0213	2442	57.55	57.739	0.189	2867	26.77	28.727	1.9571	377	2.073	2.0731	0.0001
1148	5.791	5.8127	0.0217	2443	59.09	58.925	0.1646	2868	27.45	26.979	0.471	378	2.065	2.0709	0.0059
1149	5.614	5.5940	0.0200	2444	60.27	59.663	0.607	2869	27.00	26.879	0.121	379	2.055	2.0232	0.0318
1150	5.442	5.6266	0.1846	2445	60.75	61.161	0.4109	2870	26.67	27.32	0.6499	380	2.209	2.2109	0.0019
1151	5.533	5.5122	0.0208	2446	58.41	58.011	0.3994	2871	26.51	25.468	1.0415	381	2.44	2.296	0.144
1152	5.378	5.3971	0.0191	2447	58.72	58.762	0.042	2872	26.48	26.263	0.2174	382	2.517	2.4074	0.1096
1153	5.373	5.3496	0.0234	2448	58.64	58.409	0.2309	2873	25.15	25.395	0.2445	383	2.718	2.6839	0.0341
1154	5.382	5.3735	0.0085	2449	57.87	57.762	0.1081	2874	25.57	25.555	0.0153	384	2.541	2.5246	0.0164
1155	5.507	5.5360	0.0290	2450	59.13	59.243	0.1135	2875	25.88	26.08	0.2003	385	2.566	2.5629	0.0031
1156	5.552	5.5507	0.0013	2451	60.11	60.068	0.0419	2876	25.24	25.528	0.2879	386	2.626	2.6248	0.0012
1157	5.310	5.3019	0.0081	2452	58.94	58.956	0.0155	2877	25	25.337	0.3375	387	2.587	2.5871	0.0001
1158	5.338	5.3884	0.0504	2453	59.93	59.924	0.0062	2878	25.08	24.685	0.3951	388	2.628	2.6363	0.0083
1159	5.298	5.2554	0.0426	2454	61.18	62.168	0.9876	2879	25.05	24.848	0.2024	389	2.587	2.5332	0.0538
1160	5.189	5.1644	0.0146	2455	59.66	59.381	0.2786	2880	25.89	25.638	0.2518	390	2.536	2.5374	0.0014
1161	5.082	5.0874	0.0054	2456	58.59	58.468	0.1224	2881	25.23	25.405	0.1749	391	2.42	2.3401	0.0799
1162	5.082	5.0977	0.0157	2457	58.28	58.487	0.2067	2882	25.94	25.739	0.2007	392	2.247	2.1792	0.0678
1163	5.082	5.1334	0.0514	2458	58.79	58.896	0.1058	2883	25.26	24.858	0.4025	393	2.223	2.1661	0.0569
1164	4.965	5.0340	0.0690	2459	56.23	57.202	0.9715	2884	25.25	25.147	0.1028	394	2.39	2.5122	0.1222
1165	4.767	4.9143	0.1473	2460	55.9	56.87	0.9701	2885	26.06	25.613	0.4475	395	2.38	2.3583	0.0217

In Table $A.14$, the real and LLGMM simulated price values for each of the four energy commodities: natural gas, crude oil, coal and ethanol are recorded in columns 2-3, 6-7, 10-11, and 14-15, respectively. The absolute error of each of the energy commodity's simulated value is shown in columns 4, 8, 12, 16, respectively.

Appendix A.2. State and Parameter Estimates of daily Natural gas, daily Crude oil, daily Coal, and weekly Ethanol data for initial delay $r = 20$

Table A.15: Estimates $\hat{m}_k$, $\sigma^2_{\hat{m}_k,k}$, $\mu_{\hat{m}_k,k}$ and $a_{\hat{m}_k,k}$ for initial delay $r = 20$.

t_k	Natural gas				t_k	Crude oil				t_k	Coal				t_k	Ethanol			
	$\hat{m}_k$	$\sigma^2_{\hat{m}_k,k}$	$\mu_{\hat{m}_k,k}$	$a_{\hat{m}_k,k}$		$\hat{m}_k$	$\sigma^2_{\hat{m}_k,k}$	$\mu_{\hat{m}_k,k}$	$a_{\hat{m}_k,k}$		$\hat{m}_k$	$\sigma^2_{\hat{m}_k,k}$	$\mu_{\hat{m}_k,k}$	$a_{\hat{m}_k,k}$		$\hat{m}_k$	$\sigma^2_{\hat{m}_k,k}$	$\mu_{\hat{m}_k,k}$	$a_{\hat{m}_k,k}$
21	13	0.0011	2.7056	0.0816	21	11	0.0003	24.115	0.0204	21	19	0.0042	9.1915	0.0255	21	18	0.0024	0.7591	0.0467
22	5	0.0009	2.6748	0.233	22	7	0.0003	24.215	0.0278	22	15	0.0044	9.0773	0.0601	22	4	0.0015	0.7929	-0.0272
23	3	0.0013	2.7139	0.6983	23	2	0.0006	24.013	-0.314	23	19	0.0038	9.1073	0.0319	23	8	0.0004	2.1528	0.0888
24	12	0.0021	2.6197	0.2119	24	15	0.0007	14.246	0.0009	24	10	0.0035	8.8762	0.0924	24	15	0.0025	1.0048	-0.1078
25	10	0.0022	2.6201	0.2199	25	19	0.0011	18.542	0.001	25	14	0.0049	9.1783	0.0517	25	20	0.0094	-0.4372	-0.0208
26	5	0.0015	2.567	0.2063	26	19	0.001	21.738	0.0031	26	9	0.003	8.9447	0.1	26	19	0.0094	3.1726	0.0251
27	9	0.0021	2.6295	0.1919	27	4	0.0001	22.135	0.0355	27	10	0.0031	8.9442	0.1	27	7	0.0205	2.3915	0.2198
28	17	0.0031	2.6074	0.2204	28	14	0.0007	20.045	0.0015	28	6	0.0013	9.0358	0.0767	28	17	0.0087	2.6208	0.0553
29	11	0.0022	2.6099	0.1688	29	14	0.0007	22.096	0.0034	29	3	0.0006	9.4379	0.0213	29	3	0.0218	2.3857	0.634
30	8	0.0014	2.5821	0.2593	30	9	0.0004	22.249	0.0154	30	8	0.0019	8.9685	0.1025	30	19	0.0161	2.3086	0.0752
31	7	0.0013	2.5605	0.3999	31	3	0.0002	22.739	0.0203	31	4	0.0014	8.8837	0.0869	31	18	0.0162	2.2442	0.1049
32	9	0.0016	2.5738	0.3887	32	6	0.0004	22.226	0.0427	32	15	0.0096	8.9287	0.0972	32	9	0.0279	2.3519	0.4089
33	16	0.0035	2.6195	0.2084	33	7	0.0005	22.084	0.0296	33	5	0.0013	8.7634	0.0932	33	12	0.0193	2.2912	0.2631
34	20	0.0041	2.6078	0.2483	34	11	0.001	21.683	0.0138	34	7	0.0018	8.8238	0.0869	34	6	0.0186	2.1259	0.2733
35	16	0.0033	2.6031	0.2024	35	10	0.0009	20.446	0.0041	35	8	0.0021	8.7923	0.0823	35	20	0.0218	2.2078	0.1261
36	5	0.0007	2.579	0.2816	36	3	0	21.027	0.0489	36	9	0.0023	8.7282	0.0671	36	10	0.0199	1.9158	0.0549
37	9	0.0013	2.5814	0.3453	37	4	0.0002	20.962	0.0465	37	13	0.0062	8.7653	0.0502	37	7	0.0146	1.9215	0.088
38	10	0.0014	2.5836	0.3371	38	3	0.0002	21.267	-0.0327	38	7	0.001	8.6612	0.1378	38	7	0.0127	2.0226	0.1587
39	3	0.0015	2.603	0.3923	39	13	0.0014	15.485	0.0012	39	20	0.0151	8.8225	0.0644	39	19	0.0413	2.1885	0.1729
40	18	0.0048	2.6026	0.2551	40	5	0.0004	20.617	0.028	40	17	0.0101	8.8585	0.0667	40	8	0.0112	1.9751	0.1655
...	...	...	...	...	...	...	...	...	...	...	...	...	...	...	...	...	...	...	...
...	...	...	...	...	...	...	...	...	...	...	...	...	...	...	...	...	...	...	...
1145	3	0.0001	5.7243	0.1464	2440	8	0.0007	58.338	0.0143	2865	4	0.0002	29.607	0.034	375	6	0.0013	2.1486	0.7096
1146	17	0.0033	5.7831	0.0272	2441	20	0.0033	58.546	0.0028	2866	12	0.0023	29.257	0.0209	376	3	0.0009	2.0699	0.2808
1147	15	0.0025	5.8662	0.0337	2442	10	0.0008	58.056	0.0098	2867	20	0.0054	26.256	0.0021	377	5	0.0011	2.0858	0.3308
1148	8	0.0006	5.7271	0.0741	2443	8	0.0006	58.267	0.0106	2868	14	0.0028	28.678	0.009	378	11	0.007	2.1286	0.2103
1149	5	0.0004	5.6834	0.2598	2444	7	0.0005	58.414	0.0079	2869	11	0.0019	27.482	0.0052	379	3	0.0007	2.0623	0.6096
1150	18	0.0034	5.6161	0.0138	2445	7	0.0005	65.583	0.001	2870	14	0.0026	26.136	0.0023	380	16	0.0137	2.1586	0.1983
1151	16	0.0026	5.6048	0.0268	2446	8	0.0005	58.733	0.0078	2871	12	0.0019	25.376	0.0021	381	19	0.0185	2.2115	0.1503
1152	18	0.0031	5.3059	0.0099	2447	9	0.0007	58.772	0.0078	2872	9	0.0011	26.067	0.0064	382	11	0.0066	1.7644	-0.0401
1153	9	0.0008	5.4937	0.0517	2448	20	0.0033	58.727	0.0079	2873	4	0.0003	27.22	-0.0313	383	3	0.0025	2.9233	0.1347
1154	7	0.0006	5.4044	0.0549	2449	13	0.0013	58.371	0.0087	2874	10	0.0016	25.744	0.0095	384	4	0.0025	2.5937	0.3073
1155	5	0.0003	5.4342	0.2005	2450	3	0.0001	58.48	0.0345	2875	3	0.0012	25.599	0.0532	385	5	0.0039	2.5887	0.3099
1156	7	0.0006	5.4528	0.1646	2451	9	0.0008	59.324	0.013	2876	3	0.0008	25.559	0.0541	386	3	0.006	2.5861	0.4792
1157	8	0.0006	5.4395	0.2012	2452	5	0.0005	58.955	0.0144	2877	5	0.0006	25.415	0.0446	387	4	0.0039	2.5882	0.4761
1158	14	0.002	5.4704	0.0583	2453	9	0.001	59.171	0.0135	2878	4	0.0005	25.193	0.0206	388	11	0.0087	2.6964	0.077
1159	10	0.0009	5.4035	0.1412	2454	15	0.002	59.298	0.0063	2879	3	0.0002	25.059	0.0528	389	6	0.0038	2.5952	0.4921
1160	14	0.0018	5.3501	0.0373	2455	13	0.0015	59.512	0.0126	2880	5	0.0004	25.256	0.0431	390	10	0.0075	2.5899	0.3122
1161	11	0.001	5.174	0.0277	2456	11	0.0011	59.169	0.0137	2881	5	0.0005	25.254	0.0435	391	9	0.0062	2.5817	0.4568
1162	18	0.0029	5.1069	0.016	2457	12	0.0012	59.072	0.0128	2882	9	0.002	25.431	0.0417	392	7	0.0038	2.6222	-0.3162
1163	18	0.0027	5.1426	0.0213	2458	8	0.0006	59.427	0.0112	2883	13	0.0033	25.507	0.0243	393	15	0.0142	2.5051	0.1102
1164	16	0.002	5.0554	0.0297	2459	15	0.0018	58.808	0.0092	2884	20	0.006	25.52	0.0094	394	12	0.01	2.4881	0.1156
1165	15	0.0016	5.7431	-0.0195	2460	14	0.0015	58.187	0.0042	2885	5	0.0007	25.538	0.069	395	3	0.0036	2.355	0.2939

Table $A.15$ shows the ϵ- best sub-optimal local admissible sample size $\hat{m}_k$ and the parameter estimates $a_{\hat{m}_k,k}$, $\mu_{\hat{m}_k,k}$ and $\sigma^2_{\hat{m}_k,k}$ for four energy commodities price at time t_k. This was based on the value of p and the initial real data time delay $r = 20$. We further note that the range of the ϵ-best sub-optimal local admissible sample size $\hat{m}_k$ for any time $t_k \in [21, 40] \bigcup [1145, 1165]$, $t_k \in [21, 40] \bigcup [2440, 2460]$, $t_k \in [21, 40] \bigcup [2865, 2885]$, and $t_k \in [21, 40] \bigcup [375, 395]$ for natural gas, crude oil, coal and ethanol data, respectively, is $3 \leq \hat{m}_k \leq 20$. Moreover, all comments (Remark 4.1) that are made with regard to Table 2 regarding the four energy commodities remain valid with regard to Table $A.15$

In Table $A.16$, the real and the LLGMM simulated price values for each of the four energy commodities: natural gas, crude oil, coal and ethanol are exhibited in columns 2-3, 6-7, 10-11, and 14-15, respectively. The absolute error of each of the energy commodity's simulated value is shown in columns 4, 8, 12, 16, respectively.

Table A.16: Real, Simulation using the LLGMM method, and absolute error of simulation using starting delay $r = 20$

t_k	Natural gas			t_k	Crude oil			t_k	Coal			t_k	Ethanol		
	Real y_k	Simulated $y^s_{\hat{m}_k,k}$ (LLGMM)	$\lvert Error\rvert$ $\lvert y_k - y^s_{\hat{m}_k,k}\rvert$		Real	Simulated $y^s_{\hat{m}_k,k}$ (LLGMM)	$\lvert Error\rvert$ $\lvert y_k - y^s_{\hat{m}_k,k}\rvert$		Real	Simulated $y^s_{\hat{m}_k,k}$ (LLGMM)	$\lvert Error\rvert$ $\lvert y_k - y^s_{\hat{m}_k,k}\rvert$		Real	Simulated $y^s_{\hat{m}_k,k}$ (LLGMM)	$\lvert Error\rvert$ $\lvert y_k - y^s_{\hat{m}_k,k}\rvert$
21	2.759	2.7718	0.0128	21	24	24.025	0.025	21	8.69	8.6747	0.0153	21	1.895	1.9024	0.0074
22	2.659	2.6566	0.0024	22	23.9	24.093	0.193	22	8.63	8.6175	0.0125	22	1.95	1.9315	0.0185
23	2.742	2.7353	0.0067	23	23.05	23.051	0.001	23	8.69	8.6862	0.0038	23	1.974	1.9788	0.0048
24	2.562	2.5757	0.0137	24	22.3	22.887	0.587	24	8.94	8.9184	0.0216	24	2.7	2.5529	0.1471
25	2.495	2.5332	0.0382	25	22.45	22.126	0.324	25	9.31	9.3069	0.0031	25	2.515	2.5134	0.0016
26	2.54	2.5336	0.0064	26	22.35	22.409	0.059	26	8.94	8.8992	0.0408	26	2.29	2.3306	0.0406
27	2.592	2.5631	0.0289	27	21.75	22.12	0.37	27	8.94	8.8745	0.0655	27	2.44	2.3718	0.0682
28	2.57	2.5797	0.0097	28	22.1	22.137	0.037	28	9.13	9.1162	0.0138	28	2.415	2.3927	0.0223
29	2.541	2.4846	0.0564	29	22.4	22.315	0.085	29	9.19	9.234	0.044	29	2.3	2.3311	0.0311
30	2.618	2.6245	0.0065	30	22.5	22.531	0.031	30	8.57	8.5495	0.0205	30	2.1	2.072	0.028
31	2.564	2.5469	0.0171	31	22.65	22.712	0.062	31	8.69	8.7241	0.0341	31	2.04	2.0323	0.0077
32	2.667	2.6763	0.0093	32	21.95	22.003	0.053	32	8.88	8.8866	0.0066	32	2.16	2.1561	0.0039
33	2.633	2.6308	0.0022	33	21.6	21.853	0.253	33	8.57	8.5084	0.0616	33	2.13	2.0796	0.0504
34	2.515	2.5021	0.0129	34	21	21.099	0.099	34	8.75	8.7447	0.0053	34	2.155	2.2141	0.0591
35	2.53	2.5136	0.0164	35	20.95	21.012	0.062	35	8.63	8.6003	0.0297	35	2.01	1.9687	0.0413
36	2.549	2.5458	0.0032	36	21.1	20.971	0.129	36	8.44	8.412	0.028	36	1.93	1.8762	0.0538
37	2.603	2.5835	0.0195	37	20.8	20.786	0.014	37	8.44	8.4465	0.0065	37	1.9	1.9186	0.0186
38	2.603	2.5822	0.0208	38	20.3	20.048	0.252	38	8.94	8.9538	0.0138	38	1.975	1.9052	0.0698
39	2.603	2.6075	0.0045	39	20.25	20.244	0.006	39	9	9.0064	0.0064	39	1.98	2.019	0.039
40	2.815	2.8728	0.0578	40	20.75	20.734	0.016	40	8.94	8.8655	0.0745	40	2	1.9385	0.0615
...	...	....	...	...	...	...	....	...	...	...	...	...	...	...	...
...	....	....	...	....	...	....	....	...	...	...	...	...	...	...	...
1145	5.712	5.7577	0.0457	2440	57.35	57.376	0.026	2865	29.31	29.291	0.019	375	2.073	2.09	0.017
1146	5.588	5.6488	0.0608	2441	56.74	56.447	0.293	2866	28.68	28.8	0.12	376	2.02	2.0589	0.0389
1147	5.693	5.7062	0.0132	2442	57.55	57.523	0.027	2867	26.77	26.891	0.121	377	2.073	2.0601	0.0129
1148	5.791	5.7917	0.0007	2443	59.09	58.968	0.122	2868	27.45	27.316	0.134	378	2.065	2.0312	0.0338
1149	5.614	5.5799	0.0341	2444	60.27	60.278	0.008	2869	27	27.189	0.189	379	2.055	2.0725	0.0175
1150	5.442	5.4099	0.0321	2445	60.75	60.737	0.013	2870	26.67	26.812	0.142	380	2.209	2.2254	0.0164
1151	5.533	5.5035	0.0295	2446	58.41	58.494	0.084	2871	26.51	26.709	0.199	381	2.44	2.462	0.022
1152	5.378	5.407	0.029	2447	58.72	58.614	0.106	2872	26.48	26.54	0.06	382	2.517	2.51	0.007
1153	5.373	5.3682	0.0048	2448	58.64	58.95	0.31	2873	25.15	25.313	0.163	383	2.718	2.6979	0.0201
1154	5.382	5.3827	0.0007	2449	57.87	57.865	0.005	2874	25.57	25.47	0.1	384	2.541	2.5164	0.0246
1155	5.507	5.4896	0.0174	2450	59.13	58.967	0.163	2875	25.88	26.078	0.198	385	2.566	2.5328	0.0332
1156	5.552	5.5423	0.0097	2451	60.11	59.937	0.173	2876	25.24	25.208	0.032	386	2.626	2.5831	0.0429
1157	5.31	5.318	0.008	2452	58.94	59.068	0.128	2877	25	25.138	0.138	387	2.587	2.5606	0.0264
1158	5.338	5.3794	0.0414	2453	59.93	60.141	0.211	2878	25.08	25.306	0.226	388	2.628	2.6322	0.0042
1159	5.298	5.3541	0.0561	2454	61.18	61.53	0.35	2879	25.05	25.16	0.11	389	2.587	2.5651	0.0219
1160	5.189	5.1838	0.0052	2455	59.66	59.792	0.132	2880	25.89	25.509	0.381	390	2.536	2.53	0.006
1161	5.082	5.3804	0.2984	2456	58.59	58.481	0.109	2881	25.23	25.278	0.048	391	2.42	2.4268	0.0068
1162	5.082	4.9802	0.1018	2457	58.28	58.224	0.056	2882	25.94	25.961	0.021	392	2.247	2.2228	0.0242
1163	5.082	5.1933	0.1113	2458	58.79	58.928	0.138	2883	25.26	25.255	0.005	393	2.223	2.2072	0.0158
1164	4.965	5.1925	0.2275	2459	56.23	56.329	0.099	2884	25.25	25.298	0.048	394	2.39	2.4141	0.0241
1165	4.767	4.7917	0.0247	2460	55.9	54.676	1.224	2885	26.06	25.882	0.178	395	2.38	2.4265	0.0465

Appendix B. Formulation of Aggregated Generalized Method of Moment (AGMM):

In this section, using the theoretical basis of the LLGMM and Remark 2.5 (Section 2), we generated aggregated state and parameter estimates based on the method for state and parameter estimation problems. The generalized method is then applied to energy commodity dynamic model (2.8). The results are compared with the LLGMM method.

Appendix B.1. AGMM Method Applied to Energy Commodities:

In this Subsection, using the aggregated parameter estimates $\bar{a}$, $\bar{\mu}$, and $\overline{\sigma^2}$ described by the mean value of the estimated samples $\{a_{\hat{m}_i,i}\}_{i=0}^{N}$, $\{\mu_{\hat{m}_i,i}\}_{i=0}^{N}$ and $\{\sigma^2_{\hat{m}_i,i}\}_{i=0}^{N}$ (Remark 2.5), respectively, we discuss the simulated price values for the four energy commodities. $\bar{a}$, $\bar{\mu}$, and $\overline{\sigma^2}$ defined in (2.19) are referred to as aggregated parameter estimates of a, μ, and σ^2 over the given entire finite interval of time. These estimates are derived using the following discretized system:

$$y_i^{ag} = y_{i-1}^{ag} + \bar{a}(\bar{\mu} - y_{i-1}^{ag})y_{i-1}^{ag}\Delta t + \overline{\sigma^2}^{1/2} y_{i-1}^{ag}\Delta W_i \tag{B.1}$$

where y_k^{ag} denotes the simulated value for y_k at time t_k. The overall descriptive data statistic regarding the four energy commodities price and estimated parameters are recorded in Table B.17 below.

Table B.17: Descriptive Statistics for a, μ and σ^2 using initial delay $r = 20$.

Data Set Y	$\bar{Y}$	Std(Y)	$\overline{\Delta ln(Y)}$	var($\Delta ln(Y)$)	$\bar{a}$	Std(a)	$\bar{\mu}$	Std(μ)	$\overline{\sigma^2}$	std(σ^2)	95% C. I. $\bar{\mu}$
Nat. Gas	4.5504	1.5090	0.0008	0.0015	0.1867	0.3013	4.5538	2.3565	0.0013	0.0017	(4.4196, 4.6880)
Crude Oil	54.0093	31.0248	0.0003	0.0006	0.0215	0.0517	54.0307	37.4455	0.0005	0.0008	(51.8978, 56.1636)
Coal	27.1441	17.8394	0.0003	0.0015	0.0464	0.0879	27.0567	21.3506	0.0014	0.0022	(25.8405, 28.2729)
Ethanol	2.1391	0.4455	0.0011	0.0020	0.3167	0.8745	2.1666	0.7972	0.0018	0.0030	(2.0919,2.2414)

Table B.17 shows the descriptive statistics for a, μ and σ^2 with time delay $r = 20$. Moreover, $\bar{\mu}$ is approximately close to the overall descriptive statistics of the mean $\bar{Y}$ of the real data for each of the energy commodity shown in column 2. Also, $\overline{\sigma^2}$ is approximately close to the overall descriptive statistics of the variance of $\Delta \ln(Y) = \ln(Y_i) - \ln(Y_{i-1})$ in Column 5. Moreover, column 12 shows that the mean of the actual data set in Column 2 falls within the 95% confidence interval of $\bar{\mu}$. This exhibits that the parameter $\mu_{\hat{m}_k,k}$ is the mean level of y_k at time t_k.

Using the aggregated parameter estimates $\bar{a}$, $\bar{\mu}$, and $\overline{\sigma^2}$ in Table B.17 (Column 6, 8, and 10), the simulated price values for the four energy commodities are shown in columns 3, 6, 9 and 12 of Table B.18.

Table B.18: Real, Simulation value using AGMM with $r = 20$.

t_k	Natural gas		t_k	Crude oil		t_k	Coal		t_k	Ethanol	
	Real	Simulated y_k^{ag} (AGMM)		Real	Simulated y_k^{ag} (AGMM)		Real	Simulated y_k^{ag} (AGMM)		Real	Simulated y_k^{ag} (AGMM)
21	2.759	2.649	21	24.00	23.974	21	8.690	9.111	21	1.895	1.834
22	2.659	2.651	22	23.900	24.204	22	8.630	9.028	22	1.950	1.854
23	2.742	2.636	23	23.050	25.229	23	8.690	9.192	23	1.974	1.798
24	2.562	2.625	24	22.300	25.586	24	8.940	9.032	24	2.700	1.858
25	2.495	2.593	25	22.450	26.470	25	9.310	8.938	25	2.515	1.830
26	2.54	2.525	26	22.350	25.953	26	8.940	8.792	26	2.290	1.954
27	2.592	2.513	27	21.750	26.229	27	8.940	9.035	27	2.440	1.926
28	2.57	2.399	28	22.100	26.555	28	9.130	9.255	28	2.415	1.939
29	2.541	2.485	29	22.400	26.402	29	9.190	9.018	29	2.300	1.883
30	2.618	2.506	30	22.500	27.34	30	8.570	8.687	30	2.100	1.880
31	2.564	2.460	31	22.650	26.24	31	8.690	8.985	31	2.040	1.817
32	2.667	2.295	32	21.950	26.765	32	8.880	9.339	32	2.160	1.810
33	2.633	2.534	33	21.600	26.358	33	8.570	9.359	33	2.130	1.774
34	2.515	2.514	34	21.000	26.87	34	8.750	9.310	34	2.155	1.717
35	2.53	2.573	35	20.950	26.835	35	8.630	9.302	35	2.010	1.658
36	2.549	2.592	36	21.100	26.725	36	8.440	9.543	36	1.930	1.607
37	2.603	2.456	37	20.800	26.439	37	8.440	9.288	37	1.900	1.645
38	2.603	2.428	38	20.300	26.916	38	8.940	9.155	38	1.975	1.635
39	2.603	2.505	39	20.250	26.989	39	9.000	8.469	39	1.980	1.629
40	2.815	2.526	40	20.750	26.759	40	8.940	8.899	40	2.00	1.745
...	...	....	...	...	...	...	....	...	...	...	.....
...	....	....	...	....	...	....	....	...	...	...	.....
1145	5.712	5.218	2440	57.350	48.179	2865	29.310	17.839	375	2.073	2.625
1146	5.588	5.414	2441	56.740	48.239	2866	28.680	18.563	376	2.02	2.784
1147	5.693	5.460	2442	57.550	46.984	2867	26.770	19.577	377	2.073	2.558
1148	5.791	5.464	2443	59.090	47.418	2868	27.450	19.841	378	2.065	2.670
1149	5.614	5.544	2444	60.270	48.137	2869	27.000	18.876	379	2.055	2.565
1150	5.442	5.700	2445	60.750	49.185	2870	26.670	18.465	380	2.209	2.796
1151	5.533	5.710	2446	58.410	48.271	2871	26.510	18.139	381	2.44	2.783
1152	5.378	5.936	2447	58.720	48.384	2872	26.480	17.963	382	2.517	2.659
1153	5.373	5.869	2448	58.640	47.509	2873	25.150	18.151	383	2.718	2.739
1154	5.382	5.778	2449	57.870	48.654	2874	25.570	17.987	384	2.541	2.681
1155	5.507	5.732	2450	59.130	46.883	2875	25.880	18.393	385	2.566	2.631
1156	5.552	5.816	2451	60.110	46.403	2876	25.240	18.492	386	2.626	2.638
1157	5.31	6.000	2452	58.940	45.564	2877	25.000	18.621	387	2.587	2.542
1158	5.338	6.162	2453	59.930	44.177	2878	25.080	18.806	388	2.628	2.491
1159	5.298	5.899	2454	61.180	43.112	2879	25.050	19.384	389	2.587	2.392
1160	5.189	6.008	2455	59.660	43.47	2880	25.890	20.131	390	2.536	2.393
1161	5.082	6.175	2456	58.590	41.531	2881	25.230	21.099	391	2.42	2.534
1162	5.082	6.191	2457	58.280	40.452	2882	25.940	21.499	392	2.247	2.687
1163	5.082	5.814	2458	58.790	41.968	2883	25.260	21.38	393	2.223	2.701
1164	4.965	5.701	2459	56.230	44.359	2884	25.250	20.786	394	2.39	2.703
1165	4.767	5.871	2460	55.90	44.679	2885	26.060	20.892	395	2.38	2.655
1166	4.675	5.998	2461	56.420	43.081	2886	26.030	21.269	396	2.366	2.559
1167	4.79	5.952	2462	58.010	44.235	2887	26.660	20.371	397	2.335	2.575
1168	4.631	5.782	2463	57.280	43.199	2888	27.120	19.822	398	2.428	2.466
1169	4.658	5.673	2464	60.30	42.655	2889	26.400	19.644	399	2.409	2.369
1170	4.57	5.936	2465	60.970	43.498	2890	26.940	20.602	400	2.29	2.222

Figure $B.20$ below shows a comparison between the real data set, simulated price using LLGMM and AGMM methods.

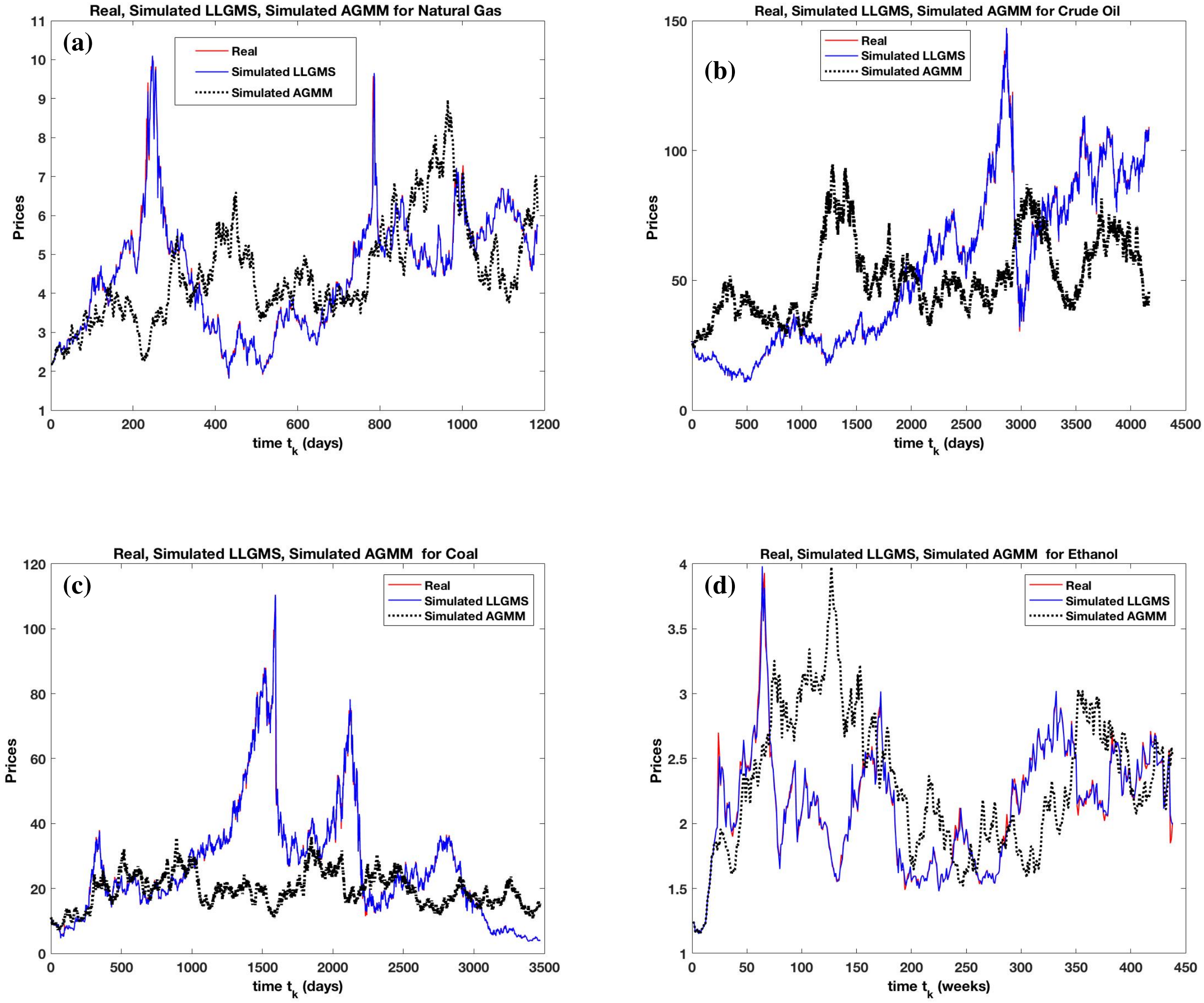

Figure B.20: Real, Simulated Prices using LLGMM, and Simulated Prices using AGMM: initial delay $r = 20$.

Figure B.20: **(a), (b), (c) and (d)** show the graphs of the real, simulated prices using the local lagged adaptive generalized method (LLGMM), and the simulated price using the average of the parameters for Henry Hub natural gas data [14] , daily crude oil data [13], daily coal data [12], and weekly ethanol data [48], respectively, for $r = 20$. The red line represents the real data set y_k, the blue line represent the simulated prices using the LLGMM method, while the black line represent the simulated price (AGMM) using the aggregated parameter estimates $\bar{a}$, $\bar{\mu}$, and $\overline{\sigma^2}$ in Table B.17, Columns 6, 8, and 10, respectively. From these simulated graphs, it is clear that the LLGMM simulation results are more realistic than the AGMM simulation results. This exhibits the superiority of LLGMM over AGMM.

Comparison of Goodness-of-fit Measures for the LLGMM and AGMM methods using initial delay $r = 20$.

Table B.19: Comparison of Goodness-of-fit Measures for the LLGMM and AGMM methods using initial delay $r = 20$.

Goodness of-fit Measure	LLGMM				AGMM			
	Natural gas	Crude oil	Coal	Ethanol	Natural gas	Crude oil	Coal	Ethanol
$\widehat{RAMSE}$	0.0674	0.4625	0.4794	0.0375	1.4968	30.7760	17.7620	0.4356
$\widehat{AMAD}$	1.1318	24.5010	9.4009	0.3213	0.0068	0.0857	0.0833	0.0035
$\widehat{AMB}$	1.1371	27.2707	12.8370	0.3566	1.2267	27.3050	13.1060	0.3579

Appendix B.2. Formulation of Aggregated Generalized Method of Moment (AGMM) for U.S. Treasury Bill and U.S.-U.K. Foreign Exchange rate

The overall descriptive statistics of data sets regarding U.S. Treasury Bill interest rate and U.S.-U.K. foreign exchange rate are recorded in the following table for initial delay $r = 20$.

Table B.20: Descriptive Statistics for $\bar{\beta}, \bar{\mu}, \bar{\delta}, \overline{\sigma}$, and $\bar{\gamma}$ for Interest rate data using initial delay $r = 20$.

$\bar{Y}$	Std(Y)	$\bar{\beta}$	Std(β)	$\bar{\mu}$	Std(μ)	$\bar{\delta}$	Std(δ)	$\bar{\sigma}$	std(σ)	$\bar{\gamma}$	Std(γ)
0.05667	0.0268	0.8739	1.8129	-3.8555	8.7608	1.4600	0.00	0.3753	0.5197	1.4877	0.1357

Table B.21: Descriptive Statistics for $\bar{\beta}, \bar{\mu}, \bar{\delta}, \overline{\sigma}$, and $\bar{\gamma}$ for U.S.-U.K. foreign exchange rate data using initial delay $r = 20$.

$\bar{Y}$	Std(Y)	$\bar{\beta}$	Std(β)	$\bar{\mu}$	Std(μ)	$\bar{\delta}$	Std(δ)	$\bar{\sigma}$	std(σ)	$\bar{\gamma}$	Std(γ)
1.6249	0.1337	1.5120	2.1259	-1.1973	1.6811	1.4892	0.00	0.0243	0.0180	1.08476	1.0050

Tables $B.20$ and $B.21$ show the descriptive statistics for $\bar{\beta}, \bar{\mu}, \bar{\delta}, \overline{\sigma}$, and $\bar{\gamma}$ for the U.S. TBYIR and the U.S.-U.K. FER data, respectively.

In Table $B.22$, the real and the LLGMM simulated rates of the US-TBYIR and the U.S.-U.K. foreign exchange rate (US-UK FER) are exhibited in the first and second columns, respectively. Using the aggregated parameter estimates $\bar{\beta}, \bar{\mu}, \bar{\delta}, \overline{\sigma}$ and $\bar{\gamma}$ in the respective Tables $B.20$ (columns 3, 5, 7, 9 and 11) and Table $B.21$ (columns 3, 5, 7, 9, and 11), the simulated rates for the U.S. TYBIR and the U.S.-U.K. FER are shown in column 3 of Table $B.22$. These estimates are derived using the following discretized system:

$$y_i^{ag} = y_{i-1}^{ag} + (\bar{\beta} y_{i-1}^{ag} + \bar{\mu}(y_{i-1}^{ag})^{\bar{\delta}}) + \bar{\sigma}(y_{i-1}^{ag})^{\bar{\gamma}} \Delta W_i \tag{B.2}$$

where AGMM, y_k^{ag}, y_k at time t_k are defined in $(B.1)$.

Table B.22: Estimates for Real, Simulated value using LLGMM and AGMM methods for U.S. TYBIR and the U.S.-U.K. FER, respectively for initial delay $r = 20$.

t_k	Interest Rate Data			t_k	U.S.-U.K. Rate Data		
	Real	Simulated LLGMM	Simulated AGMM		Real Real	Simulated LLGMM	Simulated AGMM
21	0.0465	0.0459	0.0326	21	1.7448	1.6732	1.655
22	0.0459	0.0467	0.0299	22	1.7465	1.7711	1.6588
23	0.0462	0.0463	0.0342	23	1.7638	1.7588	1.6096
24	0.0464	0.0463	0.034	24	1.874	1.8423	1.6251
25	0.045	0.0457	0.0365	25	1.7902	1.7971	1.6221
26	0.048	0.048	0.0447	26	1.7635	1.7668	1.5984
27	0.0496	0.0496	0.0449	27	1.74	1.7362	1.6368
28	0.0537	0.053	0.0538	28	1.7763	1.7755	1.5795
29	0.0535	0.0529	0.0535	29	1.8219	1.8224	1.5708
30	0.0532	0.0536	0.0489	30	1.8985	1.9002	1.6174
31	0.0496	0.0495	0.0575	31	1.9166	1.8897	1.6403
32	0.0472	0.0479	0.0548	32	1.992	1.9361	1.6425
33	0.0456	0.0453	0.0385	33	1.7741	1.7738	1.6409
34	0.0426	0.0423	0.042	34	1.5579	1.5601	1.6759
35	0.0384	0.0413	0.0339	35	1.5138	1.5017	1.5287
36	0.036	0.0363	0.0384	36	1.5102	1.5028	1.5445
37	0.0354	0.0358	0.0457	37	1.4832	1.5171	1.6334
38	0.0421	0.0434	0.0321	38	1.4276	1.4353	1.6666
39	0.0427	0.043	0.023	39	1.51	1.4972	1.606
40	0.0442	0.044	0.0299	40	1.5734	1.588	1.662
41	0.0456	0.0463	0.0301	41	1.5633	1.5556	1.6305
42	0.0473	0.0462	0.0365	42	1.4966	1.4856	1.5987
43	0.0497	0.0512	0.0341	43	1.4868	1.4914	1.5832
44	0.05	0.0505	0.042	44	1.4864	1.4785	1.621
45	0.0498	0.0497	0.0451	45	1.4965	1.4854	1.6208
⋮	⋮	⋮	⋮		⋮	⋮	⋮
420	0.045	0.0449	0.0337	155	1.5581	1.5635	1.6326
421	0.0457	0.045	0.0309	156	1.6097	1.6195	1.574
422	0.0455	0.0459	0.0389	157	1.6435	1.6089	1.6232
423	0.0472	0.047	0.0306	158	1.5793	1.5817	1.6669
424	0.0468	0.0464	0.0385	159	1.5782	1.5826	1.649
425	0.0486	0.0481	0.0179	160	1.6108	1.6206	1.5725
426	0.0507	0.0499	0.0191	161	1.6368	1.6256	1.6879
427	0.052	0.0514	0.0257	162	1.662	1.6444	1.6681
428	0.0532	0.0539	0.029	163	1.6115	1.6156	1.6534
429	0.0555	0.0546	0.0379	164	1.571	1.5708	1.6387
430	0.0569	0.0588	0.0404	165	1.6692	1.6912	1.6243
431	0.0566	0.056	0.0487	166	1.6766	1.6832	1.5822
432	0.0579	0.0587	0.0432	167	1.7188	1.7224	1.5764
433	0.0569	0.0571	0.0436	168	1.7856	1.7785	1.6206
434	0.0596	0.0602	0.0393	169	1.8225	1.7952	1.6044
435	0.0609	0.0601	0.04	170	1.8699	1.8896	1.6792
436	0.06	0.0601	0.0483	171	1.8562	1.8964	1.5417
437	0.0611	0.0604	0.0292	172	1.772	1.7717	1.6087
438	0.0617	0.0617	0.031	173	1.8398	1.8372	1.5426
439	0.0577	0.0583	0.0379	174	1.8207	1.8214	1.6147
440	0.0515	0.0509	0.0464	175	1.8248	1.8242	1.6544
441	0.0488	0.05	0.0476	176	1.7934	1.7795	1.5929
442	0.0442	0.0441	0.0516	177	1.7982	1.8056	1.5845
443	0.0387	0.0445	0.0675	178	1.8335	1.835	1.6625
444	0.0362	0.0313	0.0484	179	1.934	1.9301	1.5832
445	0.0349	0.0386	0.0484	180	1.9054	1.8939	1.5472

In Table $B.22$, we show a side by side comparison of the estimates for the simulated value using LLGMM and AGMM methods for U.S. Treasury Bill interest rate and U.S.-U.K. foreign exchange rate using initial delay $r = 20$.

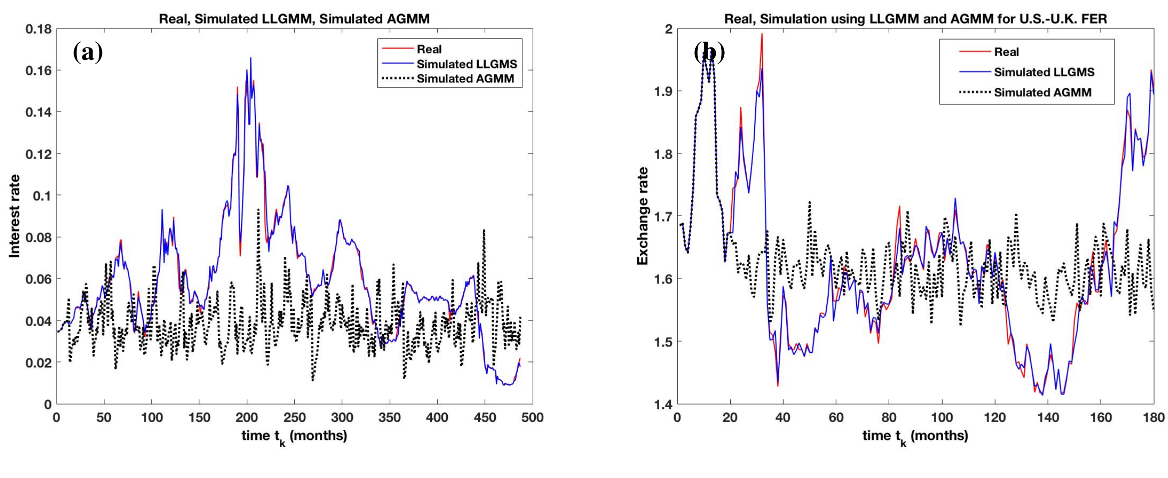

Figure B.21: Real, Simulated paths using LLGMM and AGMM methods for U.S. Treasury Bill interest rate and U.S.-U.K. foreign exchange rate for initial delay $r = 20$.

Appendix C. Comparative study of the LLGMM with OCBGMM Methods:

In this Appendix, an additional detailed comparisons regarding the theoretical, graphical and performance of the LLGMM and OCBGMM methods are presented in *Appendix C*.1, *Appendix C*.2, and *Appendix C*.3, respectively. In fact, by employing three statistical goodness-of-fit measures [11], a comparative performance analysis of forecasting and ranking of the LLGMM and OCBGMM based methods are presented in *Appendix C*.3.

Appendix C.1. Theoretical Comparison Between LLGMM and OCBGMM

Based on the foundations of the analytical, conceptual, computational, mathematical, practical, statistical and theoretical motivations and developments outlined in Sections 2, 3, 4, 5 and 6, we summarize the comparison between the innovative approach LLGMM with the existing and newly developed OCBGMM methods in separate tables in a systematic manner.

In the following, we state the differences between the LLGMM method and existing orthogonality condition based GMM/IRGMM-Algebraic and the newly formulated GMM/IRGMM-Analytic methods together with AGMM.

Table C.23: Mathematical Comparison Between the LLGMM and OCBGMM

Feature	LLGMM	OCBGMM-Algebraic	OCGMM-Analytic	Justifications
Composition:	Seven components	Five components	Five components	Sections 1, 2
Model:	Development	Selection	Development/ Selection	Sections 1, 2
Goal:	Validation	Specification/Testing	Validation/Testing	Sections 1, 2
Discrete-Time Scheme:	Constructed from SDE	Using Econometric specification	Constructed from SDE	Remark 2.8
Formation of Orthogonality Vector:	Using stochastic calculus	Formed using algebraic manipulation	Using Stochastic calculus	Remarks 2.2, 2.7, 2.8

Table C.24: Intercomponent Interaction Comparison Between LLGMM and OCBGMM

Feature	LLGMM	OCBGMM-Algebraic	OCGMM-Analytic	Justifications
Moment Equations:	Local Lagged adaptive process	Single/ global system	Single/ global system	Remarks 3.2a, and 3.2b
Type of Moment Equations:	Local lagged adaptive process	Single-shot	Single-shot	Remarks 2.6, 2.8, and 2.9
Component Interconnections:	Strongly connected	Weakly connected	Weakly connected	Remarks 2.6, 2.7, 2.8, 2.9, and 3.2
Dynamic and Static:	Discrete-time Dynamic	Static	Static	Remarks 3.2 and Lemma 1 (Section 2)

Table C.25: Conceptual Computational Comparison Between LLGMM and OCBGMM

Feature	LLGMM	OCBGMM-Algebraic	OCGMM-Analytic	Justifications
Local admissible Lagged Data Size:	Multi-choice	Single-choice/data size	Single-choice/data size	Definition 3.3, Remark 3.2, Subsection 3.2
Local admissible class of lagged finite restriction sequences	Multi-choice	Single-choice data sequence	Single-choice data sequence	Adapted finite restricted sample data: Definition 3.4, Remark 3.2, Subsection 3.2
Local admissible finite sequence parameter estimates:	Multi-choice	Single-shot estimate	Single-shot estimates	Subsection 3.2
Local admissible sequence of finite state simulation values:	Multi-choice	Single-choice	Single-choice	Remark 3.2, Subsection 3.3
Quadratic Mean Square ϵ-sub-optimal errors:	Multi-choice	Singe-error	Single-error	Remark 3.2, Subsection 3.3
ϵ-sub-optimal local lagged sample size:	Multi-choice	Single-choice	Single-choice	Definition 12, Remark 3.2, Subsection 3.3
ϵ-best sub optimal sample size:	ϵ-best sub optimal choice	No-choice	No-choice	Remark 3.2, Subsection 3.3
ϵ-best sub optimal parameter estimated:	ϵ-best estimators	No-choice	No-choice	Remark 3.2, Subsection 3.3
ϵ-best sub optimal state estimate:	ϵ-best sub optimal choice	No-choice	No-choice	Remark 3.2, Subsection 3.3

Table C.26: Theoretical Performance Comparison Between LLGMM and OCBGMM

Feature	LLGMM	OCBGMM-Algebraic	OCGMM-Analytic	Justifications
Data Size:	Reasonable Size	Large Data Size	Large Data Size	For Respectable results
Stationary Condition:	Not required	Need Ergotic/ Asymptotic stationary	Need Ergodic / Asymptotic	For Reasonable results
Multi-level optimization:	At least 2 level hierarchical optimization	Single-shot	Single-shot	Not comparable
Admissible Strategies:	Multi-choices	Single-shot	Single-shot	Not comparable
Computational Stability:	Algorithm Converges in a single / double digit trials	Single-choice	Single-choice	Simulation results
Significance of lagged adaptive process:	Stabilizing agent	Non-existence of the feature	Non-existence	Not comparable
Operation:	Operates like Discrete time Dynamic Process	Operates like a static dynamic process	Operates like static process	Obvious, details see Sections 3, 4, 5, 6 and 7

Appendix C.2. Graphical Comparison of the LLGMM with OCBGMM Methods

Parameter Estimates of (7.1) **using LLGMM and OCBGMM Methods:** Using the LLGMM method, the parameter estimates $\alpha_{\hat{m}_k,k}$, $\beta_{\hat{m}_k,k}$, $\sigma_{\hat{m}_k,k}$, and $\gamma_{\hat{m}_k,k}$ of (7) in USTBIR are shown in Table *C*.27. Here, we use $\epsilon = 0.001$, $p = 2$, and initial delay $r = 20$.

Table C.27: Estimates for $\hat{m}_k$, $\alpha_{\hat{m}_k,k}$, $\beta_{\hat{m}_k,k}$, $\sigma_{\hat{m}_k,k}$, $\gamma_{\hat{m}_k,k}$ for U.S. Treasury Bill interest rate data using LLGMM.

t_k	interest Rate				
	$\hat{m}_k$	$\alpha_{\hat{m}_k,k}$	$\beta_{\hat{m}_k,k}$	$\sigma_{\hat{m}_k,k}$	$\gamma_{\hat{m}_k,k}$
21	**2**	**0.0334**	**-0.7143**	**0.0446**	**1.5**
22	**3**	**0.0427**	**-0.9254**	**0.0766**	**1.5**
23	**4**	**0.0425**	**-0.9198**	**0.0914**	**1.5**
24	**5**	**0.0413**	**-0.8937**	**0.09**	**1.5**
25	**4**	**0.1042**	**-2.2619**	**0.1003**	**1.5**
26	**19**	**0.0002**	**0.0083**	**0.1043**	**1.5**
27	**14**	**0.0024**	**-0.0359**	**0.1281**	**1.5**
28	**5**	**-0.023**	**0.5207**	**0.3501**	**1.5**
29	**13**	**0.0037**	**-0.0573**	**0.1652**	**1.5**
30	**18**	**0.0008**	**0.001**	**0.1447**	**1.5**
31	**3**	**-0.3827**	**7.1316**	**0.26**	**1.5**
32	**19**	**0.006**	**-0.1213**	**0.1828**	**1.5**
33	**6**	**0.0063**	**-0.1359**	**0.343**	**1.5**
34	**19**	**0.0081**	**-0.1705**	**0.1993**	**1.5**
35	**4**	**-0.0166**	**0.2984**	**0.3509**	**1.5**
36	**4**	**-0.0059**	**0.0721**	**0.2318**	**1.5**
37	**9**	**-0.0035**	**0.0324**	**0.3114**	**1.5**
38	**14**	**0.0051**	**-0.1186**	**0.3385**	**1.5**
39	**20**	**0.0059**	**-0.1294**	**0.282**	**1.5**
40	**12**	**0.0075**	**-0.185**	**0.3447**	**1.5**
41	**12**	**0.0099**	**-0.2379**	**0.3579**	**1.5**
42	**4**	**-0.0089**	**0.2335**	**0.3562**	**1.5**
43	**7**	**0.0074**	**-0.1289**	**0.4654**	**1.5**
44	**7**	**0.0182**	**-0.3677**	**0.4206**	**1.5**
45	**6**	**0.0106**	**-0.2031**	**0.2356**	**1.5**
⋮	**⋮**	**⋮**	**⋮**	**⋮**	**⋮**
420	**3**	**0.0836**	**-1.9**	**0.1006**	**1.5**
421	**8**	**0.0428**	**-0.9671**	**0.783**	**1.5**
422	**3**	**0.0359**	**-0.7857**	**0.1702**	**1.5**
423	**8**	**0.0127**	**-0.2766**	**0.1719**	**1.5**
424	**6**	**0.0178**	**-0.3857**	**0.1636**	**1.5**
425	**6**	**0.0177**	**-0.3685**	**0.1829**	**1.5**
426	**18**	**0.0146**	**-0.3172**	**0.3871**	**1.5**
427	**8**	**0.0017**	**-0.012**	**0.1788**	**1.5**
428	**4**	**0.009**	**-0.1489**	**0.1341**	**1.5**
429	**9**	**-0.0059**	**0.1469**	**0.1616**	**1.5**
430	**13**	**-0.0046**	**0.116**	**0.191**	**1.5**
431	**9**	**0.0039**	**-0.0532**	**0.1369**	**1.5**
432	**9**	**0.0027**	**-0.0287**	**0.1109**	**1.5**
433	**3**	**0.0857**	**-1.5**	**0.0952**	**1.5**
434	**9**	**0.0102**	**-0.1661**	**0.1197**	**1.5**
435	**9**	**0.0075**	**-0.114**	**0.107**	**1.5**
436	**5**	**0.029**	**-0.485**	**0.1446**	**1.5**
437	**4**	**0.0476**	**-0.784**	**0.2163**	**1.5**
438	**9**	**0.0122**	**-0.1966**	**0.1054**	**1.5**
439	**4**	**0.1626**	**-2.6824**	**0.1248**	**1.5**
440	**20**	**0.0072**	**-0.1278**	**0.1916**	**1.5**
441	**19**	**0.0084**	**-0.1502**	**0.2016**	**1.5**
442	**17**	**0.0024**	**-0.0479**	**0.2369**	**1.5**
443	**7**	**-0.0153**	**0.2236**	**0.2687**	**1.5**
444	**3**	**0.0054**	**-0.2188**	**0.3887**	**1.5**
445	**16**	**-0.0076**	**0.1177**	**0.2528**	**1.5**

Table *C*.27 shows the parameter estimates of $\hat{m}_k$, $\alpha_{\hat{m}_k,k}$, $\beta_{\hat{m}_k,k}$, $\sigma_{\hat{m}_k,k}$, $\gamma_{\hat{m}_k,k}$ in the model (7.1) for U.S. Treasury Bill interest rate data. As noted before, the range of the ϵ-best sub-optimal local admissible sample size $\hat{m}_k$ for ant time $t_k \in [21, 45] \bigcup [420, 445]$ is $2 \le \hat{m}_k \le 20$. We also draw the similar conclusions (a) to (e) as outlined in Remark 4.1.

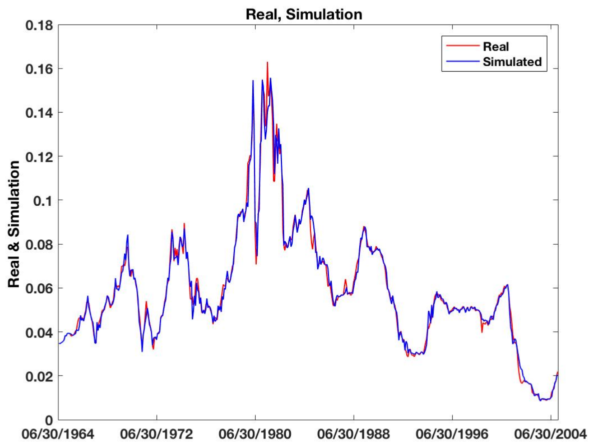

Figure C.22: Real and simulated path using LLGMM method

Figure *C*.22 shows the real and simulated path of the monthly interest rate data [44] using the LLGMM method. The root mean square error of the simulated value is 0.0027.

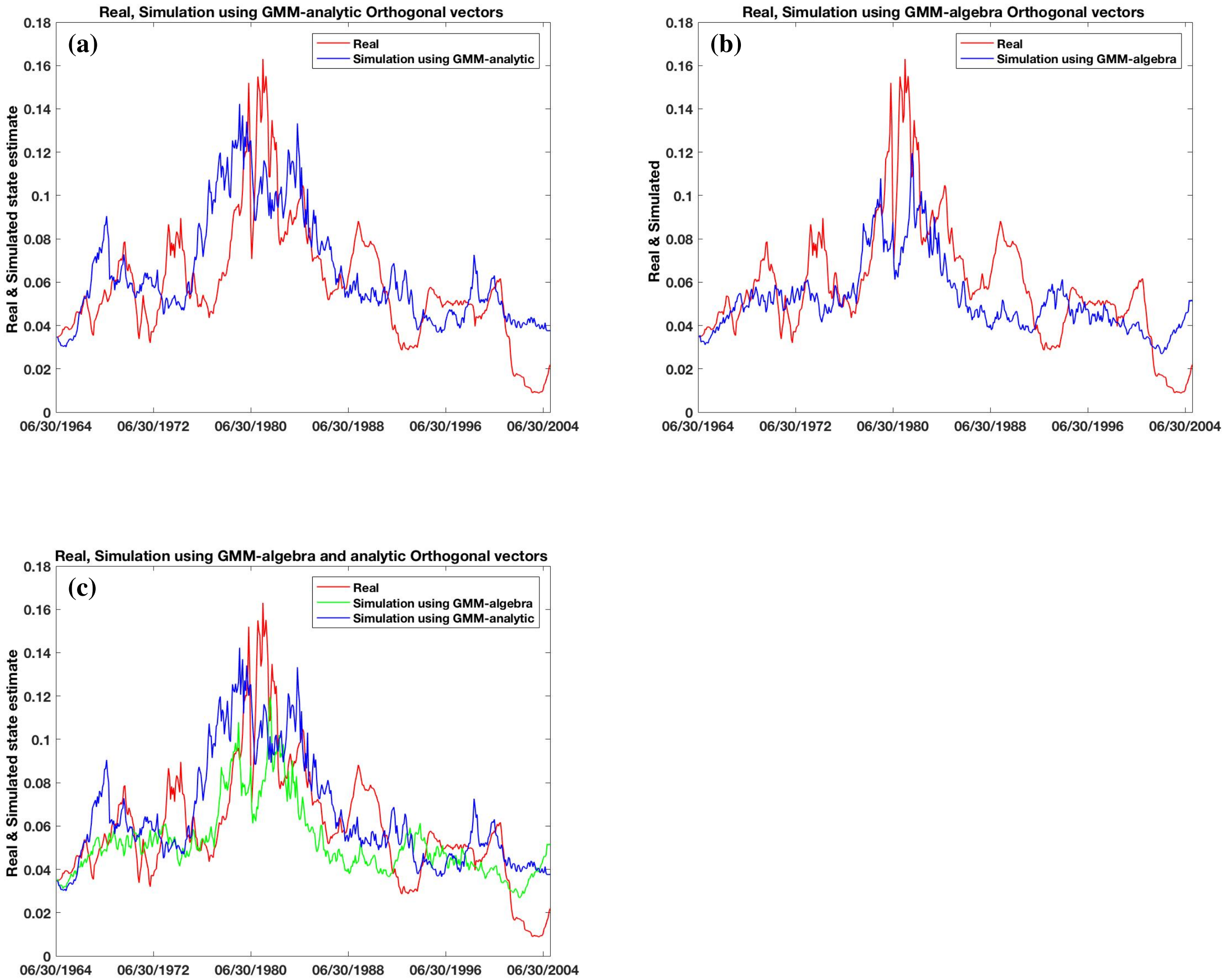

Figure C.23: Comparison of simulation result using GMM-Analytic and GMM-Algebraic methods

Figures *C*.23 (a) and (b) show the real and simulated value of the monthly interest rate data [44] using the GMM-Analytic and GMM-Algebraic methods, respectively. The root mean square errors of simulated values are shown in Table 10. Figure *C*.23(c) shows the comparison between the real and simulated values of GMM-Analytic and GMM-Algebraic methods. The red, green, and blue line represent the real data path [44], the simulated path using GMM-Algebraic, and the GMM-Analytic, respectively.

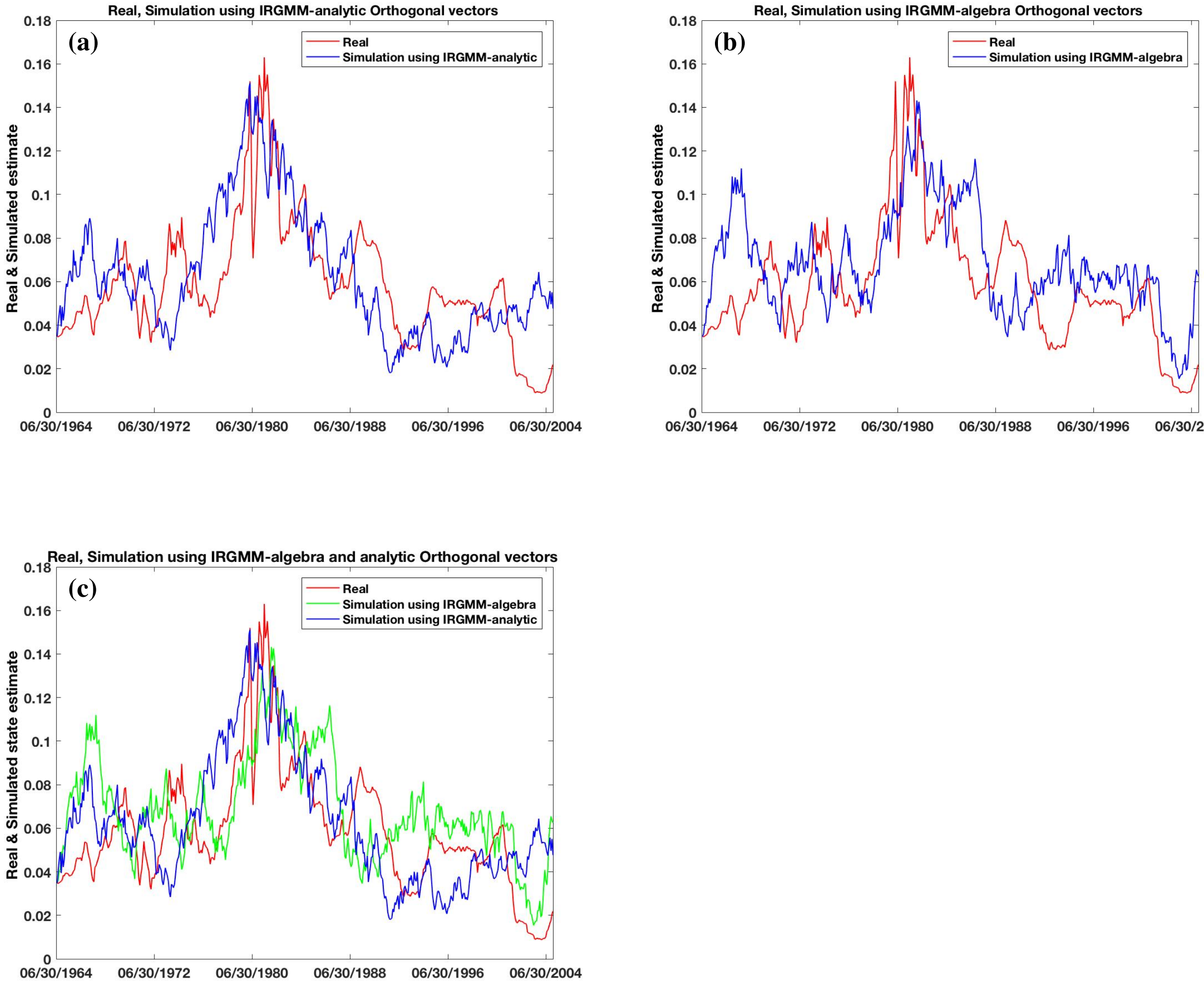

Figure C.24: Comparison of simulation result using IRGMM-Analytic and IRGMM-Algebraic methods

Figures C.24(a) and (b) show the real and simulated value of the monthly interest rate data [44] using the IRGMM-Analytic and IRGMM-Algebraic, respectively. The root mean square errors of simulated values are shown in Table 10. Figure C.24(c) shows the comparison between the real and simulated values of IRGMM-Analytic and IRGMM-Algebraic method. The red, green, and blue curve represents the real data path [44], simulated path using IRGMM-Algebraic, and GMM-Analytic, respectively.

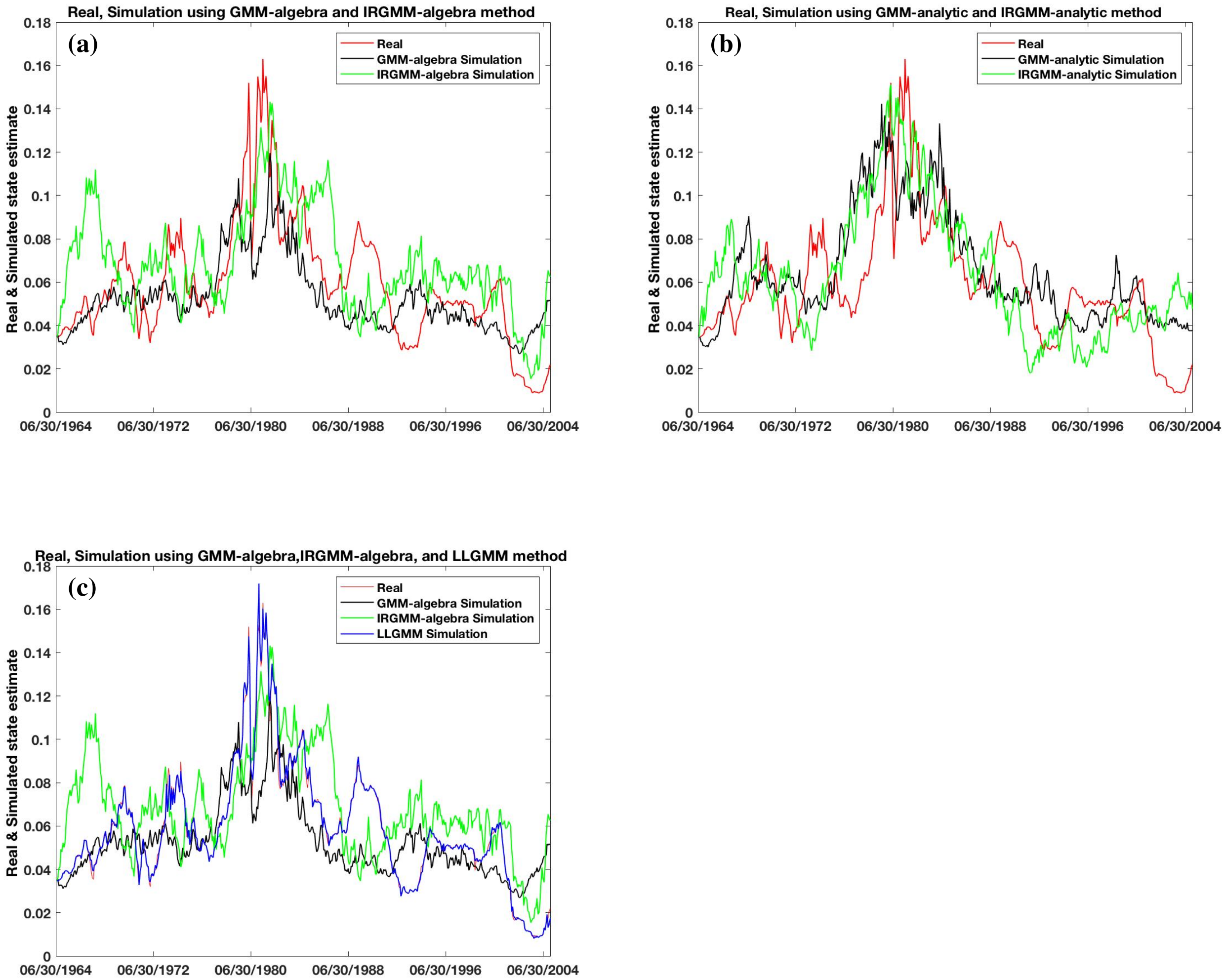

Figure C.25: Comparison of simulation results of GMM-analytic, IRGMM-analytic, GMM-algebraic and IRGMM-algebraic methods together with AGMM method

Figure C.25(a) compares the simulation results using GMM-algebraic and IRGMM-algebraic. The blue denotes the GMM-algebraic simulation curve while the green line represents the IRGMM-algebraic simulation curve. Figure C.25(b) compares the simulation results using the GMM-Analytic, and IRGMM-Analytic represented by the black, and green lines, respectively. Figure C.25(c) compares the simulation results using the GMM-Algebra, IRGMM-Algebra, and LLGMM represented by the black, green, and blue lines, respectively.

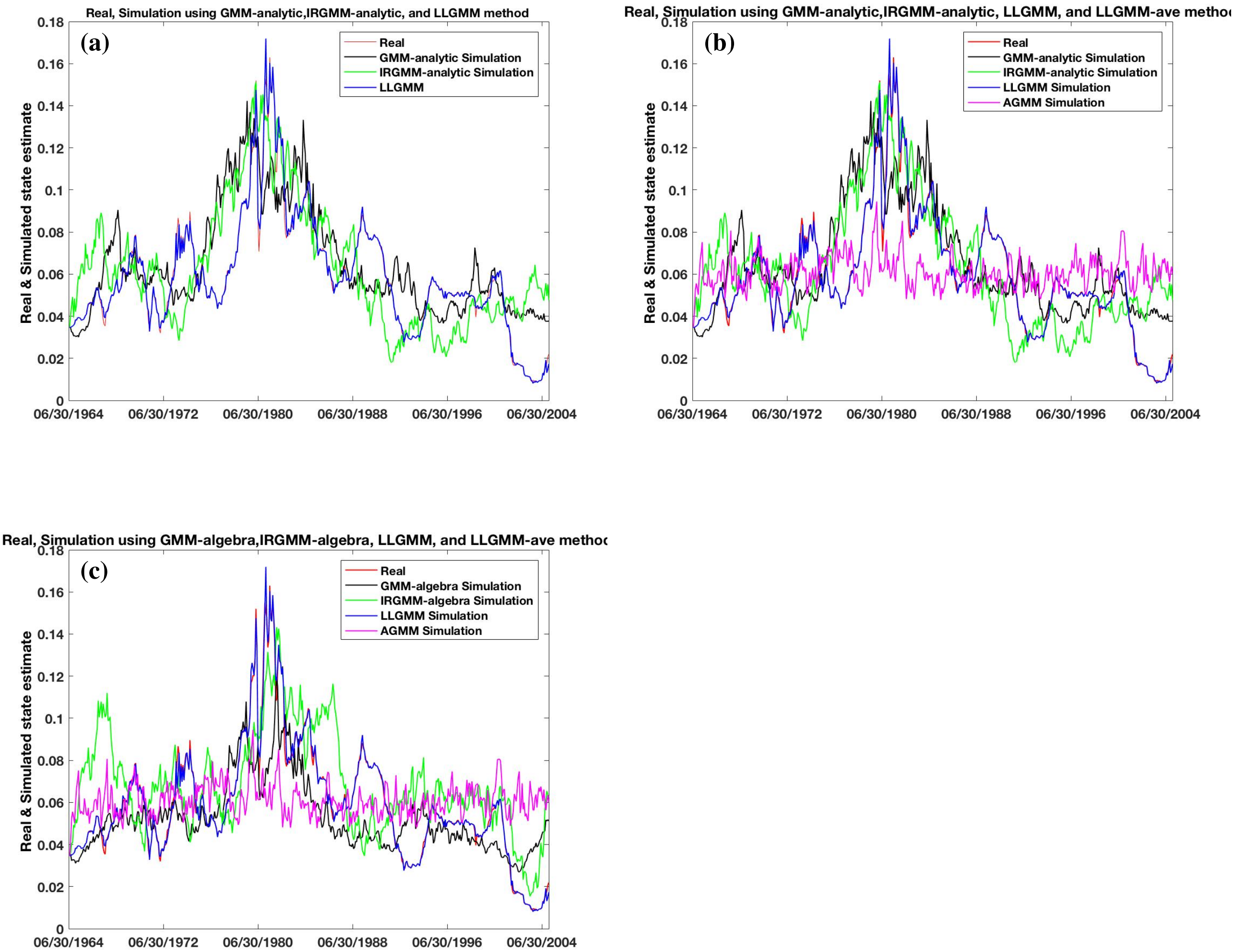

Figure C.26: Comparison of simulation results for GMM-Analytic, IRGMM-analytic, GMM-Algebraic and IRGMM-Algebraic methods as well as the LLGMM and AGMM methods

Figure C.26(a) compares the simulation results using GMM-analytic, IRGMM-analytic and the LLGMM methods. The GMM-analytic, IRGMM-analytic and the LLGMM simulation results are exhibited by the black, green and blue lines, respectively. Figure C.26(b) compares the simulation results using the GMM-Algebraic, IRGMM-Algebraic, LLGMM and AGMM methods represented by the black, green, blue and magenta lines, respectively. Figure C.26(c) compares the simulation results using the GMM-Analytic, IRGMM-Analytic, LLGMM and AGMM methods represented by the black, green, blue and magenta curves, respectively.

Comparative Analysis of Forecasting with 95% **Confidence Intervals:** Using data set from June 1964 to December 1989, the parameters of model (7.1) are estimated. Using these parameter estimates, we forecasted the monthly interest rate for January 1, 1990 to December 31, 2004. Table C.28 shows the parameter estimates in the context of the data from June 1964 to December 1989.

Table C.28: Parameter estimates in (7.1) in the context of data July 1964-December 1989

Method	α	β	σ	γ
GMM-Algebraic	0.0033	-0.051	0.4121	1.5311
GMM-Analytic	0.0009	-0.0155	0.0197	0.4854
IRGMM-Algebraic	0.0023	-0.0421	0.3230	1.3112
IRGMM-Analytic	0.0084	-0.1436	0.1073	1.3641
AGMM	0.0154	-0.2497	0.2949	1.4414

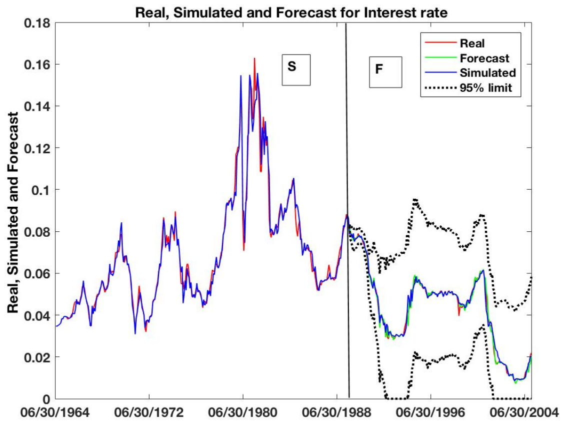

Figure C.27: Real, Simulation and Forecast state estimates using LLGMM method

In Figure $C.27$, region S shows the real, simulated value using the monthly interest rate data from June 30, 1964 to December 31, 1989 [44]. In the F region (forecasting region), the estimated parameters in the context of the data set [44] are used to forecast interest rate from January 1, 1990 to December 31, 2004 using the LLGMM method.

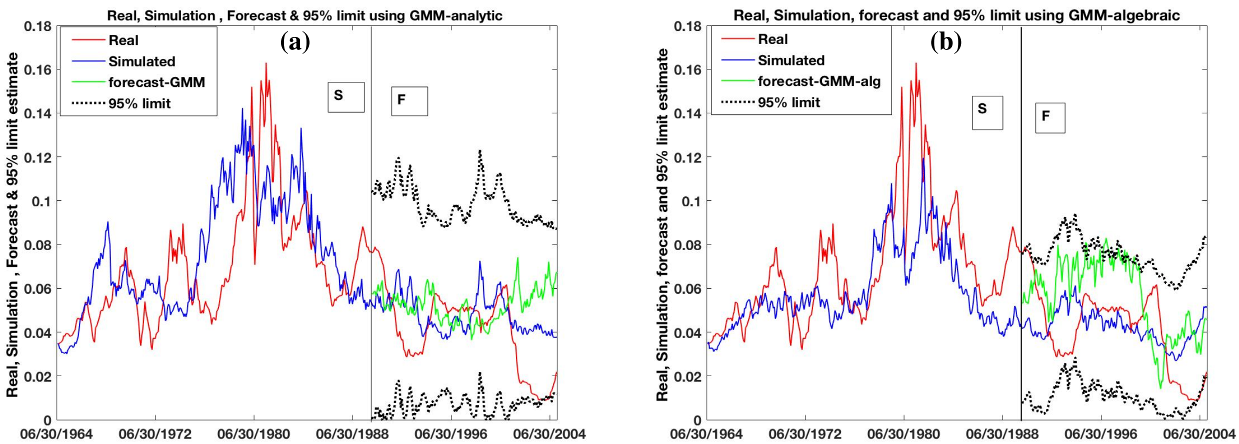

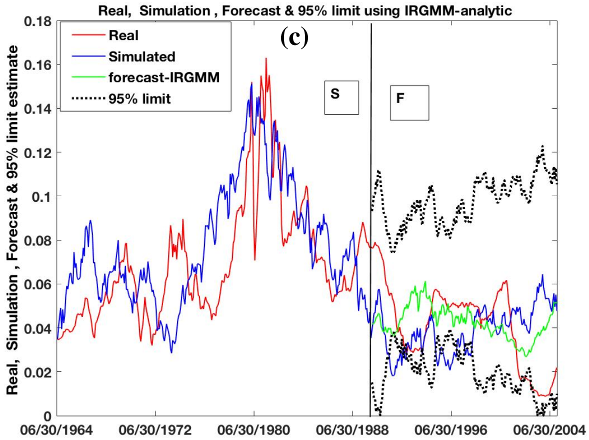

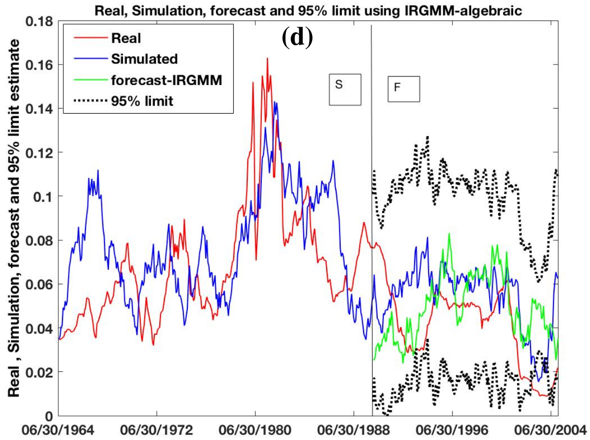

Figure C.28: Real, Simulation and Forecast estimates using GMM-Algebraic, GMM-Analytic, IRGMM-Algebraic and IRGMM-Analytic methods

Figure C.28(a), (b), (c) and (d) exhibit the side-by-side comparison of the simulated forecasting results of the GMM-Analytic, GMM-Algebraic, IRGMM-Analytic, and IRGMM-Algebraic methods, respectively. The S region represents the simulation region based on the real data while the F region represents the forecasting region. In addition, the 95% confidence level of the simulation results are also shown (in black).

Appendix C.3. Performance Comparisons of LLGMM Method with Existing and Newly Introduced OCBGMM Methods Using Energy Commodity Stochastic Model

Using the stochastic dynamic model in (2.8) of energy commodity represented by stochastic differential equation:

$$dy = ay(\mu - y)dt + \sigma(t, y_t)ydW(t), \quad y(t_0) = y_0, \tag{C.1}$$

the orthogonality condition parameter vector (OCPV) is described in (2.13) in Remark (2.2). Based on discretized scheme using the econometric specification [9], the orthogonality condition parameter vector in the context of algebraic manipulation is as [9]: OCBGMM looks like

$$\begin{cases} y_t - y_{t-1} - ay_{t-1}(\mu - y_{t-1})\Delta t \\ y_{t-1}\left(y_t - y_{t-1} - ay_{t-1}(\mu - y_{t-1})\Delta t\right) \\ \left(y_t - y_{t-1} - ay_{t-1}(\mu - y_{t-1})\Delta t)^2 - \sigma^2 y_{t-1}^2\right] \end{cases} \tag{C.2}$$

The goodness-of-fit measures are computed using pseudo-data sets of the same sample size as the real data set: (i) $N = 1184$ days for natural gas data, (ii) $N = 4165$ days for crude oil data, (iii) $N = 3470$ for coal data, and (iv) $N = 438$ weeks for ethanol data. The smallest value of $\widehat{RAMSE}$ for all method is italicized.

Table C.29: Comparison of Parameter estimates of model (C.1) using GMM-Algebraic, GMM-Analytic, IRGMM-Algebraic, IRGMM-Analytic and AGMM for natural Gas Data

Method	a	μ	σ^2	$\widehat{RAMSE}$	$\widehat{AMAD}$	$\widehat{AMB}$
GMM-Algebraic	0.0023	5.3312	0.0019	1.5119	0.0663	1.1488
GMM-Analytic	0.0018	5.4106	0.0015	1.5014	0.0538	1.1677
IRGMM-Algebraic	0.2000	4.4996	0.0010	1.4985	0.0050	1.2299
IRGMM-Analytic	0.1998	4.4917	0.0011	1.4901	0.0044	1.2329
AGMM	0.1867	4.5538	0.0013	1.4968	0.0068	1.2267
LLGMM				*0.0674**	1.1318	1.1371

Table C.30: Comparison of Parameter estimates of model (C.1) using GMM-Algebraic, GMM-Analytic, IRGMM-Algebraic, IRGMM-Analytic and AGMM for crude oil data

Method	a	μ	σ^2	$\widehat{RAMSE}$	$\widehat{AMAD}$	$\widehat{AMB}$
GMM-Algebraic	0.0023	54.4847	0.0005	39.2853	0.3577	29.1587
GMM-Analytic	0.0021	51.2145	0.0006	38.8007	0.5181	28.7414
IRGMM-Algebraic	0.0000	88.5951	0.0005	30.7511	0.0920	27.5791
IRGMM-Analytic	0.0021	51.2195	0.0005	28.9172	0.2496	27.3564
AGMM	0.0215	54.0307	0.0005	30.776	0.0857	27.3050
LLGMM				*0.4625**	24.501	27.2707

Table C.31: Comparison of Parameter estimates of model (C.1) using GMM-Algebraic, GMM-Analytic, IRGMM-Algebraic, IRGMM-Analytic and AGMM for coal Data

Method	a	μ	σ^2	$\widehat{RAMSE}$	$\widehat{AMAD}$	$\widehat{AMB}$
GMM-Algebraic	0.0000	94.4847	0.0006	22.6866	0.2015	16.3444
GMM-Analytic	0.0000	94.4446	0.0006	21.6564	0.2121	16.3264
IRGMM-Algebraic	0.0027	34.4838	0.0013	17.6894	0.3438	13.4981
IRGMM-Analytic	0.0021	23.1151	0.0005	17.6869	0.3448	13.4989
AGMM	0.0464	27.0567	0.0014	17.7620	0.0833	13.106
LLGMM				*0.4794**	9.4009	12.8370

Table C.32: Comparison of Parameter estimates of model (C.1) using GMM-Algebraic, GMM-Analytic, IRGMM-Algebraic, IRGMM-Analytic and AGMM for Ethanol data

Method	a	μ	σ^2	$\widehat{RAMSE}$	$\widehat{AMAD}$	$\widehat{AMB}$
GMM-Algebraic	0.0000	94.4847	0.0006	22.6866	0.2015	16.3444
GMM-Analytic	0.0000	94.4446	0.0006	21.6564	0.2121	16.3264
IRGMM-Algebraic	0.0014	3.4506	0.0026	0.5844	0.0322	0.4346
IRGMM-Analytic	0.0015	3.4506	0.0026	0.5813	0.0336	0.4303
AGMM	0.3167	2.166	0.0018	0.4356	0.0035	0.3579
LLGMM				*0.0375**	0.3213	0.3566

Tables $C.29$, $C.30$, $C.31$, and $C.32$ show a comparison parameter estimates of model ($C.1$) and the goodness-of-fit measures $\widehat{RAMSE}$, $\widehat{AMAD}$ and $\widehat{AMB}$ using GMM-Algebraic, GMM-Analytic, IRGMM-Algebraic, IRGMM-Analytic, AGMM and LLGMM method for the daily natural gas data [14] , daily crude oil data [13], daily coal data [12], and weekly ethanol data [48], respectively. The LLGMM estimates are derived using initial delay $r = 20$, $p = 2$ and $\epsilon = 0.001$. Among all methods under study, the LLGMM method generates the smallest $\widehat{RAMSE}$ value. In fact, the $\widehat{RAMSE}$ value is smaller than the 1/22, 1/62, 1/36, and 1/10 of any other $\widehat{RAMSE}$ values regarding the natural gas, crude oil, coal and ethanol, respectively. This exhibits the superiority of the LLGMM method over all other methods. We further observe that the LLGMM approach yields the smallest $\widehat{AMB}$ and highest $\widehat{AMAD}$ value regarding the natural gas, crude oil, coal and ethanol. The high value of $\widehat{AMAD}$ for the LLGMM method signifies that LLGMM method captures the influence of random environmental fluctuations on the dynamic of energy commodity process. From Remark 4.3, the smallest $\widehat{RAMSE}$, highest $\widehat{AMAD}$ and smallest $\widehat{AMB}$ value under the LLGMM method exhibits the superior performance under the three goodness-of-fit measures.

Ranking of Methods under Goodness of Fit Measure

Method	RANK OF METHODS UNDER GOODNESS OF FIT MEASURE											
	Natural gas			Crude oil			Coal			Ethanol		
	$\widehat{RAMSE}$	$\widehat{AMAD}$	$\widehat{AMB}$	$\widehat{RAMSE}$	$\widehat{AMAD}$	$\widehat{AMB}$	$\widehat{RAMSE}$	$\widehat{AMAD}$	$\widehat{AMB}$	$\widehat{RAMSE}$	$\widehat{AMAD}$	$\widehat{AMB}$
GMM-Algebraic	6	2	2	6	3	6	6	5	6	6	3	6
GMM-Analytic	5	3	3	5	2	5	5	4	5	5	2	5
IRGMM-Algebraic	4	5	5	3	5	4	4	3	3	4	5	4
IRGMM-Analytic	2	6	6	2	4	3	3	2	4	3	4	3
AGMM	3	4	4	4	6	2	2	6	2	2	6	2
LLGMM	1	1	1	1	1	1	1	1	1	1	1	1

Table C.33: Ranking result for Natural gas, Crude oil, Coal and Ethanol Under three Statistical measures.

Remark Appendix C.1. The ranking of LLGMM is top one in all three Goodness-of-fit statistical measures for all four energy commodity data sets. Moreover, one of the IRGMM-Analytic and AGMM is ranked either as top two or three under $\widehat{RAMSE}$ measure. This exhibits the influence of the usage of stochastic calculus based orthogonality condition parameter vectors (OCPV-Analytic).

Appendix D. Comparative analysis of LLGMM with Existing Nonparametric Statistical Methods

In this section, we compare our LLGMM method with existing nonparametric methods. We consider the following existing nonparametric methods.

Appendix D.1. Nonparametric estimation of nonlinear dynamics by metric-based local linear approximation (LLA)

The LLA method [39] assumes no functional form of a given model but estimates from experimental data by approximating the curve implied by the function of the tangent plane around the neighborhood of a tangent point. Suppose the state of interest x_t at time t is differentiable with respect to t and satisfies $dx_t = f(x_t)dt$, where $f : \Re^k \to \Re$

is a smooth map, $x_t \in \Re^k$. The approximation of the curve $f(x_t)$ in a neighborhood $U_\epsilon(x_0) = \{x : \ d(x, x_0) < \epsilon\}$ is defined by a tangent plane at x_0:

$$y_t = f(x_0) + \sum_{i=1}^{k} \frac{\partial f}{\partial x_i}(x_0)(x_i - x_0),$$

where d is a metric on $\Re^k$. Allowing error in the equation and assigning a weight $w(x_t)$ to each error terms ϵ_t, the method reduces to estimating parameters $\beta_i = \frac{\partial f}{\partial x_i}(x_0)$, $i = 1, 2, ..., k$ in the equation

$$w(t)y_t = \beta_0 \cdot w(x_t) + \sum_{i=1}^{k} \beta_i \cdot w(x_t)(x_{t,i} - x_{0,i}).$$

Applying the standard linear regression approach, the least square estimate $\hat{\boldsymbol{\beta}}$ is given by

$$\hat{\boldsymbol{\beta}} = \left(\tilde{\mathbf{X}}^T \tilde{\mathbf{X}}\right)^{-1} \tilde{\mathbf{X}}^T \tilde{\mathbf{Y}}, \tag{D.1}$$

where

$$\begin{aligned}
\tilde{\mathbf{x}}_i &= \left(w(x_{t_1})(x_{t_1,i} - x_{0,i}), ..., w(x_{t_n})(x_{t_n,i} - x_{0,i})\right)^T, \quad i = 1, ..., k \\
\tilde{\mathbf{w}} &= \left(w(x_{t_1}), ..., w(x_{t_n})\right)^T \\
\tilde{\mathbf{Y}} &= \left(w(x_{t_1})y_{t_1}, ..., w(x_{t_n})y_{t_n}\right)^T \\
\tilde{\mathbf{X}} &= (\tilde{\mathbf{w}}, \tilde{\mathbf{x}}_1, ..., \tilde{\mathbf{x}}_k)
\end{aligned}$$

Particularly, the trajectory $f(x_{t_i})$ is estimated by choosing $x_0 = x_{t_i}$, for each $i = 1, 2, ..., n$. As discussed in [39], we use $d(x, x_0) = |x - x_0|$, where $|.|$ is the standard Euclidean metric on $\Re^k$, and $w(x) = \phi(d(x, x_0))$, where $\phi(u) = K(u/\epsilon)$ and K is the Epanechnikov Kernel [39] $K(x) = 0.75(1 - x^2)_+$.

Appendix D.2. Risk Estimation and Adaptation after Coordinate Transformation (REACT) method

Given n pairs of observations (x_1, Y_1), ..., (x_n, Y_n). Using the REACT method [47], the response variable Y is related to the covariate x (called a feature) by the equation

$$Y_i = r(x_i) + \sigma\epsilon_i, \tag{D.2}$$

where $\epsilon_i \sim N(0,1)$ are identically independently distributed, and $x_i = \frac{i}{n}$, $i = 1, 2, ..., n$ and the function $r(x)$, approximated using orthogonal cosine basis $\phi_i,\ i = 1, 2, 3, ...$ of $[0, 1]$ described by

$$\phi_1(x) \equiv 1, \quad \phi_j(x) = \sqrt{2}\cos((j-1)\pi x), \quad j \geq 2. \tag{D.3}$$

is expanded as

$$r(x) = \sum_{j=1}^{\infty} \theta_j \phi_j(x), \tag{D.4}$$

where $\theta_j = \int_0^1 \phi_j(x) r(x) dx$, is approximated. The function estimator $\hat{r}(x) = \sum_{j=1}^{\hat{J}} Z_j \phi_j(x)$, where $Z_j = \frac{1}{n} \sum_{i=1}^{n} Y_i \phi_j(x_i)$, $j = 1, 2, ..., n$ and $\hat{J}$ is found so that the risk estimator $\hat{R}(J) = \frac{J\hat{\sigma}^2}{n} + \sum_{j=J+1}^{n} \left(Z_j^2 - \frac{\hat{\sigma}^2}{n}\right)$ is minimized, $\hat{\sigma}^2$ is the estimator of variance of Z_j.

Appendix D.3. Exponential Moving Average method (EMA)

The EMA [27] for an observation y_t at time t may be calculated recursively as

$$S_t = \alpha y_t + (1-\alpha) S_{t-1}, \quad t = 1, 2, 3, ..., n \tag{D.5}$$

where $0 < \alpha \leq 1$ is a constant that determines the depth of memory of S_t.

Appendix D.4. ***Goodness-of-fit Measures for the LLA, REACT, and EMA methods***

In this subsection, we show the Goodness-of-fit Measures for the LLA, REACT, and EMA methods. We use $\hat{J} = 183$ for the REACT method and $\alpha = 0.5$ for the EMA method.

Goodness of-fit Measure	LLGMM method				LLA method				REACT method				EMA method			
	Natural gas	Crude oil	Coal	Ethanol	Natural gas	Crude oil	Coal	Ethanol	Natural gas	Crude oil	Coal	Ethanol	Natural gas	Crude oil	Coal	Ethanol
$\widehat{RAMSE}$	0.0674	0.4625	0.4794	0.0375	0.3114	1.9163	2.1645	0.2082	0.1895	2.0377	2.0162	0.0775	0.1222	0.7845	0.8233	0.0682
$\widehat{AMAD}$	1.1318	24.5010	9.4009	0.3213	1.1406	24.3266	9.4511	0.3290	1.1779	24.6967	9.3791	0.3291	1.1336	24.5858	9.4183	0.3159
$\widehat{AMB}$	1.1371	27.2707	12.8370	0.3566	1.2375	27.2713	12.8388	0.3677	1.12352	27.2711	12.8369	0.3566	1.2352	27.2710	12.8370	0.3567

Table D.34: Goodness-of-fit Measures for the LLGMM, REACT, and EMA methods

Comparison of the results derived using these non-parametric methods with the LLGMM method show that the results derived using the LLGMM method is far better than the results of the nonparametric methods.

Graphical Comparison of the LLGMM with LLA, REACT, and EMA Methods:

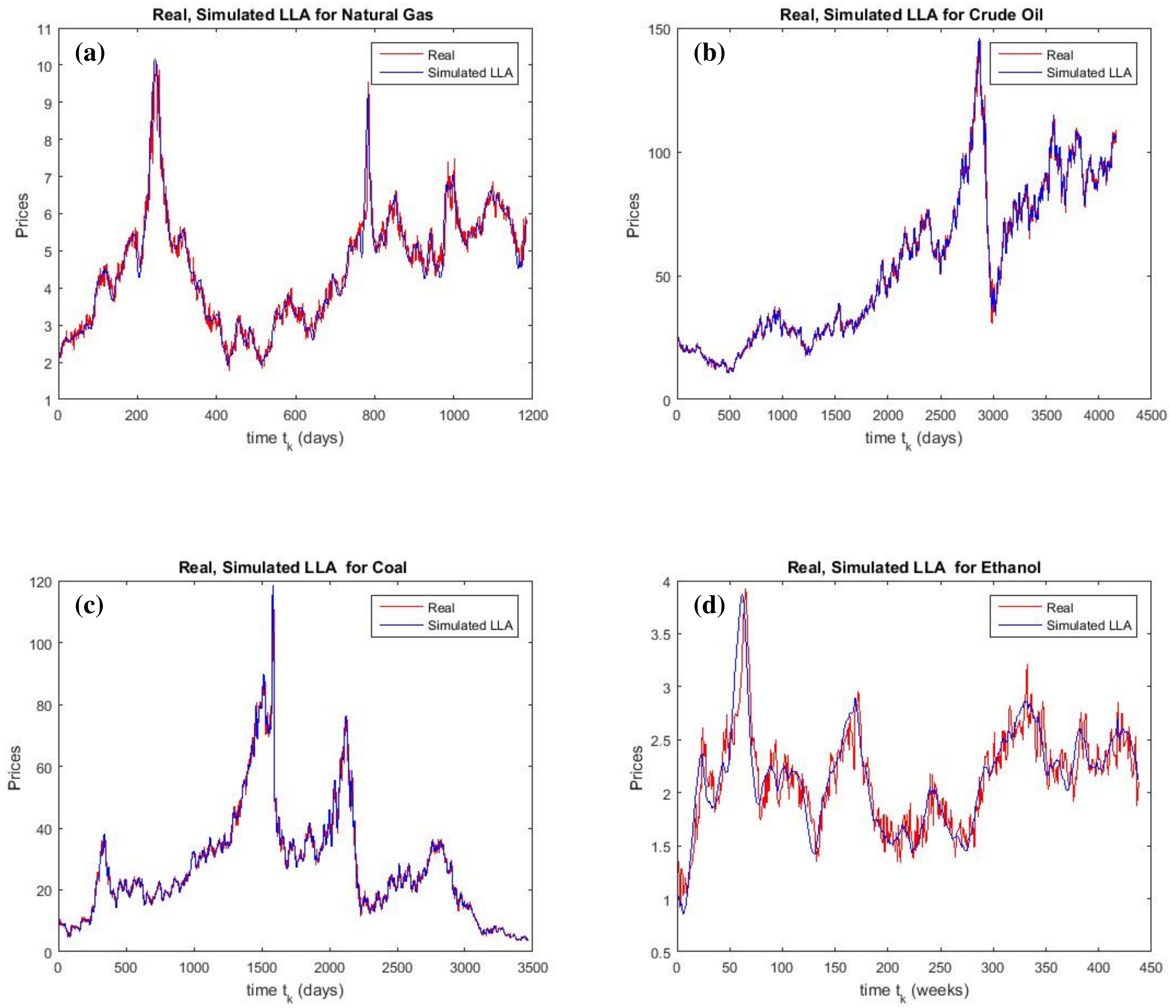

Figure D.29: Real and simulated curve using LLA method

Figure *D*.29: **(a), (b), (c) and (d)** show the graphs of the Real and Simulated Spot Prices for the daily Henry Hub natural gas data [14], daily crude oil data [13], daily coal data [12], and weekly ethanol data [48], respectively, using LLA method. The red line represents the real data y_k while the blue line represents the simulated value.

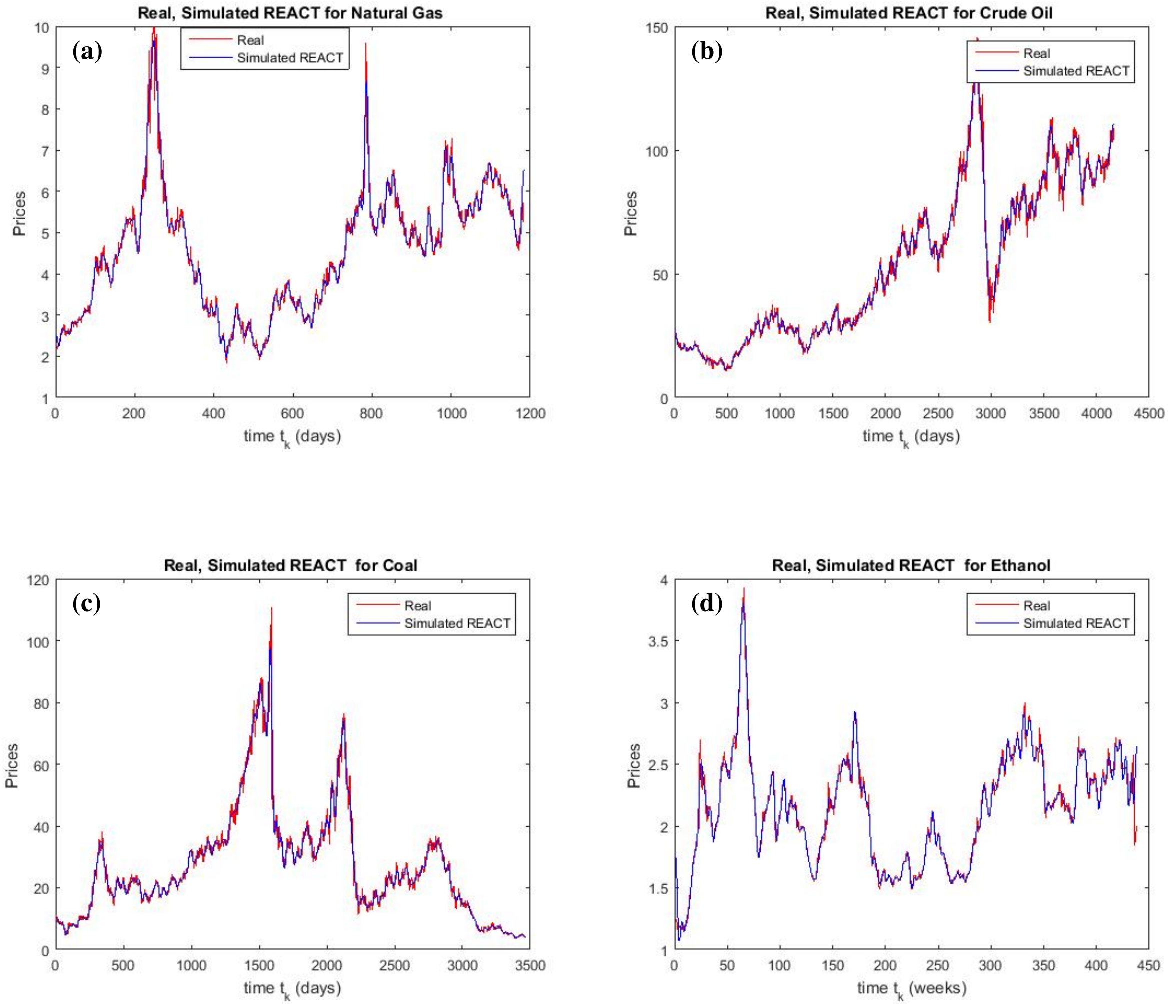

Figure D.30: Real and simulated curve using REACT method

Figure $D.30$: **(a), (b), (c) and (d)** show the graphs of the Real and Simulated Spot Prices for the daily Henry Hub natural gas data [14], daily crude oil data [13], daily coal data [12], and weekly ethanol data [48], respectively, using the REACT method. The red line represents the real data y_k while the blue line represents the simulated value.

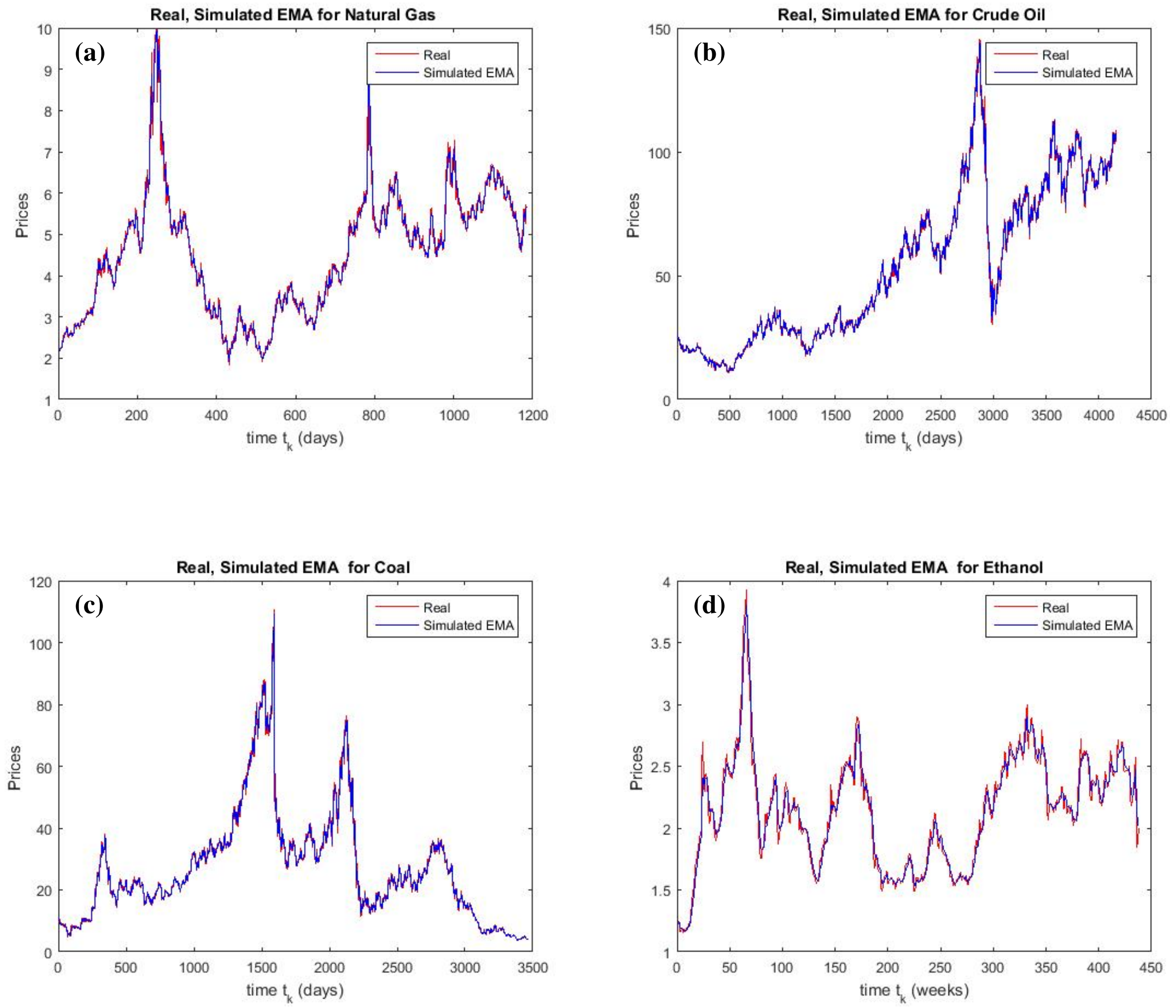

Figure D.31: Real and simulated curve using EMA method

Figure $D.31$: **(a), (b), (c) and (d)** show the graphs of the Real and Simulated Spot Prices for the daily Henry Hub natural gas data [14], daily crude oil data [13], daily coal data [12], and weekly ethanol data [48], respectively, using the EMA method. The red line represents the real data y_k while the blue line represents the simulated value.

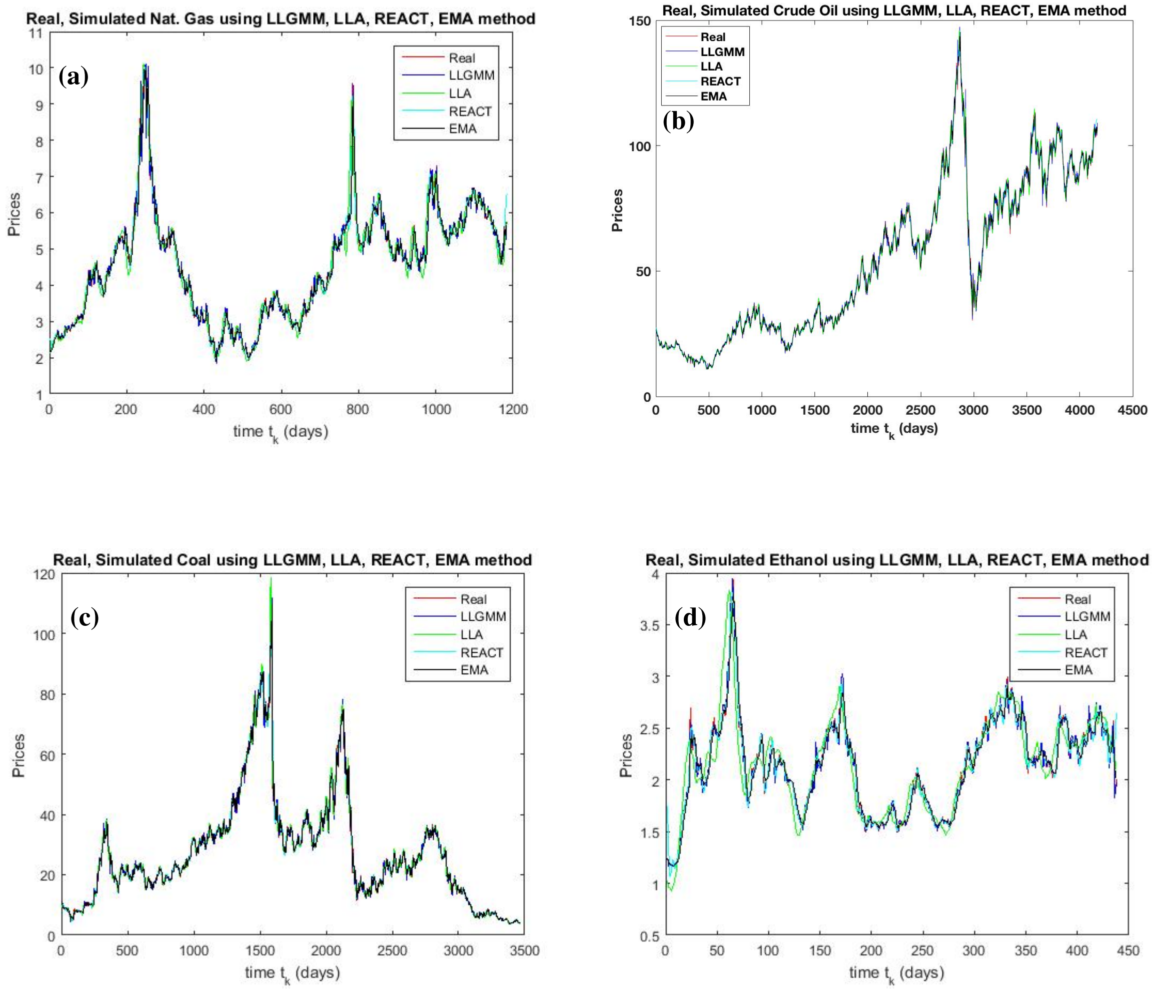

Figure D.32: Comparison of Real and simulated curve using LLGMM, LLA, REACT, and EMA method

Figure *D*.32: **(a), (b), (c) and (d)** show the graphs of the Real and Simulated Spot Prices for the daily Henry Hub natural gas data [14], daily crude oil data [13], daily coal data [12], and weekly ethanol data [48], respectively, using the LLGMM, LLA, REACT, and EMA method. The red line represents the real data.

Acknowledgements

This research is supported by the Mathematical Sciences Division, the U.S. Army Office, under Grant Numbers W911NF-12-1-0090 and W911NF-15-1-0182.

References

[1] Andrews, Donald W. K. , Generalized Method of Moments Estimation When a Parameter Is on a Boundary, *Business Economic Statistics*, 20(4) (2002): 530-544.

[2] Apostol, Tom M., Mathematical Analysis, Addison-Wesley Publishing Company, Inc., 1974.

[3] Bergstrom, A. R., Statistical Inference in Continuous Time Economic Models, Amsterdam: North-Holland, Amsterdam, 1976.

[4] Bollerslev, T., Generalized Autoregressive Conditional Heteroskedasticity, *Econometrics* 31 (1986): 307-327.

[5] Bollerslev, T., Chou, R., and Kroner, K., ARCH modeling in finance: A review of the theory and empirical evidence, *Econometrics*, 52 (1986): 5-59

[6] Box, George E. P., Jenkins, Gwilym M. , and Reinsel, Gregory C. , Time Series Analysis Forecasting and Control, Third Edition, Prentice-Hall, Inc., Englewood Cliffs, NJ, 1994.

[7] Carlstein, E, The Use of Subseries Values for Estimating the Variance of a General Statistics from a Stationary Sequence, *Ann. Statist.*, 14 (1986): 1171-1179.

[8] Casella, George and Berger, Roger L. , Statistical Inference, Second Edition, Duxbury Advanced Series, Pacific Grove, California, 2002.

[9] Chan, K. C. , Karolyi, G. Andrew , Longstaff, F. A. , and Sanders, Anthony B., *An Empirical Comparison of Alternative Models of the Short-Term Interest Rate*, *Finance*, 47(3) (1992): 1209-1227

[10] Chow, G. C., Usefulness of Adaptive and Rational Expectations in Economics, CEPS Working Paper, No. 221, Princeton University, 2011.

[11] Czella, Veronika , Karolyi, G. Andrew , and Ronchetti, Elvezio , Indirect Robust Estimation of the Short-term Interest Rate Process, *Empirical Finance*, 14 (2007), 546-563.

[12] Daily Coal data for the period 01/03/2000 − 10/25/2013, Arch Coal Incorporation, URL http://finance.yahoo.com/q/hp?s=ACI..

[13] Daily Crude Oil data for the period 01/07/1997 − 06/02/2008, *U.S. Energy Information Administration Website, URL http: //www.eia.gov/.*

[14] Daily Henry Hub natural gas data for the period 01/04/2000-09/30/2004, *U.S. Energy Information Administration Website, URL http: //www.eia.gov/.*

[15] Donnet, Sophie , and Samson, Adeline , A Review on Estimation of Stochastic Differential Equations for Pharmacokinetic/Pharmacodynamic Models, *Advanced Drug Delivery Reviews*, 65(7) (2013), 929-939.

[16] Engle, R. F. , Autoregressive Conditional Heteroscedasticity with Estimates of the Variance of United Kingdom Inflation, *Econometrica*, 50(4) (1982), 987-1007.

[17] Hansen, Lars Peter . Large Sample Properties of Generalized Method of Moments Estimators, *Econometrica*, 50(4) (1982), 1029-1054.

[18] Hansen, Lars Peter , and Scheinkman, Jose Alexandre ,Back to the Future: Generating Moment Implications for Continuous-Time Markov Processes, *Econometrica*, 63(4) (1995), 767-804.

[19] Jeisman, Joseph , Estimation of the Parameters of Stochastic Differential Equations, (PhD Dissertation, Queensland Uni. of Tech., 2005).

[20] Kenney, J. F. and Keeping, E. S., Moving Averages, *Mathematics of Statistics*, Pt. 1, 3rd ed. Princeton, NJ: Van Nostrand, (1962) 221-223.

[21] Kloeden, P. E. and Platen, E., Numerical Solution of Stochastic Differential Equations, Springer-Verlag, New York, 1992.

[22] Kulkarni, R and Ladde, G. S. , Stochastic Stability of Short-Run Market Equilibrium, *The Quarterly Journal of Economics*, 93(4) (1979), 731-735.

[23] Ladde, Anil G. and Ladde, G. S. , An Introduction to Differential Equations: Deterministic Modelling, Methods and Analysis, Volume 1, World Scientific Publishing Company, Singapore, 2012.

[24] Ladde, Anil G. and Ladde, G. S. , An Introduction to Differential Equations: Stochastic Modelling Methods and Analysis, Volume 2, World Scientific Publishing Company, Singapore, 2013.

[25] Ladde, G.S. , Stability and Oscillations in single-species process with past memory, *Int. J. Systems Sci.*, 10(6) (1979), 639-647.

[26] Ladde, G.S., Lakshmikantham, V. and Vatsala, A. S. ,Monotone Iterative Techniques for Nonlinear Differential equations, Pitman Publishing, Inc., Marshfield, Massachusetts, 1985.

[27] Lucas M. James and Saccucci S. Michael, Exponentially Weighted Moving Average Control Schemes: Properties and Enhancements American Statistical Association, *American Society for Quality Control*, 32(1) (1990), 1-12

[28] Mohinder S. Grewal, Angus P. Andrews, Kalman Filtering, Theory and Practice using Matlab, John Wiley and Sons, 1, 2008.

[29] Otunuga, Olusegun M. , Non-Linear Stochastic Modeling of Energy Commodity Spot Price Processes , (Ph. D. Dissertation, University of South Florida, 2014).

[30] Otunuga, Olusegun M. , Gangaram S. Ladde and Nathan G. Ladde, Local Lagged Adapted Generalized Method of Moments and Applications, *Stochastic Analysis and Applications*, 35:1 (2017), 110-143, DOI: 10.1080/07362994.2016.1213640

[31] Ozaki T, Nonlinear time series models and dynamical systems, *Handbook of Statistics*, Amsterdam: North-Holland, 5 (1985), 25-83.

[32] Ozaki T, A Bridge between Nonlinear Time Series Models and Nonlinear Stochastic Dynamical Systems: A local Linearization Approach, *Stat. Sin.*, 2 (1992) , 115-135.

[33] Paothong, Arnut and Ladde, G. S. , Adaptive Expectations and Dynamic Models for Network Goods, *Economic Analysis and Policy*, 43 (2013) , 353-373.

[34] Paothong, Arnut and Ladde, G. S. , Agent-Based Modeling Simulation under Local Network Externality, *Economic Interaction and Coordination*, 9 (2014), 1-26.

[35] Phillips, A. W., The Estimation of Parameters in Systems of Stochastic Differential Equations, *Biometrika*, 46 (1959), 67-76.

[36] Robinson, P. M., The Estimation of Linear Differential Equations with Constant Coefficients, *Econometrica*, 44 (1976), 751-764.

[37] Ronchetti, E. and , Trojani, F., Robust inference with GMM estimators, *Econometrics*, 101 (2001), 37-69.

[38] Shoji, Isao and Ozaki, Tohru , Comparative Study of Estimation Methods for Continuous Time Stochastic Processes, The *Time Series Analysis*, 18(5) (1997), 485-506.

[39] Shoji, Isao , Nonparametric Estimation of Nonlinear Dynamics by Metric-based Local Linear Approximation, *Statistical Methods Applications*, 22 (2013), 341-353.

[40] Singer, H, Continuous-time Dynamical Systems with Sampled Data Errors of Measurement and Unobserved Components, *Time Series Analysis*, 14 (1993), 527-545.

[41] Singer, Hermann, A Survey of Estimation Methods for Stochastic Differential Equations, 6th International Conference on Social Science Methodology, Amsterdam, 2004.

[42] Steiger, Natalie M. , Lada, Emily K. , Wilson, James R., Jeffrey A. Jones, Christos Alesopoulos, and David Goldsman, ASAP3: A batch means procedure for steady-State Simulation Analysis, *ACM Transactions on Modeling and Computer Simulation*, 15(1) (2005), 39-73.

[43] Trevezas, Samis and Nikolaos Limnios, Variance Estimation in the Central Limit Theorem for Markov Chains, *Statistical Planning and Inference*, 139, 7 (2009), 2242-2253.

[44] U.S. Treasury Bill Yield Data for the period of June 1, 1964 to December 1, 2004, *Center for Research in Security Prices*.

[45] U.S.-U.K. Foreign Exchange Rate data January 1990-December 2004, *Forex Database*.

[46] Walter Rudin, Principles of Mathematical Analysis, International series in pure and applied mathematics, McGraw-Hill, Inc., 1976.

[47] Wasserman Larry , *All of Nonparametric Statistics*, Springer science, Business Media Inc., New York, NY, 2007.

[48] Weekly Ethanol data for the period $03/24/2005 - 09/26/2013$. *Agricultural Marketing Resource Center*.

[49] Wei Biao Wu, Recursive Estimation of Time-average Variance Constants, *The Annals of Applied Probability*, 19(4) (2009), 1529-1552.

[50] Yuriy, K. , Anatoliy S. and Jianhong W., A Continuous-Time GARCH model For Stochastic Volatility with Delay, *Canadian Applied Mathematics Quarterly*, Summer, 13(2) (2005), 121-149.